

1-1-1980

Conformation and branching studies of polymers: using gel permeation chromatography coupled with on-line low angle laser light scattering photometry.

Robert Francis Jenkins
University of Massachusetts Amherst

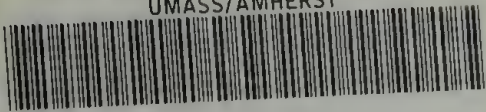
Follow this and additional works at: https://scholarworks.umass.edu/dissertations_1

Recommended Citation

Jenkins, Robert Francis, "Conformation and branching studies of polymers: using gel permeation chromatography coupled with on-line low angle laser light scattering photometry." (1980). *Doctoral Dissertations 1896 - February 2014*. 652.
https://scholarworks.umass.edu/dissertations_1/652

This Open Access Dissertation is brought to you for free and open access by ScholarWorks@UMass Amherst. It has been accepted for inclusion in Doctoral Dissertations 1896 - February 2014 by an authorized administrator of ScholarWorks@UMass Amherst. For more information, please contact scholarworks@library.umass.edu.

UMASS/AMHERST



312066 0015 5915 6

CONFORMATION AND BRANCHING STUDIES OF POLYMERS:
USING GEL PERMEATION CHROMATOGRAPHY COUPLED
WITH ON-LINE LOW ANGLE LASER LIGHT
SCATTERING PHOTOMETRY

A Dissertation Presented

By

ROBERT FRANCIS JENKINS

Submitted to the Graduate School of the
University of Massachusetts in partial fulfillment
of the requirements for the degree of

DOCTOR OF PHILOSOPHY

September 1980

Polymer Science and Engineering



Robert Francis Jenkins

1980

All Rights Reserved

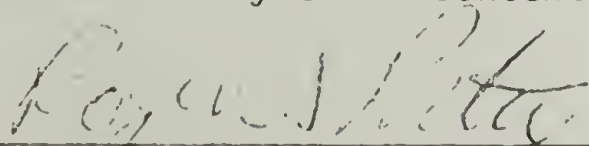
CONFORMATION AND BRANCHING STUDIES OF POLYMERS:
USING GEL PERMEATION CHROMATOGRAPHY COUPLED
WITH ON-LINE LOW ANGLE LASER LIGHT
SCATTERING PHOTOMETRY

A Dissertation Presented

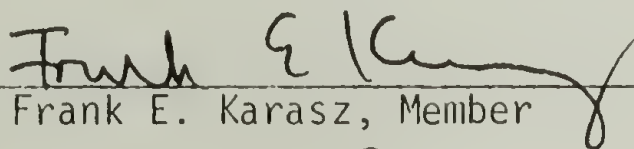
By

ROBERT FRANCIS JENKINS

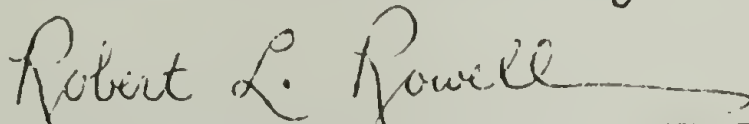
Approved as to style and content by:



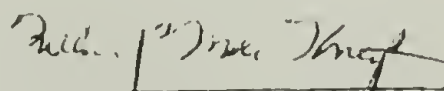
Dr. Roger S. Porter, Chairperson of Committee



Dr. Frank E. Karasz, Member



Dr. Robert L. Rowell, Member



Dr. William J. MacKnight, Department Head
Polymer Science and Engineering

To my parents, for providing me with the opportunity to pursue the career of my choice; and to Betty for her love and patience throughout the course of this work.

ACKNOWLEDGEMENTS

I wish to thank my advisor, Professor Roger S. Porter, for his guidance and support during the course of this research. I am especially grateful for his encouragement to present my work at national scientific meetings and for providing me with the opportunity to do so.

I would also like to extend my appreciation to Dr. Bernd Appelt for numerous and prolonged scientific discussions as well as for the hours of experimental assistance. I am especially grateful for his assistance in the early stages of my work. Without it this research would certainly have progressed more slowly.

ABSTRACT

Conformation and Branching Studies of Polymers:
Using Gel Permeation Chromatography Coupled
With On-Line Low Angle Laser Light
Scattering Photometry

(September 1980)

Robert Francis Jenkins, B.S., Northeastern University,

M.S., Ph.D., University of Massachusetts

Directed by: Professor Roger S. Porter

Several applications of a Gel Permeation Chromatograph, GPC, coupled with an on-line Low Angle Laser Light Scattering photometer, LALLS, are presented. These involve using the GPC/LALLS system to generate a series of values for the molecular weight, M_{wi} , and the intrinsic viscosity, $[\eta]_i$, from the distribution of the polymer sample. These values are first applied to obtaining estimates of the unperturbed dimensions for a series of stereoregular poly(methyl methacrylate), PMMA, samples, and later to measure the degree of long chain branching in poly(vinyl acetate), PVAc.

Six different stereoregular forms of PMMA, ranging from 15% to 100% isotactic dyad content, were analyzed by the GPC/LALLS method. Comparison of the intrinsic viscosity and molecular weight values generated by the GPC/LALLS method with those obtained by more conventional means (i.e., intrinsic viscosity and light scattering

measurements) showed very good agreement. Our results for "conventional" (23% isotactic dyads) PMMA gave Mark-Houwink constants of $K = 0.956 \times 10^{-4}$ (dl/gm), and $\alpha = 0.695$, as compared to $K = 1.04 \times 10^{-4}$ (dl/gm) and $\alpha = 0.697$ as obtained by conventional viscometry. Using these intrinsic viscosity and molecular weight values, the unperturbed dimensions, as well as the polymer-solvent interaction parameter, B , were evaluated by means of viscosity plots for the six stereoregular forms of PMMA.

Results showed the unperturbed dimensions of isotactic PMMA to be approximately 35% larger than the syndiotactic form. In addition, the dimensions of isotactic PMMA in a thermodynamically good solvent, tetrahydrofuran at 25°C, were determined to be larger than for the syndiotactic polymer, as exhibited by the larger intrinsic viscosity obtained for a given molecular weight. Isotactic PMMA was also found to exhibit a smaller degree of polymer-solvent interaction as reflected in the smaller value of the polymer-solvent interaction parameter, B , by the smaller value of the second virial coefficient, A_2 ; and by the smaller value of the Mark-Houwink exponent, α .

It is proposed that the larger unperturbed and perturbed dimensions as well as the smaller degree of polymer-solvent interaction exhibited by isotactic PMMA is a result of the presence of helical segments in the isotactic polymer. The presence of helical segments, because they are the conformation of lowest potential energy for the isotactic polymer, is believed to be possible in dilute solution as well as the bulk state. As a result of the helical segments, the isotactic polymer would be expected to be more extended than the

syndiotactic in both theta solvents and thermodynamically good solvents. In addition, the combination of bulky side groups and the helical segments is expected to shield the polymer from solvent molecules, resulting in the smaller degree of polymer-solvent interaction observed for isotactic PMMA.

The GPC/LALLS system was also applied to the determination of long chain branching in PVAc. Basically, polymers with long chain branching have been found to exhibit smaller hydrodynamic volumes than linear polymers of the same molecular weight. Since the intrinsic viscosity is essentially a measure of the volume, the change in intrinsic viscosity is used as a measure of the degree of long chain branching.

In this study PVAc was subjected to chain scission by mechanical as well as chemical methods to investigate the effect of shear on the branching distribution. It was concluded from this work that: (a) the branches through the acetate group are long and are ruptured preferentially on shearing, (b) the branches through the α - and β carbons are not broken on shearing, (c) the extent of long branches through the acetate group is about 67% of the total branching, (d) on shearing, 80% of the decrease in molecular weight is due to rupture of the long branches through the acetate group. The remaining 20% of the decrease in molecular weight results from main chain scission, and (e) poly(vinyl alcohol) derived from branched PVAc contains a smaller but nevertheless significant amount of branching.

TABLE OF CONTENTS

ACKNOWLEDGMENTS	v
ABSTRACT	vi
LIST OF TABLES	xii
LIST OF FIGURES	xiii
Chapter	
I. REVIEW: UNPERTURBED DIMENSIONS OF STEREOREGULAR POLYMERS	1
Abstract	1
Introduction	2
Historical	3
Measurement of the Unperturbed Dimensions	7
Direct measures of unperturbed dimensions	7
Methods	7
Stereoregular systems	10
Indirect measures of unperturbed dimensions	26
Methods	26
Stereoregular systems	33
Data Analysis	34
Dependence of dimensions on stereoregularity	34
Error analysis	35
Statistical Calculations	35
Discussion	42
References	43
II. SYNTHESIS AND CHARACTERIZATION OF STEREOREGULAR POLY(METHYL METHACRYLATE)	48
Introduction	48
Preparation of Stereoregular Poly(Methyl Methacrylate)	48
Monomer preparation	49
Preparation of samples 4, 5, 6, 7, and 8	51
Sample 4	51
Sample 5	52
9-Fluorenyl Lithium	52
Polymer preparation	53
Sample 6	53

Sample 7	53
Sample 8	54
Stereoregularity Determination	55
Carbon-13 nuclear magnetic resonance spectroscopy	55
Infrared analysis	58
Thermal Analysis	62
References	66
III. MEASUREMENT OF THE SPECIFIC REFRACTIVE INDEX INCREMENT	67
Introduction	67
Background	68
Calibration	68
Specific Refractive Index Increment for Polystyrene as a Function of Molecular Weight	69
Specific Refractive Index Increment for Stereoregular Poly(Methyl Methacrylate)	71
Discussion	81
Calculation of the specific volume	81
Specific Refractive Index Increments for Branched Poly(Vinyl Acetate)	88
Conclusions	92
References	93
IV. MEASUREMENT OF THE UNPERTURBED DIMENSIONS USING A GEL PERMEATION CHROMATOGRAPH COUPLED WITH A LOW ANGLE LASER LIGHT SCATTERING PHOTOMETER	94
Introduction	94
Experimental	94
Calculations of the Incremental Molecular Weights and Intrinsic Viscosities	100
Universal calibration	100
Determination of the spreading function	103
Recycle GPC	105
Correction for spreading	106
Calculation of the Unperturbed Dimensions	119
Conclusion	121
References	125
V. MEASUREMENT OF THE UNPERTURBED DIMENSIONS OF STEREOREGULAR POLY(METHYL METHACRYLATE)	127
Introduction	127
Measurement of the Molecular Weights and Intrinsic Viscosities	127
Calculation of Unperturbed Dimensions	131
Measurement of K_θ	131

Calculation of the characteristic ratio	141
Statistical calculations of unperturbed dimensions	142
Discussion	144
References	150
VI. CHARACTERIZATION OF BRANCHED POLY(VINYL ACETATE) BY GEL PERMEATION CHROMATOGRAPHY WITH ON-LINE LOW ANGLE LASER LIGHT SCATTERING PHOTOMETRY	151
Abstract	151
Introduction	152
Experimental	154
Materials	154
Saponification	154
Reacetylation	156
High-speed stirring	156
Refractive index increment measurements	156
Gel permeation chromatography on-line with low angle laser light scattering photometry	157
Calculation of the incremental intrinsic viscosity and molecular weight values	157
Results and Discussion	158
References	166
VII. SUGGESTIONS FOR FUTURE WORK	168
Gel Permeation Chromatography Coupled With On-Line Low Angle Laser Light Scattering Photometry	168
Dimensions of polymer	168
Branching studies	169
Alternative axial dispersion corrections	170
Calculation of the intrinsic viscosity	170
Rigid rods in GPC	171
Differential Refractometry	172
Conformational and branching effects	172
Helix-coil transitions	173
References	174

LIST OF TABLES

1.1.	Unperturbed Dimensions of Stereoregular PMMA	11
1.2.	Unperturbed Dimensions of Stereoregular PS	14
1.3.	Unperturbed Dimensions of Stereoregular PMS	15
1.4.	Unperturbed Dimensions of Stereoregular PIPA	16
1.5.	Unperturbed Dimensions of Stereoregular PB-1	17
1.6.	Unperturbed Dimensions of Stereoregular PP	19
1.7.	Unperturbed Dimensions of Stereoregular PPT-1	21
1.8.	Unperturbed Dimensions of Stereoregular PMA	22
1.9.	Temperature Coefficient for PMMA	25
2.1.	Synthesis and Characterization of Stereoregular PMMA	50
2.2.	Infrared Analysis of Stereoregular PMMA	61
3.1.	Calibration of KMX-16 Using Sodium Chloride	70
3.2.	Specific Refractive Index Increments for Polystyrene	72
3.3.	Specific Refractive Indices for PMMA	77
3.4.	Comparison of $\Delta n/\Delta c$ for Stereoregular PMMA	82
3.5.	Estimation of the Specific Volume	85
3.6.	Specific Refractive Index Increments for PVAc	90
4.1.	Mark-Houwink Constants for PS in THF	102
4.2.	Recycle GPC Data for Polystyrene	107
4.3.	K_θ Values Obtained by Various Methods	123
5.1.	$[\eta]$, M_w Relations for Stereoregular PMMA	129
5.2.	K Values for Stereoregular PMMA	140
5.3.	Slopes Obtained for Equations 5.1 to 5.6	145
5.4.	The Polymer-Solvent Interaction Parameter for PMMA	147
6.1.	Description of Poly(Vinyl Acetate) Samples	155
6.2.	Comparison of Poly(Vinyl Acetate) Samples	164

LIST OF FIGURES

1.1.	$[\eta]$ versus M for PS in toluene	4
1.2.	$[\eta]$ versus M for PS in benzene	5
1.3.	Fox-Flory plot for isotactic PPT-1	29
1.4.	Kurata-Stockmayer plot for isotactic PPT-1	30
1.5.	Stockmayer-Fixman plot for isotactic PPT-1	31
1.6.	Berry plot for isotactic PPT-1	32
1.7.	Characteristic ratio for $\{\text{CH}_2\text{-CHR}\}_n$	36
1.8.	Characteristic ratio for polystyrene	37
1.9.	Characteristic ratio for polypropylene	38
1.10.	Characteristic ratio for poly(α -methyl styrene)	39
1.11.	Characteristic ratio for poly(methyl methacrylate)	40
1.12.	Characteristic ratio for poly(methyl acrylate)	41
2.1.	Stereoregular triads for poly(methyl methacrylate)	56
2.2.	^{13}C -NMR characterization of poly(methyl methacrylate)	57
2.3.	Infrared spectra for poly(methyl methacrylate)	59
2.4.	Infrared absorbance as a function of stereoregularity	60
2.5.	Infrared characterization using the J value	63
2.6.	The effect of tacticity on T_g	65
3.1.	dn/dc versus concentration for polystyrene	73
3.2.	dn/dc versus molecular weight for polystyrene	74
3.3.	dn/dc versus the reciprocal of molecular weight	75
3.4.	dn/dc versus concentration for PMMA	79
3.5.	dn/dc versus tacticity for PMMA	80
3.6.	Refractive index versus tacticity for PMMA	86
3.7.	Specific volume versus tacticity for PMMA	87
3.8.	dn/dc versus concentration for PVAc	91
4.1.	Block diagram fo the GPC/LALLS system	95
4.2.	Typical response from the dual detectors	97
4.3.	Effect of dust particles in the GPC/LALLS system	98
4.4.	$[\eta]$ versus MW for polystyrene	104
4.5.	Recycle GPC for polystyrene, MW = 51,000	108
4.6.	Effect of spreading on the $[\eta]_i$ values	110
4.7.	ϕ_e versus MW for PMMA	112
4.8.	$\phi \{1/\alpha+1\}$ versus MW for PMMA	116
4.9.	A comparison of GPC/LALLS and GPC/Viscometry	118
4.10.	Dondos/Benoit method for stereoregular PMMA	122
5.1.	$[\eta]$ versus MW for stereoregular PMMA	130
5.2.	Fox/Flory method for stereoregular PMMA	133
5.3.	Stockmayer/Fixman method for stereoregular PMMA	134
5.4.	Berry method for stereoregular PMMA	135
5.5.	Dondos/Benoit method for stereoregular PMMA	136
5.6.	Cowie method for stereoregular PMMA	137
5.7.	Inagaki method for stereoregular PMMA	138

5.8.	The characteristic ratio for stereoregular PMMA	143
6.1.	$[\eta]$ versus M_w for branched PVAc	160
6.2.	G versus M_w for branched PVAc	162

CHAPTER I

REVIEW: UNPERTURBED DIMENSIONS OF STEREOREGULAR POLYMERS

Abstract

Results from numerous studies of unperturbed dimensions for vinyl polymers are tabulated for the first time. A comparison is made between results from theta temperature measurement and those estimated from measurements in good solvents. Data for poly(1-pentene)⁽³⁸⁾ was used by the authors to obtain figures 1.3-1.6. This data had not previously been used to obtain estimates of the unperturbed dimensions. It is concluded that these estimation procedures are generally quite acceptable, giving values usually within 8% of those determined in theta solvents. Statistical calculations for the dependence of the unperturbed dimensions on stereoregularity are considered in the light of the available data. The calculations predict an increase in the characteristic ratio, C_∞ , at intermediate tacticities for vinylidene polymers whereas a decrease is predicted for vinyl polymers. It is shown that little experimental data currently exists to confirm these predictions. It is pointed out that this is not a result of insufficient experimental studies, but rather insufficient characterization of those polymers which were studied.

Introduction

Since the initial advancements in the synthesis of stereoregular polymers by Natta et al.⁽¹⁾ in the late fifties, attempts have been made to obtain stereoregular forms of many polymers. With the synthesis of these new polymers came a large number of reports on their properties, both in the bulk state and in solution. Among the properties studied have been crystallinity, and the effect of stereoregularity on the unperturbed dimensions. In this review we are concerned exclusively with the latter. A thorough understanding of the effect of stereoregularity on the unperturbed dimensions is essential since they are a direct result of the chain conformations. Knowledge of the effect of stereoregularity on a chains conformations is importance since the conformations determine many of the properties of polymers, both in the bulk state and in solution. Properties such as rubber elasticity, the hydrodynamics and thermodynamics of polymer solutions, and optical properties are only several of the properties that are dependent on chain conformations. Although it is now possible to obtain specific stereoregular forms for many polymers, we are concerned here only with stereoregular vinyl and vinylidene polymers.

There appears to be no prior reviews concerned with the effect of stereoregularity on unperturbed chain dimensions. Our intent is to compile the reliable data and to elucidate whatever trends may exist. This review also reveals areas that suggest further study. Admittedly, the data given in many instances is questionable. One of the many obstacles in any such study is the exactness with which stereoregularity has been determined. In all early publications little could be

reported about the absolute stereoregularity. Commonly researchers have referred to polymers as "isotactic," "syndiotactic," or simply "atactic," with little reference as to the degree. Still others chose to refer to polymer products by the method with which they were synthesized, or by the fraction number, as collected from polymer fractionation procedures. Today, with the advancements made in both polymer synthesis and characterization techniques, especially nuclear magnetic resonance spectroscopy (NMR), an increasing body of knowledge is becoming available from studies of polymers of known stereoregularity. However, data from systematic studies of well characterized stereoregular polymers is still scarce, and the data reported in this review should be received with this in mind.

Historical

The first systematic evaluation of chain dimensions of stereoregular polymers in solution were reported by Danusso and Moraglio⁽²⁾. They studied both isotactic and atactic polystyrene by viscometry and osmometry, in benzene and in toluene (both thermodynamically good solvents). They concluded that no difference could be observed in the intrinsic viscosity-molecular weight relationship, $[\eta] = kM^a$, for the two stereoregular forms (see Figure 1.1 and 1.2). However, they did find a noticeable difference between the second virial coefficients for the two stereoregular forms of equivalent molecular weight. These results were consistent with subsequent measurements on isotactic⁽³⁻⁸⁾ and atactic^(7,9-12) polystyrene, PS; isotactic⁽¹³⁻¹⁸⁾, atactic⁽¹³⁻¹⁶⁾, and syndiotactic⁽¹⁶⁾ polypropylene, PP; isotactic and atactic poly(1-pentene)⁽¹⁹⁾,

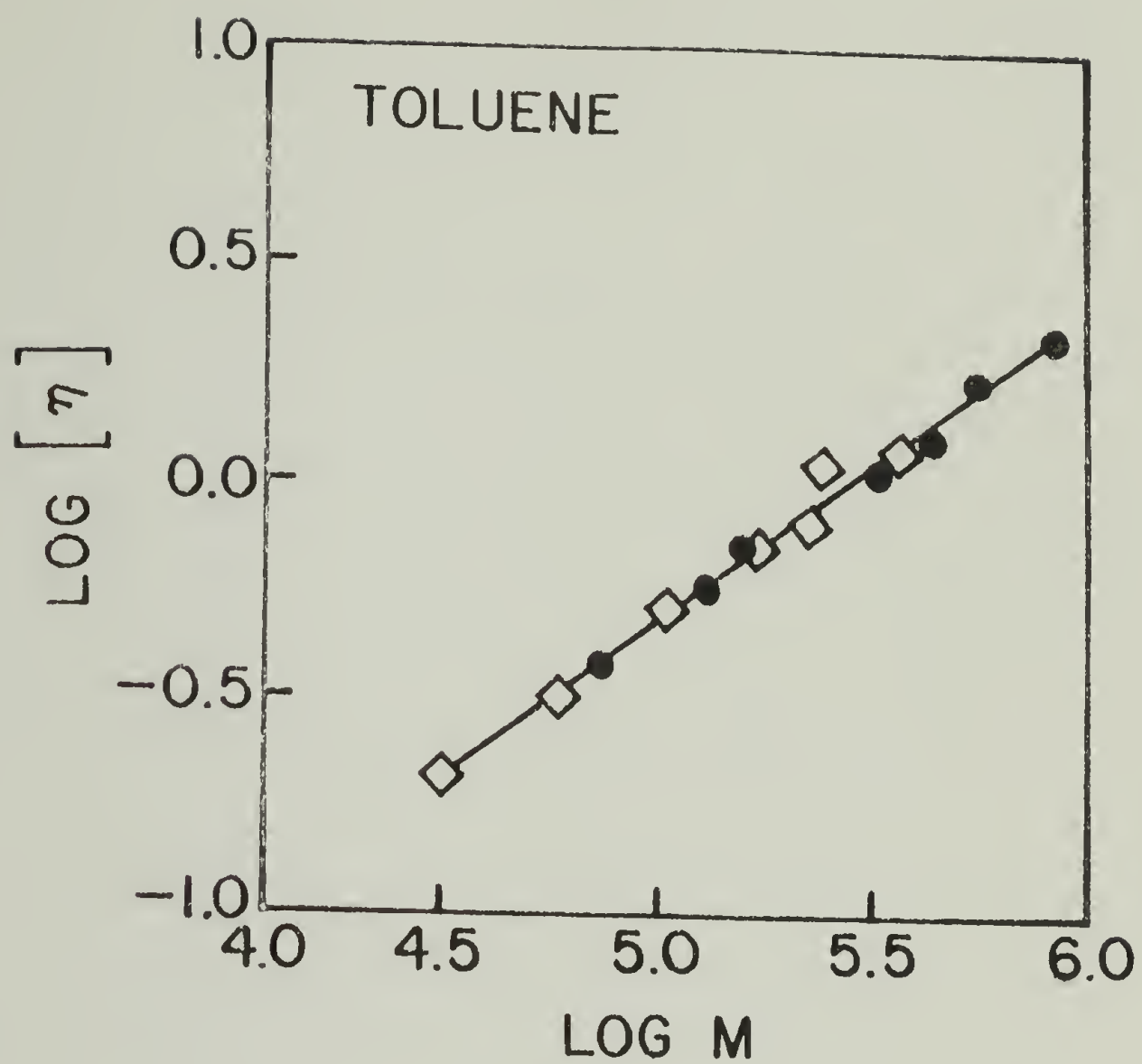


Figure 1.1. Relation between $[\eta]$ in toluene and M for fractions of polystyrene; (◇) isotactic polystyrene; (●) atactic polystyrene. From Ref. 2.

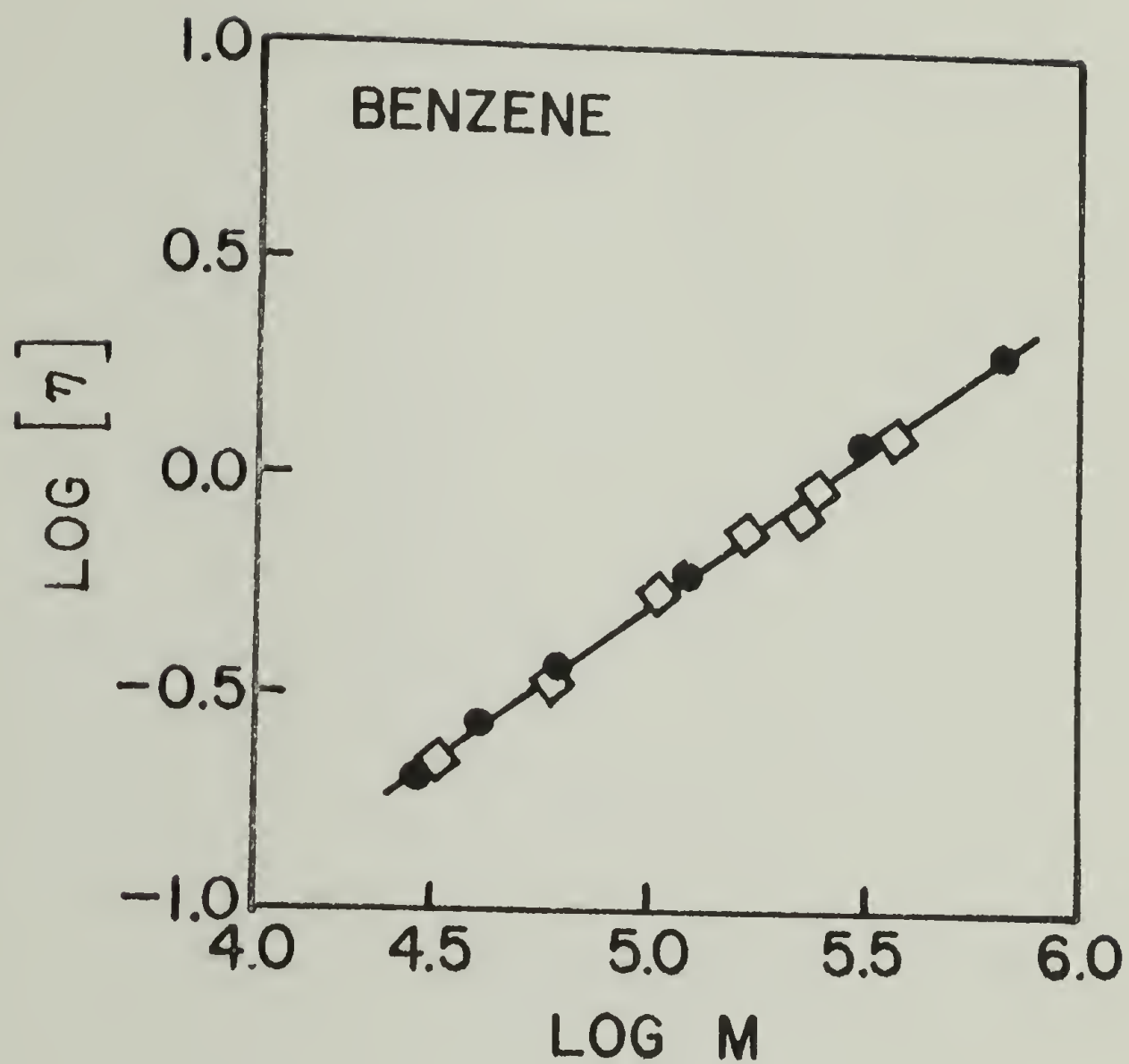


Figure 1.2. Relation between $[\eta]$ in benzene and M for fractions of polystyrene; (\diamond) isotactic polystyrene; (\bullet) atactic polystyrene. From Ref. 2.

PPT; isotactic^(10,20), atactic^(21,22), and syndiotactic⁽²³⁾ poly(methyl methacrylate), PMMA; and isotactic, atactic, and syndiotactic⁽²³⁾ poly(methyl methacrylate), PMMA; and isotactic, atactic, and syndiotactic poly(isopropyl acrylate)^(24,25), PIPA. All of these systems showed that, in thermodynamically good solvents, no differences are measurable in the intrinsic viscosity-molecular weight relationship for the different stereoregular forms. In addition, the second virial coefficient, A_2 , in every case studied was found to be larger for the syndiotactic and atactic forms than for the isotactic forms^(7,8,14,15,19,25,26).

The chain dimensions of polymer molecules in solution are influenced by both long range (excluded volume), and short range (rotational isomeric) effects⁽²⁷⁾. Long range effects are a result of thermodynamic interactions between polymer molecules and their environments. In a good solvent, where the energy of interaction between polymer and solvent is high, the molecules will tend to expand in order to increase the number of polymer-solvent contacts. As a result, the volume which one polymer segment excludes from another is large. In a poor solvent where the energy of interaction is unfavorable, the polymer will contract in order to increase the amount of polymer-polymer contacts. This decreases the amount of polymer-solvent contacts, resulting in a low excluded volume. Under theta conditions, defined as the temperature at which the second virial coefficient is zero⁽²⁷⁾, it has been shown that the excluded volume vanishes and the chain is unperturbed by long range interactions. Here the dimensions are simply a function of the short range effects and are therefore referred to as the unperturbed dimensions. Short range effects are a result of the rotational isomeric states

available to the particular molecule, and hence are indicative of the conformations of the polymer molecule itself.

Krigbaum et al.⁽⁸⁾, were the first to emphasize the necessity of measuring the dimensions of stereoregular polymers unperturbed by long range effects. They used light scattering and intrinsic viscosity measurements in thermodynamically good solvents to obtain the unperturbed dimensions of isotactic PS. Comparison with the value for atactic PS⁽⁹⁾ led to the conclusion that the unperturbed dimensions of the isotactic form were 25-30% larger than the atactic counterpart. These results were the first among many studies of the unperturbed dimensions of stereoregular polymers, and served to clearly point the way for subsequent work.

Measurement of the Unperturbed Dimensions

There are two basic ways in which measurements of the unperturbed dimensions are obtained: (1) determination of unperturbed dimensions directly, by measurements in theta solvents; and (2) determination of the perturbed dimensions in a good solvent and extrapolation of the values to the unperturbed state using one of the existing theories. Both methods have been widely used as will be shown.

Direct measures of unperturbed dimensions.

Methods. The unperturbed dimensions can be directly determined by methods such as light scattering and dilute solution viscometry on polymers dissolved in theta, θ , solvents. The light scattering technique involves graphical methods as outlined by Zimm⁽²⁸⁾ which involves obtaining light scattering data from a number of solute concentrations,

each at several different scattering angles. Equation 1.1 is used:

$$\frac{Kc}{R_\theta} = \frac{1}{M_w} (1 + (16\pi^2/3\lambda^4) \sin^2 (\theta/2) \langle \bar{S} \rangle_z^2) + 2 A_2 c + \dots \quad (1.1)$$

where; $K = 2\pi N_0^2 (dn/dc)^2 / N_a \lambda^4$, c is the solute concentration, R_θ is the Raleigh ratio and θ is the scattering angle. The ratio Kc/R_θ is plotted as a function of $\sin^2 (\theta/2) + qc$, where q is an arbitrary constant. The data obtained at a given scattering angle are then extrapolated to $c=0$. Then the data obtained at different scattering angles for the same concentrations are extrapolated to $\theta=0$. Through this double extrapolation procedure, it is possible to eliminate effects due to deviations from solution ideality as well as effects due to destructive interference of the scattered light. It follows from Equation 1.1, that the mean-square-radius of gyration, $\langle \bar{S} \rangle_0^2$, may be calculated from the initial slope of the $c=0$ line from the Zimm plot. The radius of gyration from such studies is the z-average, and must be corrected for heterogeneity to obtain $\langle \bar{S} \rangle_0^2$. Assuming a linear polymer, the mean square end-to-end distance, $\langle \bar{r}_0 \rangle^2$ is:

$$\langle \bar{r}_0 \rangle^2 = 6 \langle \bar{S} \rangle_0^2 \quad (1.2)$$

Although theoretically sound, this method has proved to be difficult to impossible, in practice. In general, the light scattering method is hindered by a number of errors: optical artifacts, molecular heterogeneity, and the errors inherent in the dual extrapolation required with respect to concentration and angle. In addition, experimental difficulties, such as crystallization and fractional precipitation, often encountered when working with stereoregular polymers near theta conditions are generally formidable. As a result there are

relatively few reports of light scattering measurements of stereoregular polymers in theta solvents^(29,30,30a).

Viscosity measurements on polymers dissolved in theta solvents have proved more useful. However, again measurements are subject to difficulties due to poor solubility near the theta point. At the theta temperature the Flory-Fox relationship⁽³¹⁾ reduces to:

$$[\eta]_{\theta} = K_{\theta} M^{1/2} \quad (1.3)$$

where:

$$K_{\theta} = \Phi (6\overline{S}_0^2/\overline{M})^{3/2} = \Phi (\overline{r}_0^2/M)^{3/2} \quad (1.4)$$

and: Φ is the "universal constant" of Flory, and \overline{M} is the number average molecular weight⁽²⁷⁾. Consequently measurements of the intrinsic viscosity at the θ temperature for samples of known molecular weight allows calculation of K_{θ} . Determination of the constant Φ thus allows calculation of the unperturbed parameter $(\overline{r}_0^2/M)^{1/2}$, as well as the characteristic ratio, C_{∞} , defined in Equation 1.5:

$$C_{\infty} = (K_{\theta}/\Phi)^{2/3} M_b/l^2 \quad (1.5)$$

where M_b is the mean molecular weight per skeletal bond, l is the bond length, and Φ is again the Flory constant.

Flory⁽²⁷⁾ has stated that Φ should be independent of molecular characteristics, and should therefore be the same for all randomly coiled chains. According to Flory⁽²⁷⁾, the best value for Φ is $2.1(\pm 0.2) \times 10^{21}$, which, when corrected for heterogeneity, should yield a value of 2.5×10^{21} . This value is substantiated by Cowie⁽³²⁾, who studied anionically-produced polystyrene in several solvents, and found an average of 2.55×10^{21} . However, many authors have determined Φ from light scattering and dilute solution viscometry, and have suggested

different values. Ptitsyn et al.⁽³³⁾, as well as Stockmayer and Kurata⁽³⁴⁾, have noted that ϕ may vary from 1.9×10^{21} for measurements in good solvents to 2.9×10^{21} for measurements in theta solvents. In addition, Mark et al.⁽²⁵⁾ determined ϕ for isotactic, atactic and syndiotactic poly(isopropyl acrylate) and found values of $2.0(\pm 0.2) \times 10^{21}$, and $2.6(\pm 0.2) \times 10^{21}$ respectively. It appears that ϕ is not as constant as originally believed. In addition, the value of ϕ used in Equation 1.4 for calculation of K_θ as well as C_∞ , varies from one author to another. It should also be noted that few researchers have actually determined ϕ for their systems. As a result, until more accurate values of ϕ are obtained for narrow distribution samples for each stereoregular polymer, in the appropriate solvent, and at specific temperatures, the values reported in tables 1.1-1.8 must be taken as approximations.

Stereoregular systems. The unperturbed dimensions for a number of stereoregular polymers have been studied by dilute solution viscometry in theta solvents. Given in tables (1.1-1.8) are values of K_θ , as defined in Equation 1.4, and the corresponding values of C_∞ . As can be seen from these eight tables, comparisons can be made between the stereoregular forms for only four polymers; PMMA, PMS, PPT, and PP. For the other three polymers sufficient data from direct, theta point studies is not available. Of the four polymers for which comparisons can be made, we see that the variation in chain dimensions with tacticity is not uniform. For PMMA it appears that the isotactic form has the larger unperturbed dimensions whereas the atactic and syndiotactic forms are equivalent. This latter result may be expected since atactic PMMA is predominantly syndiotactic⁽³⁵⁾. For PMS, the isotactic form again

Table 1.1. Unperturbed Dimensions of Stereoregular Poly(Methyl Methacrylate).

Tacticity	Solvent	Exp. Temp. °C,	θ Temp. °C.	Direct Determination	$K_{\theta} \times 10^4$ (dl/gm)					\uparrow $C_{\infty} \times 10^{-21}$	Ref.
					(F-F)	(S-Γ)	(K-S)	(B)			
Atactic	4-Heptanone	33	33	4.7	--	--	--	--	7.8	2.1 ⁺	68
	Acetonitrile	45	45	4.9	--	--	--	--	8.1	2.1 ⁺	68
	3-Octanone	72	72	5.0	--	--	--	--	8.2	2.1 ⁺	68
	p-Xylene	50	50	4.9	--	--	--	--	7.1	2.5	69
m-Xylene	60-70		--	--	4.6	4.6	--	--	6.8	2.5	69
	30	30	30	4.9	--	--	--	--	7.1	2.5	69
o-Xylene	40-70		--	--	4.1	4.4	--	--	6.5	2.5	69
	40-70		-3	--	4.1	4.4	--	--	6.5	2.5	69
n-Butyl Bromide	35	35	35	4.6	--	--	--	--	6.8	2.5	69
	42-58		--	--	4.4	4.6	--	4.6	6.8	2.5	69
Isoamyl Acetate	50	50	50	4.5	--	--	--	--	6.7	2.5	69
	65-80		--	--	2.4-2.7	3.5-3.7	--	--	5.1	2.5	69
Cyclohexane	40-70		-10	--	4.6	7.0	--	4.6	7.6	2.5	69
	25	25	25	5.9	--	--	--	--	9.7	1.9 ⁺	29,70
Chloroform	30	--	--	--	4.9	--	--	--	7.1	2.5	71
Benzene	30	--	--	--	4.9	--	--	--	7.1	2.5	71
MEK	30	--	--	--	4.9	--	--	--	7.1	2.5	71
Acetone	30	--	--	--	4.9	--	--	--	7.1	2.5	71

TABLE 1.1--Continued

Tacticity	Solvent	Exp. Temp. °C.	Temp. °C.	Direct Determination	$K_0 \times 10^4$ (dl/gm)				Φ		Ref.
					(F-F)	(S-F)	(K-S)	(B)	C_∞	$\times 10^{-21}$	
Atactic	TFP	25	--	--	--	11.6	11.6	--	11.5	2.87*	70
	p-Cumene	159.7	159.7	5.7	--	--	--	--	7.2	2.87*	70
	n-Propanol	84.4	84.4	6.8	--	--	--	--	8.1	2.87*	70
	3-Heptanone	36.7	36.7	6.3	--	--	--	--	7.7	2.87*	70
Syndio- tactic	n-Butyl Bromide	35	35	5.1	--	--	--	--	7.3	2.5	73
	Butanone										
	Isopropanol	8	8	4.4	--	--	--	--	6.6	2.5	73
	2-Heptanone	5-50	30.2	--	4.8	4.8	4.8	4.8	6.5	2.83*	74
Isotactic	Nitromethane	25-45	15	--	4.8	4.8	4.8	4.8	6.5	2.83*	74
	Acetonitrile	27.5	27.5	7.6	--	--	--	--	9.5	2.55*	75
	Acetonitrile	27.6	27.6	7.6	--	--	--	--	10.8	2.1*	76
	n-Butyl Chloride	26.5	26.5	7.7	--	--	--	--	9.5	2.55*	73
	Butanone										
	Isopropanol	25	25	7.2	--	--	--	--	9.1	2.58*	73
	Ethyl Acetate	25	--	--	--	7.7	7.8	7.3	9.4	2.55*	75
	Acetone	30	--	--	7.0	--	--	--	10.1	2.1*	70
	TFP	25	--	--	--	8.2	8.7	--	9.3	2.87*	72

TABLE 1.1--Continued

Tacticity	Solvent	Exp. Temp. °C.	θ Temp. °C.	Direct Determination	$K_\theta \times 10^4 (\text{dl/gm})$					ϕ $\times 10^{-21}$	Ref.
					(F-Γ)	S-Γ)	(K-S)	(B)	c_∞		
Isotactic	TFP	25	--	--	--	8.2	8.7	--	9.3	2.87*	72
	MEK										
	Isopropanol	30.3	30.3	9.0	--	--	--	--	9.7	2.87	70
	3-Heptanone	40.0	40.0	8.7	--	--	--	--	9.5	2.87*	70
	n-Propanol	75.9	75.9	7.6	--	--	--	--	8.7	2.87*	70
	p-Cymene	152.1	152.1	5.7	--	--	--	--	7.2	2.87*	70

(*) Indicates the value of ϕ used by the respective authors.

Table 1.2. Unperturbed Dimensions of Stereoregular Polystyrene.

Tacticity	Solvent	$K_g \times 10^4 (\text{dl/gm})$						Ref.
		Exp. θ Temp. $^{\circ}\text{C.}$	Direct Determin- ation	(F-F)	(S-F)	(K-S)	(B)	
Atactic	1-Chloro-n-Decane	6.6	7.8	--	--	--	10.1	36
	1-Chloro-n-Undecane	32.8	7.9	--	--	--	10.2	36
	1-Chloro-n-Dodecane	58.6	8.1	--	--	--	10.3	36
	73% trans Decalin	18	7.7	--	--	--	10.0	77
	100% trans Decalin	24	8.2	--	--	--	10.4	77
	Diethyl Malonate	35.9	7.7	--	--	--	10.0	36
	Toluene/n-Heptane	30	8.6	--	--	--	10.8	27
	Cyclohexane	34.8	8.2	--	--	--	10.4	78
	Methyl Cyclohexane	68	7.8	--	--	--	10.1	77
	Cyclohexane	34	8.0	--	--	--	10.3	79
Isotactic	Ethyl Cyclohexane	70	7.3	--	--	--	9.6	79
	PCT	25	10.0**	--	--	--	12.2	8
	Benzene	30	--	--	--	9.0	11.1	6

(*) Indicates the value of ϕ used by the respective authors. Where no value of ϕ was suggested, we chose to use 2.5×10^{21} .

(**) Obtained by A_2 data by the method of Flory and Orfino (56).

Table 1.3. Unperturbed Dimensions of Stereoregular Poly(α -Methyl Styrene)

		$K_0 \times 10^4 \text{ (dl/gm)}$									
Tacticity	Solvent	Exp. Temp. C.	θ Temp. C.	Direct Determination	(F-F)	(S-F)	(K-S)	(B)	C_∞	$\frac{4}{C_\infty} \times 10^{-21}$	Ref.
Syndio- tactic	trans Decalin	9.5	9.5	6.7	--	--	--	--	10.3	2.5	80
	t-Decalin/ 1/1	17	17	6.8	--	--	--	--	10.4	2.5	80
	Cyclohexane	34.5	34.5	7.3	--	--	--	--	10.9	2.5	80
	t Dec./Methyl	55.5	55.5	6.9	--	--	--	--	10.5	2.5	80
	Cyclohexane/ Methyl Cyclo- hexane 1/1	58.6	58.6	7.4	--	--	--	--	11.0	2.5	80
Isntactic	t Dec./Methyl	81	81	6.8	--	--	--	--	10.4	2.5	80
	Cyclohexane 1/10	32.5	32.5	6.6	--	--	--	--	10.2	2.5	81
	Cyclohexane	37	37	7.8	--	--	--	--	11.4	2.5	81
	Cyclohexane	30	--	--	--	7.5	--	--	11.1	2.5	48
	Toluene	30	30	7.68	--	--	--	--	11.3	2.5	82

Note: Characterization of stereoregular PMS is a subject of considerable controversy. Many disagree as to whether a specific sample is syndiotactic or isotactic. As a result, the method of polymerization is usually referred to in the literature instead of the stereoregularity.

Table 1.4. Unperturbed Dimensions of Stereoregular Poly(Isopropyl Acrylate)

Tacticity	Solvent	Exp. \bar{M}_w	\bar{M}_w	Direct Determination	$K_g \times 10^4$ (dl/gm)					Ref.
					(F-F)	(S-F)	(K-S)	(B)	$C_m \times 10^{-21}$	
Atactic	Benzene	25	--	--	--	--	--	--	7.1 ⁺	25
	TFP	25	--	--	9.2	--	13.7	--	14.3	24
Syndio- tactic	Bromobenzene	60	--	--	--	--	--	--	7.2 ⁺	25
	Bromobenzene	60	--	--	--	--	--	--	9.7 ⁺	25
Isotactic	TFP	25	--	--	9.9	--	14.3	--	17.2	24

(*) Value of ϕ suggested by respective authors.

(**) Calculated using the theory of Flory and Orfino⁽⁵⁶⁾.

Table 1.5. Unperturbed Dimensions of Stereoregular Poly(1-Butene)

Tacticity	Solvent	Exp. Temp. °C.	Temp. °C.	Direct Determination	$V_B \times 10^4$ (dl/gm)					Ref.	
					(F-F)	(S-F)	(F-S)	(R)	$\bar{r}^2 \times 10^{-21}$		
Atactic	n-Nonane	35	83	21**	--	--	--	--	11.8	2.8*	26
	Anisole	83	83	10.81	--	--	--	--	6.7	2.5	83
	Isamyl Acetate	23	23	11.3	--	--	--	--	6.0	2.5	83
	Phenetole	61	61	10.5	--	--	--	--	6.6	2.5	83
	Toluene	-46	-46	13.3	--	--	--	--	7.7	2.5	83
	Benzene	30	--	--	--	--	11	--	6.8	2.5	83
	Toluene	30	--	--	--	--	11	--	6.8	2.5	83
	Decalin	30	--	--	--	--	11	--	6.8	2.5	83
	Decalin	100	--	--	--	--	10.5	--	6.6	2.5	83
	Tetralin	100	--	--	--	--	10.0	--	6.4	2.5	83
	n-Nonane	80	--	30**	--	--	--	--	14.9	2.1*	26
Isotactic	Cyclohexane n-Propanol $\frac{69}{31}$	35	35	24.7	--	--	--	--	10.7	2.87*	84
	Cyclohexane	35	--	--	24.1	25.0	24.1	--	10.6	2.87*	84
	Cyclohexane n-Propanol $\frac{90}{10}$	35	--	--	24.1	25.0	24.1	--	10.6	2.87*	84

TABLE 1.5--Continued

		$K_{\theta} \times 10^4 (\text{dl/gm})$						
Tacticity	Solvent	Exp. $\theta_{\text{C.}}$	$\theta_{\text{C.}}$	Direct Determination	(F-F)	(S-F)	(K-S)	(R)
Isotactic	Cyclohexane	80	--	--	24.1	25.0	24.1	--
	n-Propanol	20	--	--	24.1	25.0	24.1	--
	Cyclohexane	70	--	--	24.1	25.0	24.1	--
Isotactic	n-Propanol	30	--	--	24.1	25.0	24.1	--
	Cyclohexane	65	--	--	24.1	25.0	24.1	--
Isotactic	n-Propanol	35	--	--	24.1	25.0	24.1	--
	Cyclohexane	35	--	--	24.1	25.0	24.1	--

(*) Value of θ as suggested by the respective authors.

(**) Calculated from measurements in good solvents using the method of Flory and Orfino (56).

Table 1.6. Unperturbed Dimensions of Stereoregular Polypropylene.

		$K_{\theta} \times 10^4$ (dl/gm)								
Tacticity	Solvent	Exp. Temp. °C.	θ Temp. °C.	Direct Determination	(F-F)	(S-F)	(K-S)	(R)	C_{∞} $\times 10^{-21}$	Ref.
Atactic	1-Chloro Naphthalene	74	74	18.2	--	--	--	--	8.18	2.1 ⁺ 17
	Cyclohexane	92	92	17.2	--	--	--	--	7.86	2.1 ⁺ 17
	Isoamyl Acetate	34	34	16.8	--	--	--	--	6.12	2.1 ⁺ 17
	Diphenyl Ether	153	153	12.0	--	--	--	--	6.20	2.1 ⁺ 17
	? Decalin	135	--	--	--	--	12.5	--	5.6	2.5 13,14
Syndio- tactic	Isoamyl Acetate	34	34	16.8	--	--	--	--	6.9	2.5 91
	Isobutyl Acetate	58	58	15.8	--	--	--	--	6.7	2.5 91
	Diphenyl	129	129	12.8	--	--	--	--	5.8	2.5 91
	Diphenyl Ether	146	146	12.5	--	--	--	--	5.7	2.5 91
	Isoamyl Acetate	45	45	17.2	--	--	--	--	6.9	2.5 16
	Toluene	30	--	--	--	16.4	--	--	6.6	2.5 16
Isotactic	Heptane	30	--	--	--	16.4	--	--	6.6	2.5 16
	Decalin	135	--	--	--	11.2	--	--	5.2	2.5 16
	Diphenyl Ether	145	145	13.2	--	--	--	--	7.48	2.1 ⁺ 17
	Diphenyl Ether	145	145	9.4	--	--	--	--	4.6	2.5 77

TABLE 1.6--Continued

$V_a \times 10^4$ (dl/gm)											
Tacticity	Solvent	Exp. Temp. °C.	θ Temp. °C.	Direct Determination	(F-F)	(S-F)	(K-S)	(R)	C_m $\phi \times 10^{-21}$	Ref.	
Isotactic	Diphenyl Ether	145	145	6.6	--	--	--	--	4.73	2.5	85
	Diphenyl	125.1	125.1	15.2	--	--	--	--	5.80	2.87*	86
	Diphenyl Ether	142.8	142.8	13.7	--	--	--	--	5.41	2.87*	86
	Dibenzyl Ether	183.2	183.2	10.6	--	--	--	--	4.56	2.87*	86
	Diphenyl	125	125	14.1	--	--	--	--	6.2	2.5	91
	Diphenyl Ether	143	143	13.0	--	--	--	--	5.9	2.5	91

(*) Value of ϕ suggested by the respective authors.

Table 1.7. Unperturbed Dimensions of Stereoregular Poly(1 Pentene).

Tacticity	Solvent	Exp. θ Temp. θ_C	Direct Determination Temp. θ_C	$K_\theta \times 10^4$ (dl/gm)					$C_\infty \times 10^{-2}$	Ref.
				(F-F)	(S-F)	(E-S)	(B)			
Isotactic	Isamyl Acetate	31.5	31.5	12.3	--	--	--	9.5	2.4*	37
	2-Pentanol	62.4	62.4	12.1	--	--	--	9.1	2.5	38
	i-Butyl Acetate	32.5	32.5	12.03	--	--	--	9.1	2.5	38
	Phenetole	64	64	11.3	--	--	--	8.7	2.5	38
	Anisole	85	85	10.60	--	--	--	8.3	2.5	38
	Diphenyl Methane	121	121	9.77	--	--	--	7.9	2.5	38
	Phenyl Ether	149	149	9.77	--	--	--	7.9	2.5	38
	Toluene	30	--	--	12.1**	13.6**	14.8**	9.5	2.5	--
	i-Butyl Acetate	32.5	32.5	10.00	--	--	--	8.0	2.5	38
	Phenetole	64	64	9.77	--	--	--	7.9	2.5	38
Atactic	Anisole	85	85	9.86	--	--	--	7.9	2.5	38
	Phenyl Ether	149	149	9.44	--	--	--	7.7	2.5	38

(*) Value of θ suggested by the respective authors.

(**) As shown in Figs. 1.3-1.6; calculated by the authors from data in Ref. 38.

Table 1.8. Unperturbed Dimensions of Stereoregular Poly(ethyl Acrylate).

Tacticity	Solvent	Exp. Temp. °C.	θ Temp. °C.	Direct Determination	$K_{\theta} \times 10^4$ (dl/gm)					$\bar{r}^2 \times 10^{-21}$	Ref.
					(F-F)	(S-F)	(K-S)	(B)	\bar{r}^2		
Atactic	Toluene	35	--	--	6.5	6.6	6.6	--	--	2.5*	92
	Benzene	35	--	--	6.7	--	--	--	--	2.5*	92
	2-methyl Cyclohexanol	56.5	56.5	6.8	--	--	--	--	--	2.5*	30
	Isoamyl Acetate	61.7	61.7	6.8	--	--	--	--	--	2.5*	30
	Isoamyl Acetate	61.7	61.7	7.3*	--	--	--	--	--	--	--
	MEK/iso- Propanol (1/1)	27.5	27.5	7.2	--	--	--	--	--	2.5*	30
	MEK/iso-Propanol (1/1)	27.5	27.5	5.44	--	--	--	--	--	2.1*	93

(*) Value of \bar{r}^2 suggested by the respective authors.(**) Obtained from light scattering measurement under θ conditions.

exhibits larger unperturbed dimensions than the syndiotactic form. This same result is also found for PPT. However, the reverse trend is observed for PP where the isotactic form has the smaller unperturbed dimensions.

Interpretation of these results is complicated by the fact that the unperturbed parameter, K_θ , used to obtain both $(\langle \bar{r}_0^2 \rangle / M)^{1/2}$ and C_∞ , is not strictly a constant. It has been demonstrated in several studies that K_θ is subject to the combined effects of both solvent^(32,36,37,38a) and temperature^(36,38,38a), although the effect of solvent is believed to be small⁽²⁷⁾. In principle, however, solvation can perturb the relative energies of the conformations accessible to polymer chain segments⁽³⁹⁾. Since the unperturbed dimensions are determined by the conformations of the chain, solvent effects may be observed. In general, the unperturbed dimensions may be expected to be susceptible to solvent effects if the chain backbone contains polar groups. This has been shown for both poly(hexene 1-sulfone)^(40,41) and poly(dimethyl siloxane)⁽⁴²⁾, both of which contain polar backbone bonds. However, measurable solvent effects are also observed⁽³⁷⁾ for less polar chains such as PS^(32,36,37), PMMA⁽³⁷⁾ and poly(vinyl acetate)⁽³⁷⁾, PVAc. An obvious way of determining the effect of solvent is to compare the unperturbed dimensions of the same polymer in solvents that exhibit the same theta temperature. Consider the data for atactic PS given in Table 1.2; in 1-chloro-n decane, diethyl malonate, and cyclohexane. All have relatively close theta temperatures (i.e., 39.9, 34.8, 32.8). The differences in the unperturbed parameter K_θ , (7.9, 7.7, + 8.2 x 10⁻⁴), must therefore result from solvent effects⁽³⁶⁾.

The effect of temperature on unperturbed dimensions although straightforward in principle, has proved to be difficult to evaluate experimentally. Based on the rotational isomeric model, one would expect a negative temperature coefficient since as the thermal energy increases the relative populations of the g^+ and g^- states increases over the trans and consequently $(\bar{r}_0^2)^{1/2}$ and therefore K_θ should decrease. However, evaluation of the temperature coefficients for stereoregular polymers have resulted in inconsistencies^(43,44,45). These inconsistencies have been attributed in part to different techniques used to obtain the temperature coefficient, $d \ln \langle \bar{r}_0^2 \rangle / dt$.

There are two basic ways by which $d \ln \langle \bar{r}_0^2 \rangle / dt$ may be determined. The first involves measurements in dilute solution^(43,27); the second, solid state stress-temperature measurements^(46,47). The dilute solution measurements have been shown to be fraught with problems arising from solvent effects, as discussed in the preceding section. However, data obtained from stress-temperature measurements for amorphous networks are believed to be more reliable. The data in Table 1.9 shows the discouraging pattern of the available measurements of $d \ln \langle \bar{r}_0^2 \rangle / dt$ for stereoregular PMMA. All data come from solution measurements. Consequently specific effects of solvent are not eliminated. The more reliable method of determination of $d \ln \langle \bar{r}_0^2 \rangle / dt$ from the temperature coefficient of stress exhibited by a strained network has not been applied to PMMA. In general, quantitative comparisons of unperturbed dimensions for the stereoregular polymers (see Tables 1.1-1.8), may be made only after both the temperature and solvent effects have been evaluated.

TABLE 1.9 Experimental Values of the Temperature Coefficient for PMMA

Tacticity	Sign (+)	$d \ln C_{\infty}/dt$ Value (K^{-1})	Reference
Atactic		0	68
Syndiotactic	+	1.4×10^{-3}	70
	+	2.4×10^{-3}	73
	+	4.0×10^{-3}	90
Isotactic	-	-2.3×10^{-3}	70

been proposed, those of Fox and Flory⁽³¹⁾, (F-F), [Eq. 1.9]; Stockmayer and Fixman⁽⁵¹⁾, (S-F), [Eq. 1.10]; Kurata and Stockmayer⁽³⁴⁾, (K-S), [Eq. 1.11]; and Berry⁽⁵²⁾, (B), [Eq. 1.12], have been the most thoroughly tested, although several others have been proposed^(34,48,53,54,55,56).

$$\alpha^5 - \alpha^3 = 2 C_M (1/2 - x) M^{1/2} \quad (1.9)$$

$$\text{where; } C_M = \left(\frac{27}{2^{5/2} \pi} \right)^{3/2} \left(\bar{v}^{-2} / V_1 N_A \right) \left(M / \bar{r}_0^2 \right)^{3/2}$$

\bar{v} - partial specific volume of solute

N_A - Avogadro's number

V_1 - molar volume of solvent

and; x is a parameter related to polymer-solvent interaction

$$\alpha^3 = 1 + 2z \quad (1.10)$$

where; $z = (3/2\pi)^{3/2} \beta (\bar{r}_0^2 / M)^{3/2} M^{1/2}$ and; β is the "Binary cluster integral"⁽³⁴⁾

$$\alpha^3 - \alpha = 4/3 z g(\alpha) \quad (1.11)$$

where; $g(\alpha) = 8\alpha^3 (3\alpha^2 + 1)^{-3/2}$

$$\alpha^3 = 2 + .325z \quad (1.12)$$

where; $2 < z < 11$

On combining Equation 1.7 with each of Equations 1.9-1.12, relationships were obtained^(31,51,34,52,34a) whereby the value of K_θ can be graphically evaluated if $[\eta]$ and M are known. Flory and Fox⁽³¹⁾ were the first to put forward such a method; their equation was

$$[\eta]^{2/3} / M^{1/3} = K_\theta^{2/3} + K_\theta^{5/3} C_T (M / [\eta]) \quad (1.9A)$$

where; $C_T = 2 \psi_1 C_M (1 - \theta/T) = (\alpha^5 - \alpha^3) / M^{1/2}$ and; ψ_1 is an entropy

A much simpler form was proposed by Burchard^(34a), and later by Stockmayer and Fixman⁽⁵¹⁾; the latter authors suggested the equation:

$$[\eta] / M^{1/2} = K_\theta + .51 \phi B M^{1/2} \quad (1.10A)$$

where; $B = \beta/c_m^2$ and; c_m is the molar weight of a chain segment.

In addition Kurata and Stockmayer⁽³⁴⁾ proposed:

$$[\eta]^{2/3}/M^{1/3} = K_\theta^{2/3} + .363 \Phi B[g(\alpha)(M^{2/3}/[\eta]^{1/3})] \quad (1.11A)$$

While Berry⁽⁵²⁾ proposed:

$$([\eta]/M^{1/2})^{1/2} = K_\theta^{1/2} + .42 K_\theta^{3/2} B(\bar{r}_0^2/M)^{-3/2}(M/[\eta]) \quad (1.12A)$$

Typical plots for Equations 1.9A-1.12A are shown in Figures 1.3-1.6. In each case values of K_θ are obtained from the intercept of the appropriate plot. It is clear that the linear relationships proposed, Equations 1.9A-1.12A, do not hold at high molecular weights. As a result, values of K_θ must be obtained by extrapolation of the linear portion of the curves. The data used to obtain these plots (Figures 1.3-1.6), is from a study by Moraglio and Gianotti⁽³⁸⁾ on isotactic and atactic PPT. This data had not been previously used to estimate unperturbed dimensions by the theories presented here. Shown in the graphs are data for isotactic PPT in toluene, at 30°C., a thermodynamically good solvent, and isobutyl acetate, at 32.5°C., a θ solvent. Comparison of the results obtained by these four extrapolation techniques with that obtained in a θ solvent (iso-butyl acetate) shows reasonable agreement (see Table 1.7). Values of K_θ as estimated by the Stockmayer-Fixman and the Kurata-Stockmayer methods are seen to be ~10% higher than those obtained directly in a theta solvent. The values from the Fox-Flory and Berry equations are even closer to the experimental value; the Fox-Flory method within 1.6%; the Berry method within 4.8%. This is exceptional agreement since the values of K_θ obtained directly in θ solvents are generally accurate to $\pm 2\%$. Deviations from the experimental values has been attributed in part to the fact that the semi-empirical parent

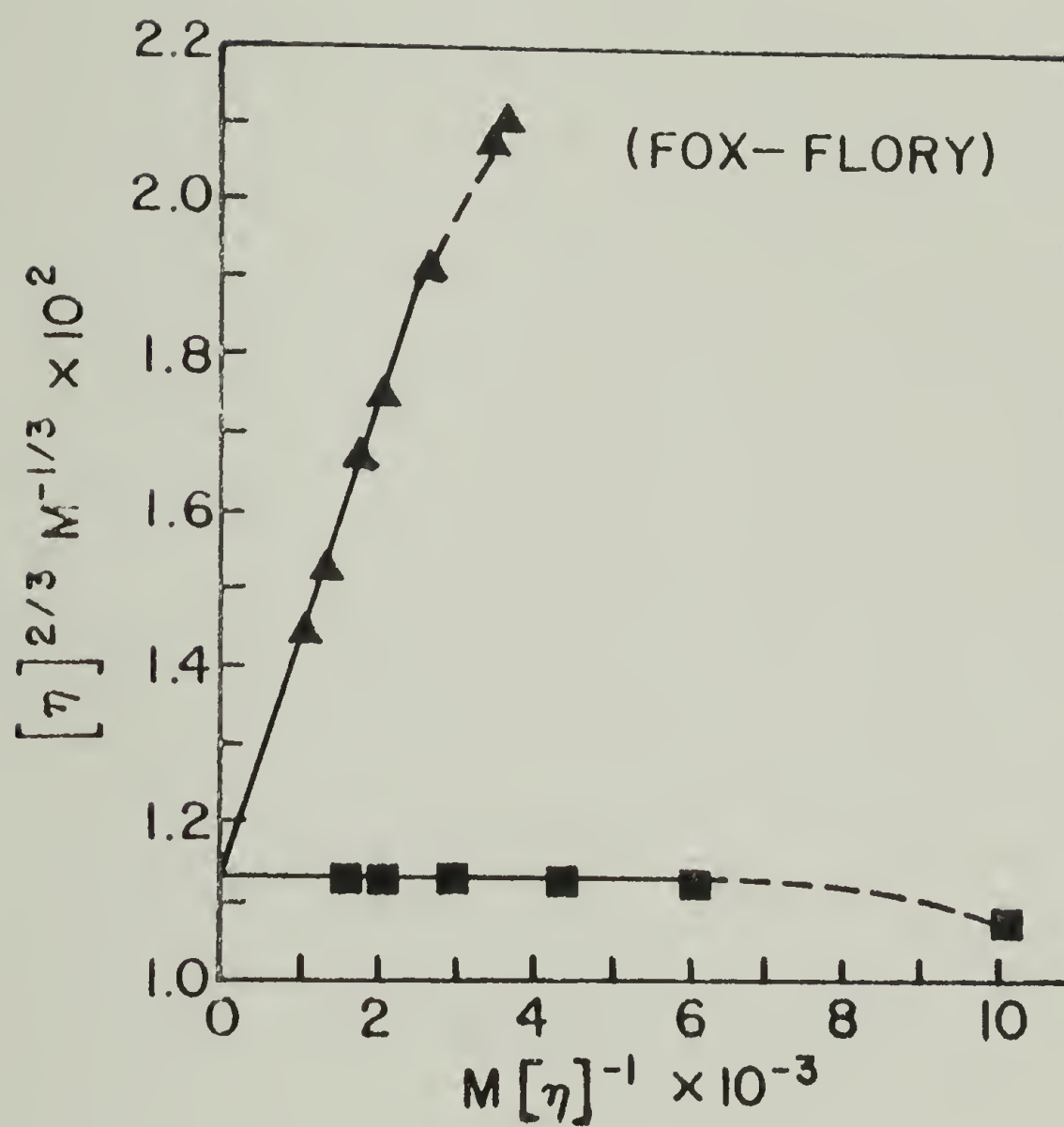


Figure 1.3. Fox-Flory plot for isotactic poly(pentene-1)⁽³⁸⁾; (▲) toluene at 30°C.; (■) i-butyl acetate at 32.5°C., θ temperature.

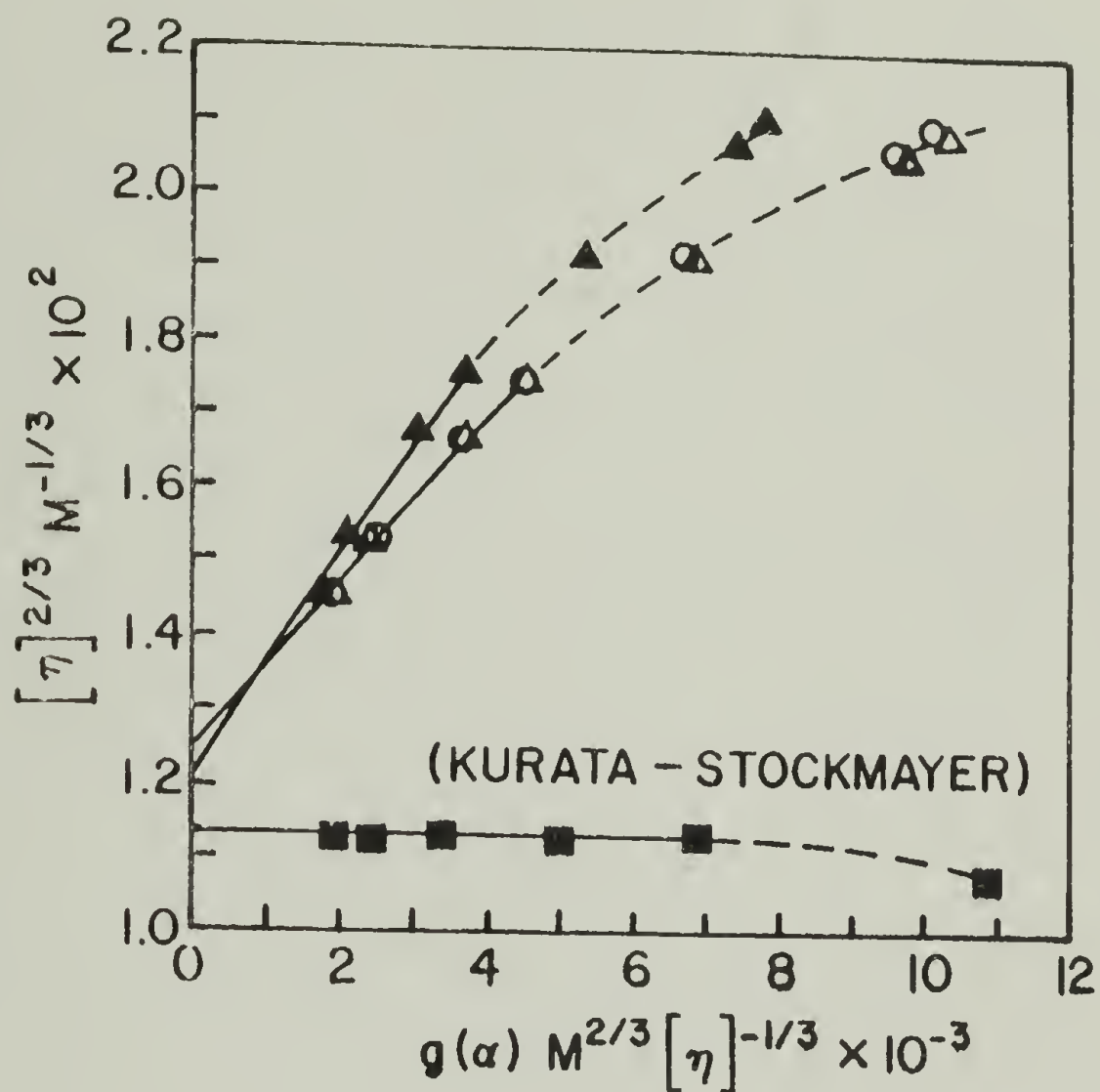


Figure 1.4. Kurata-Stockmayer plot for isotactic poly(pentene-1)⁽³⁸⁾. (Shown in the plot are three successive approximations for $g(\alpha)$ as suggested by Kurata and Stockmayer. The values are shown to converge rapidly. (▲) toluene at 30°C., first approximation; (Δ) toluene at 30°C., second approximation; (○) toluene at 30°C., third approximation; (■) i-butyl acetate at 32.5°C., θ temperature.

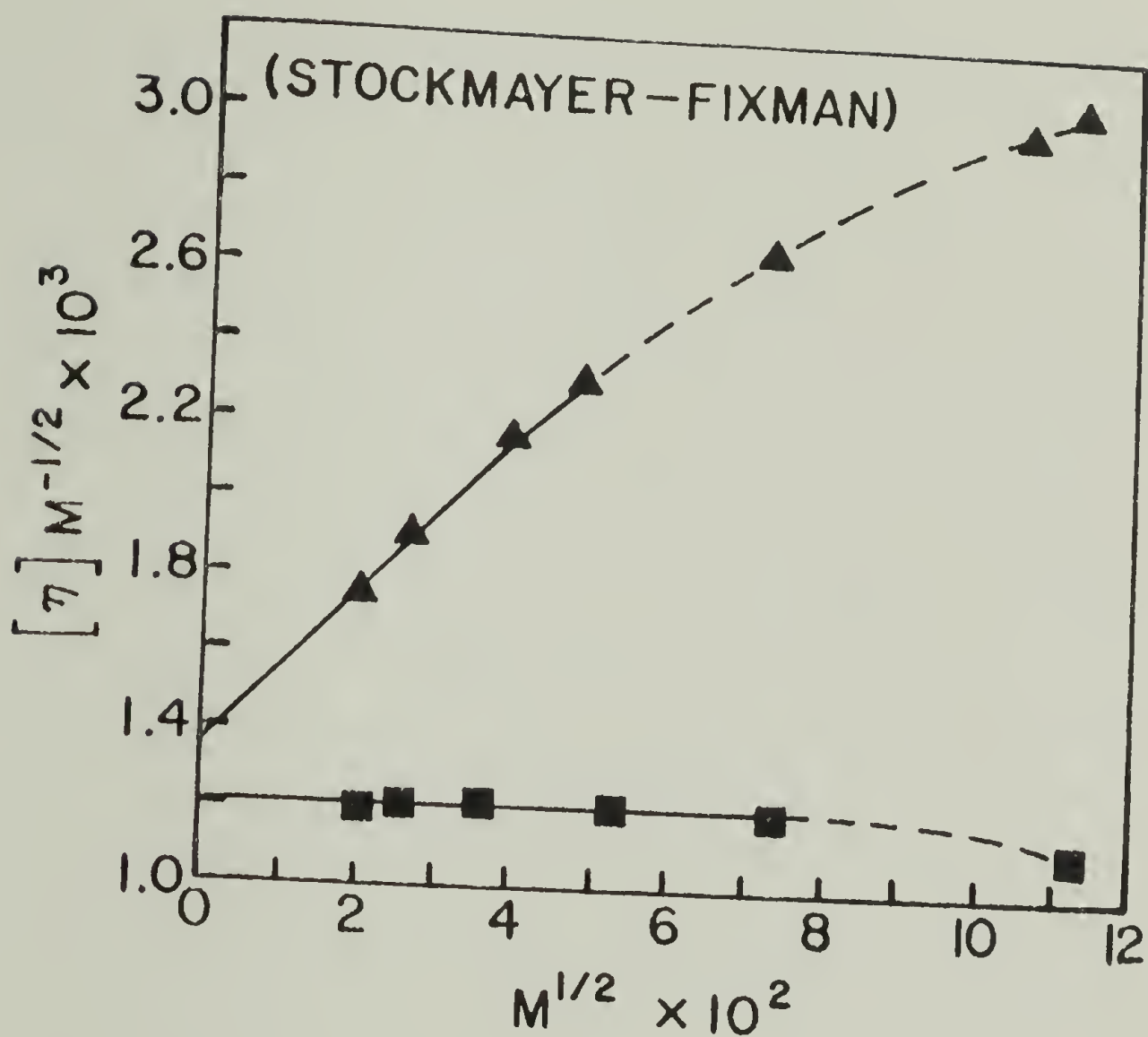


Figure 1.5, Stockmayer-Fixman plot for isotactic poly(pentene-1) (38); (\blacktriangle) toluene at 30°C.; (\blacksquare) i-butyl acetate at 32.5°C., θ temperature.

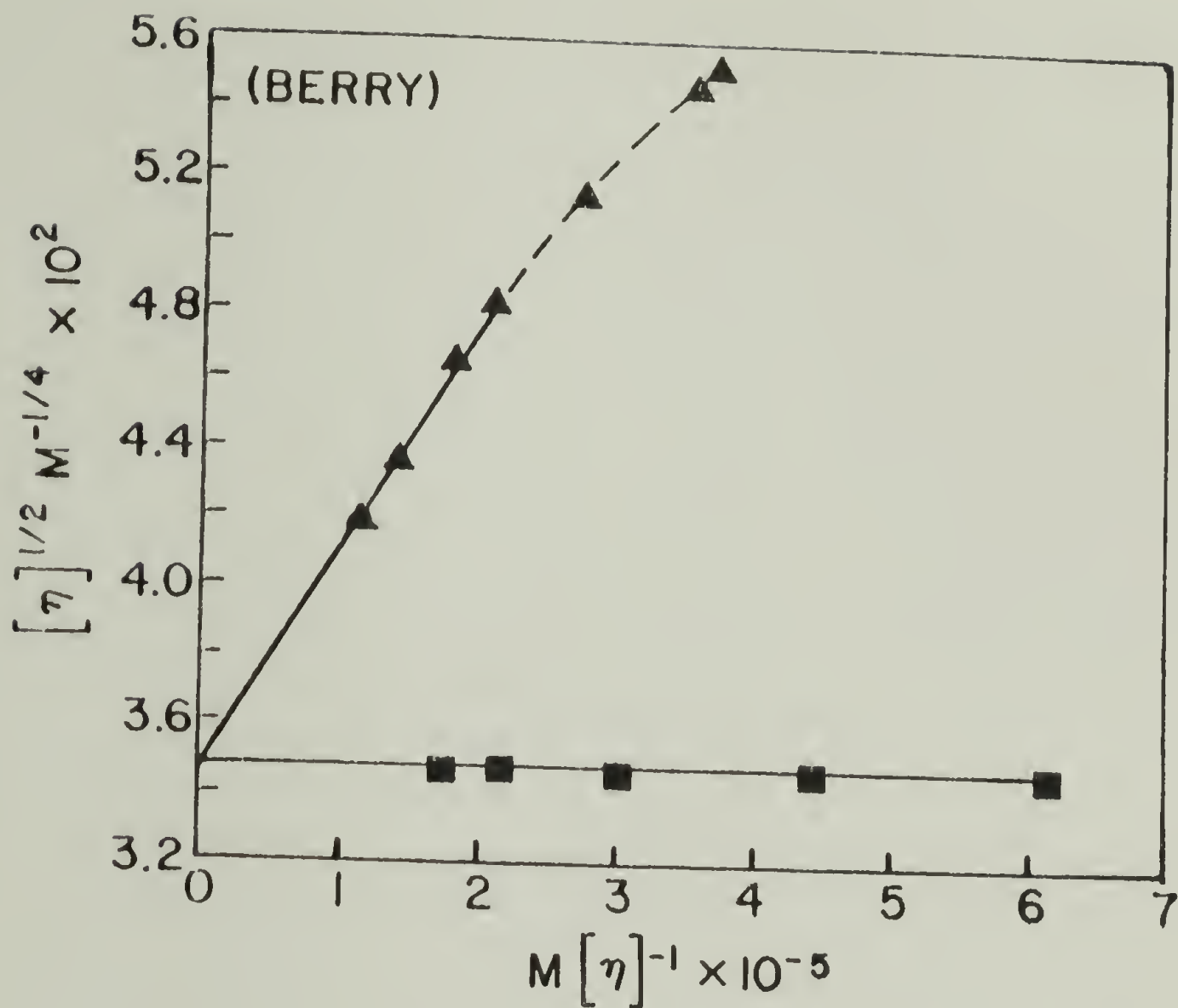


Figure 1.6. Berry plot for isotactic poly(pentene-1)⁽³⁸⁾; (\blacktriangle) toluene at 30°C.; (\blacksquare) i-butyl acetate at 32.5°C., θ temperature.

equations, Equations 1.9-1.12, are only valid over a limited range of α values⁽⁴⁸⁾. As a result, it has been suggested⁽⁴⁸⁾ that these estimation methods be used to compliment one another.

Values of K_0 derived from Equations 1.9A-1.12A from measurements at temperatures greater than θ , as well as the experimental values determined at the θ temperature, for several polymer-solvent systems, are given in Tables 1.1-1.8. It is not our purpose to critically review the various techniques for obtaining K_0 from data in non- θ solvents, as this problem has been considered elsewhere^(48,49). However, data analysis does indicate that the agreement between the experiment and calculation is generally within 8%, and often the agreement is better. This is of prime importance to those interested in stereoregular polymers since estimations of K_0 in good solvents are far easier to obtain than the corresponding values determined in θ solvents.

Stereoregular systems. Estimations of the unperturbed dimensions of several polymers^(48,57-59) have been obtained by measurements in good solvents using the extrapolation methods discussed in the previous section. However, relatively few have been concerned with the unperturbed dimensions of polymers of known stereoregularity. The data available on stereoregular polymers is given in Tables 1.1-1.8. With the exception of PMMA, data is scant for determinations of unperturbed dimensions in non- θ solvents. For PMMA the agreement is excellent among non- θ estimation techniques discussed here. For other polymers where estimates have been attempted, agreement is also satisfactory. For example, the value obtained by the Stockmayer-Fixman method for syndiotactic PP and that obtained by direct measurement at the θ temperature are

in reasonable agreement. In addition, the data available for atactic PMA (Table 1.8), shows good agreement between the values of K_θ obtained by the Fox-Flory, Stockmayer-Fixman, and Kurata-Stockmayer methods, and those obtained by direct measurements at the θ temperature. Also, the limited data available for isotactic PPT as interpreted here, shows good agreement with those values determined in θ solvents at the same temperature. In general, values of K_θ obtained from the estimation methods discussed here, have thus been shown to give good agreement with the values as determined directly in theta solvents^(48,49).

Data Analysis

Dependence of dimensions on stereoregularity. Immediately obvious, is the dependence of the unperturbed dimensions on the stereoregularity. For PMMA, the K_θ values for the isotactic form are $\sim 50\%$ larger than those of either the atactic or syndiotactic forms. Although only limited data is available for PB-1, indications are that the isotactic form is $\sim 40\%$ larger. For PIPA and PPT, the isotactic form is $\sim 25\%$ larger than either the atactic or syndiotactic forms. Although the isotactic content of PMS is not high ($\sim 11\%$ isotactic triads), the "isotactic" polymer is $\sim 10\%$ larger than the syndiotactic form. No data is available for syndiotactic PS. However, the isotactic form does exhibit a K_θ $\sim 25\%$ larger than the atactic form. On the other hand, the data for PP, although considerably scattered, appears to indicate that K_θ for the syndiotactic and atactic forms is larger than that of the isotactic form by $\sim 25\%$.

Error analysis. Due to the errors inherent in the methods used to obtain K_0 , the values are believed to be accurate to $\pm 10\%$. The observed differences of $\geq 25\%$ are therefore considered real. However, a question that arises on comparing unperturbed dimensions, as obtained by solution studies, is to what extent the differences observed are manifestations of specific effects of solvent or temperature, as pointed out in the previous section. Another problem which arises on trying to compare the dimensions of stereoregular polymers is that of insufficient characterization. It is likely that we are never dealing with either 100% iso or syndiotactic forms. Consequently reported differences between forms depend on the level of stereoregularity. For most data in Tables 1.1-1.7, there is no exact information on stereoregularity. As a result, comparisons between experimentally observed unperturbed dimensions of the stereoregular forms of these polymers must be deemed as qualitative. As later shown, even trends deduced from such data may be spurious.

Statistical Calculations

Flory⁽⁶⁰⁾ has shown that the unperturbed dimensions of polymers may be predicted through statistical evaluations of molecular conformations based solely on the rotational isomeric model. These calculations have been applied to stereoregular polymers with considerable success⁽⁶¹⁾. Among the stereoregular systems for which statistical conformational studies have been attempted are PMA^(62,62a), PMMA⁽⁴⁴⁾, PS^(63,64), PP^(65,66), PPT⁽⁶³⁾, PBT⁽⁶³⁾, and PMS⁽⁶⁷⁾. The results of these calculations for the polymers in Tables 1.1-1.8 are shown graphically in Figures 1.7-1.12. These plots are the result of employing Monte Carlo

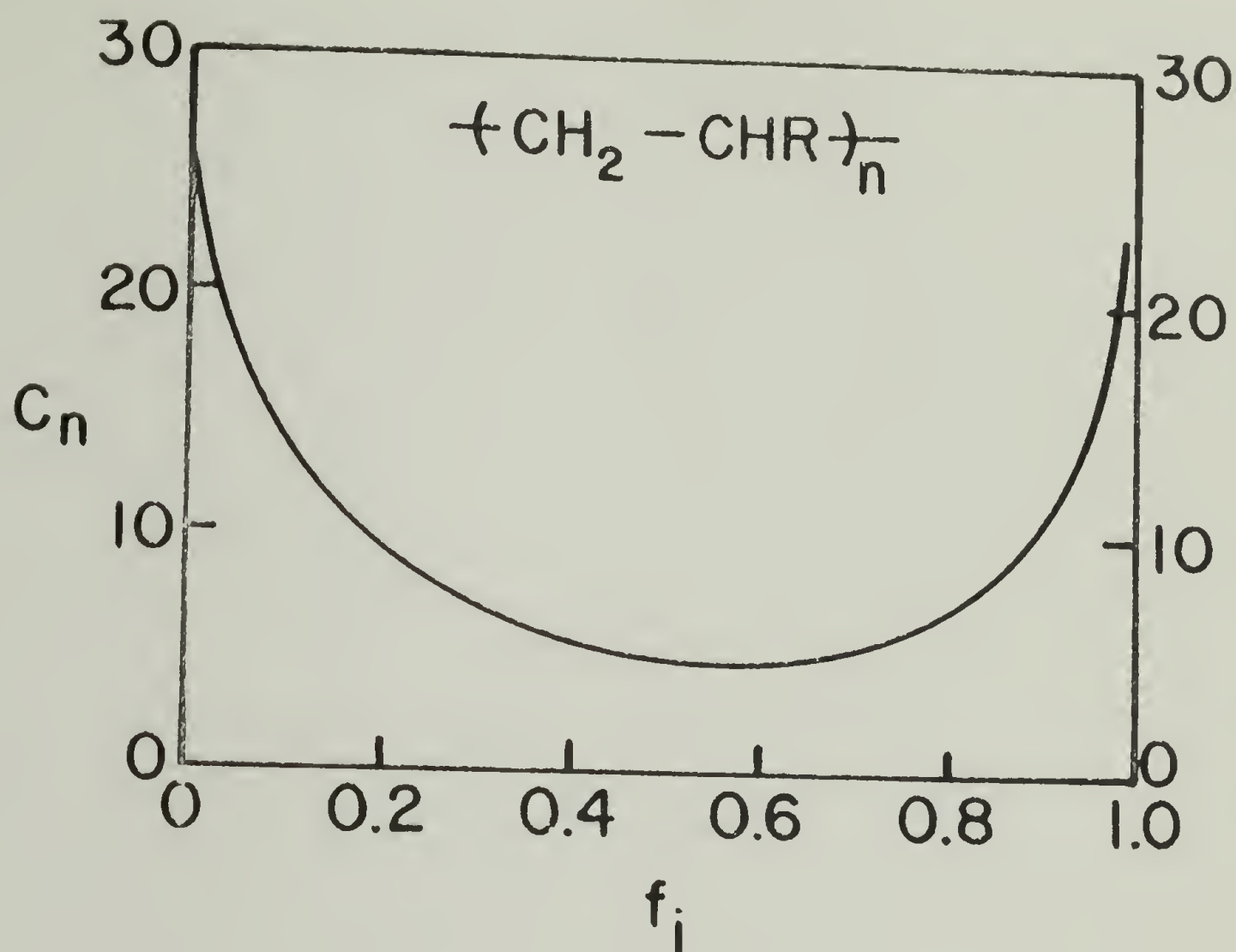


Figure 1.7. The characteristic ratio as a function of stereoregularity, calculated for a system with $R = (CH_2)_zCH_3$ ($z \geq 1$). The parameters used are $E_\tau^*/RT = 2.3$, $E_{\omega''}/RT = 5 \pm 1$ and $\Delta\phi = 20^\circ$, respectively.

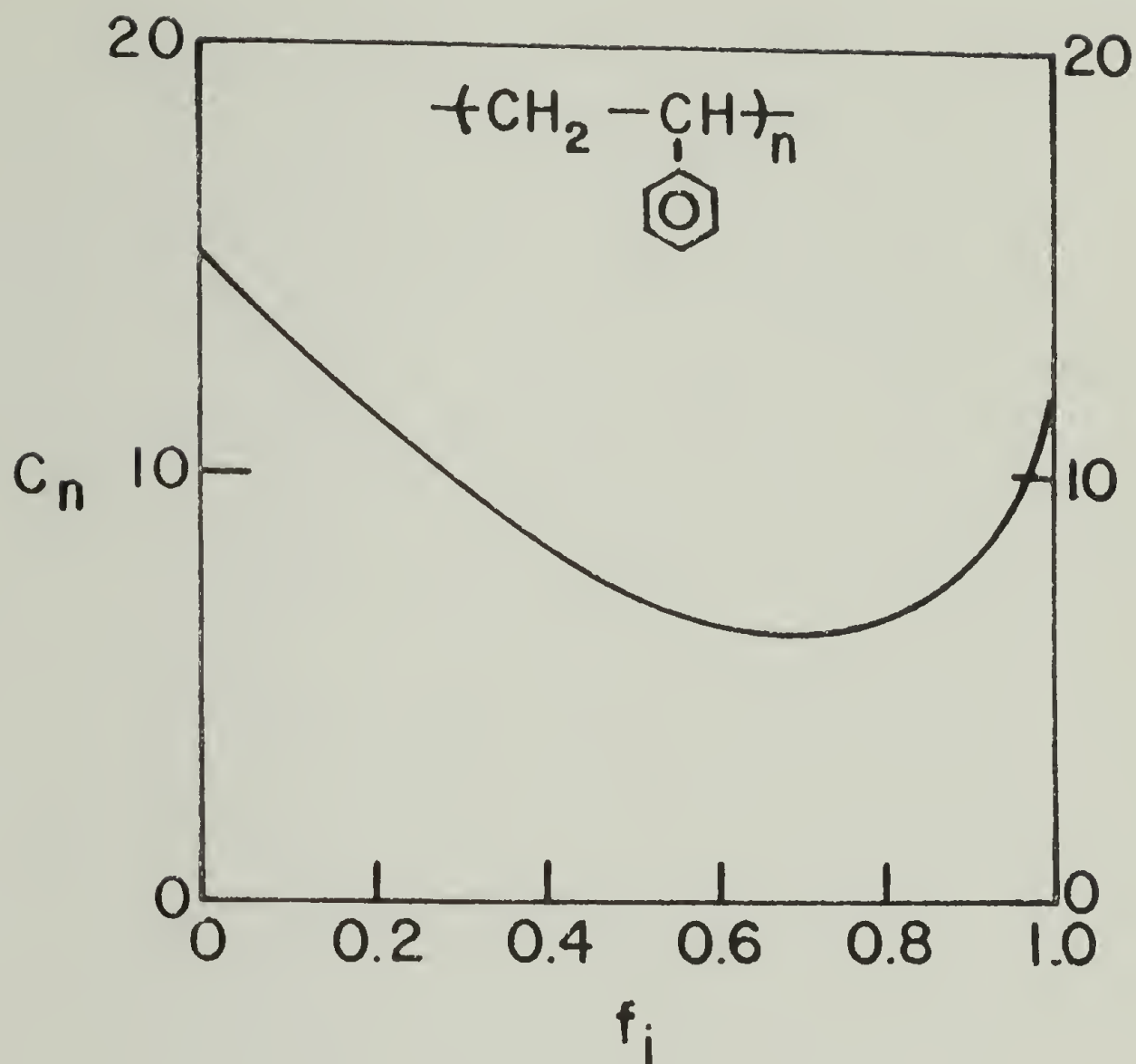


Figure 1.8. The characteristic ratios for Monte Carlo chains of 100 units each as a function of f_i , the fraction of meso dyads in the chain. The curve shown above represents results of calculations carried out with $E_{\tau''}/RT = E_{\omega}/RT = 5$. From Ref. 63.

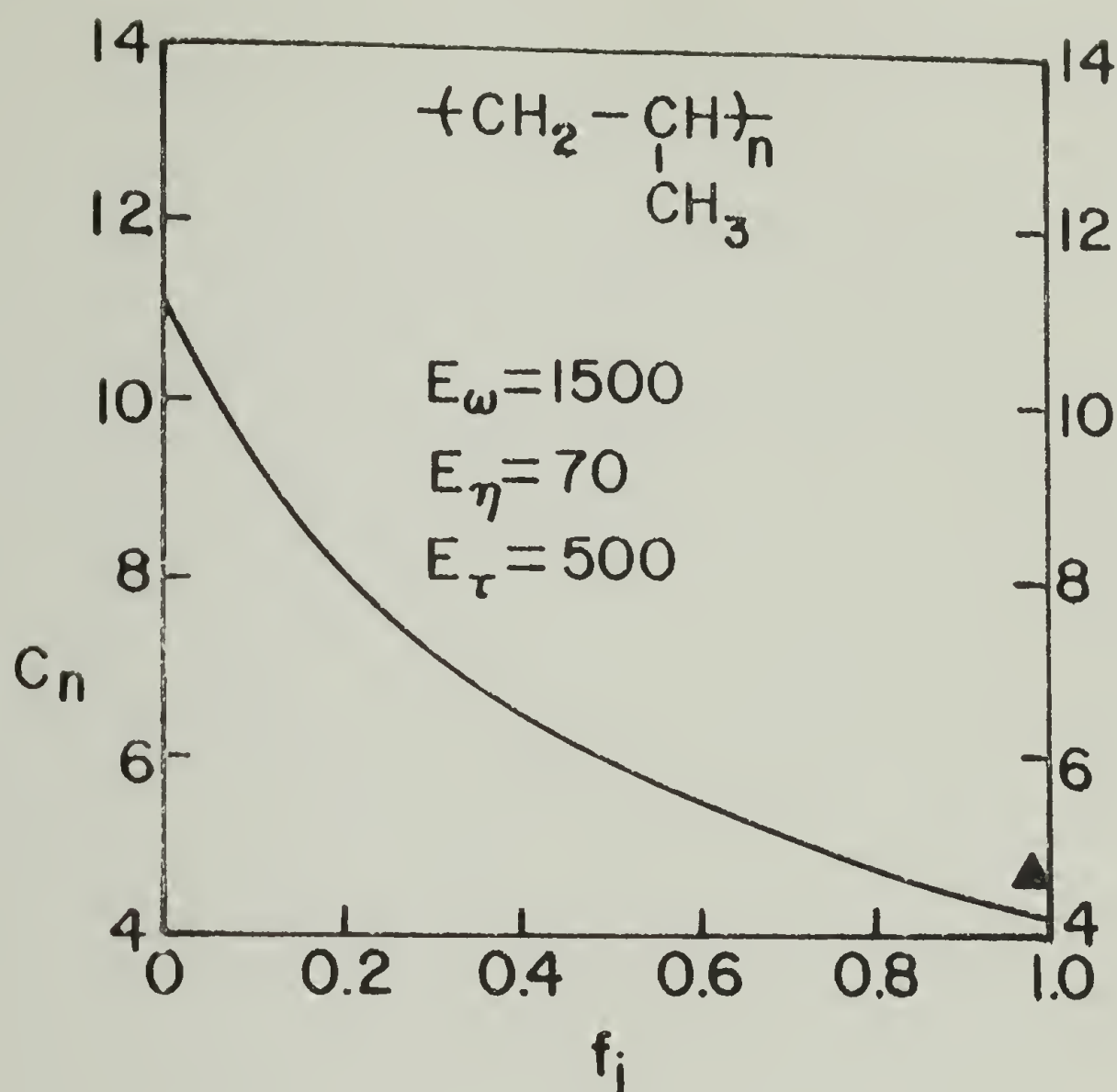


Figure 1.9. The characteristic ratios for Monte Carlo chains of 200 units each as a function of f_i , the fraction of meso dyads in the chain. The curve shown above represents results of calculations carried out for a temperature of 140°C . with the conformational parameters chosen as indicated, in cal. mol.^{-1} . The experimental values of Bovey and Heatley⁽⁸⁵⁾ (\blacktriangle) are shown. From Ref. 65.

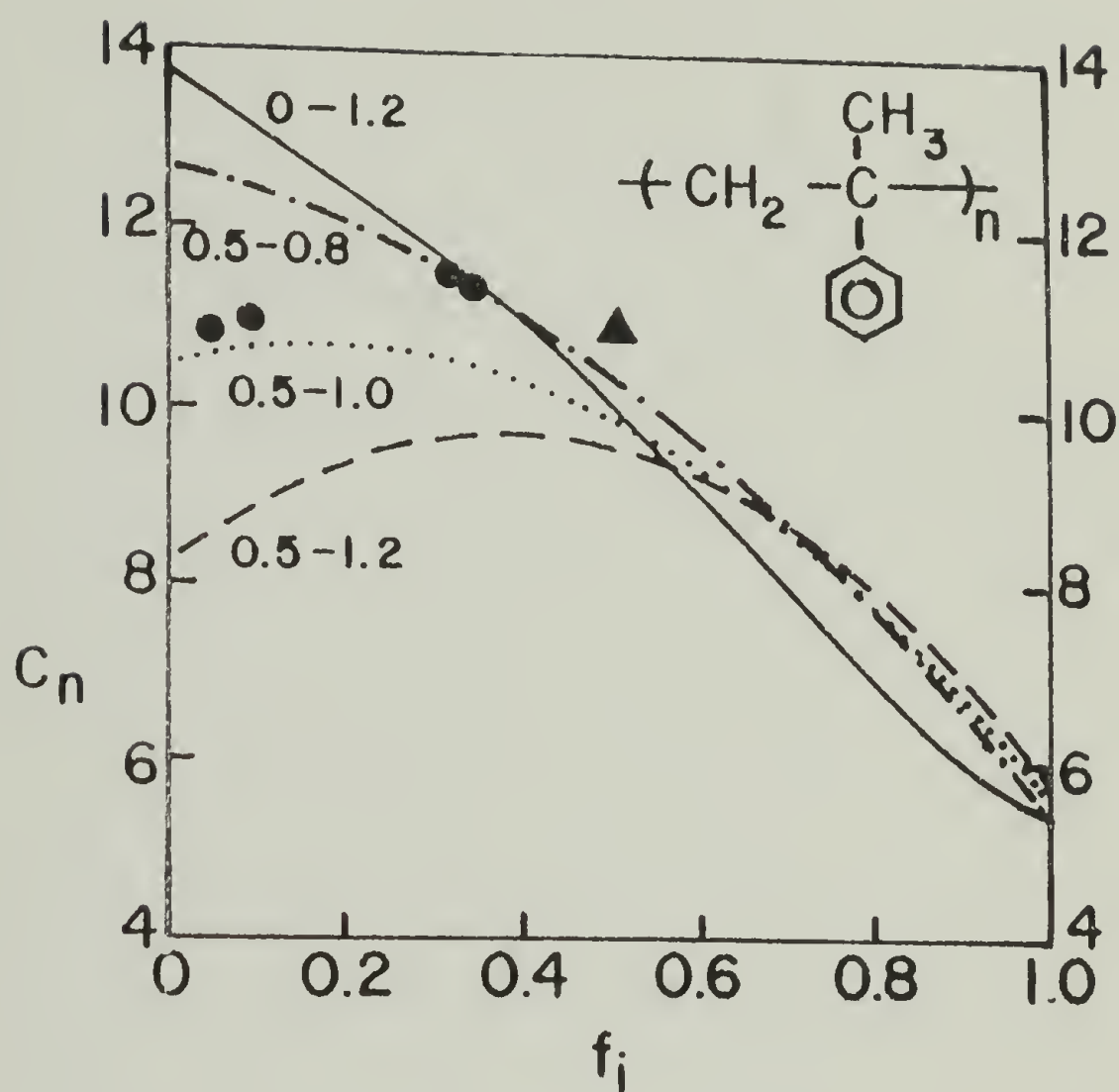


Figure 1.10. The characteristic ratios for Monte Carlo chains of 200 units each as a function of f_i , the fraction of meso dyads in the chain. The values of E_α and E_β in that order, in Kcal. mol.⁻¹, are marked on the curves. The experimental values of Cowie and Bywater⁽⁸¹⁾ (●), and Noda et al. (80) (▲) are shown. From Ref. 67.

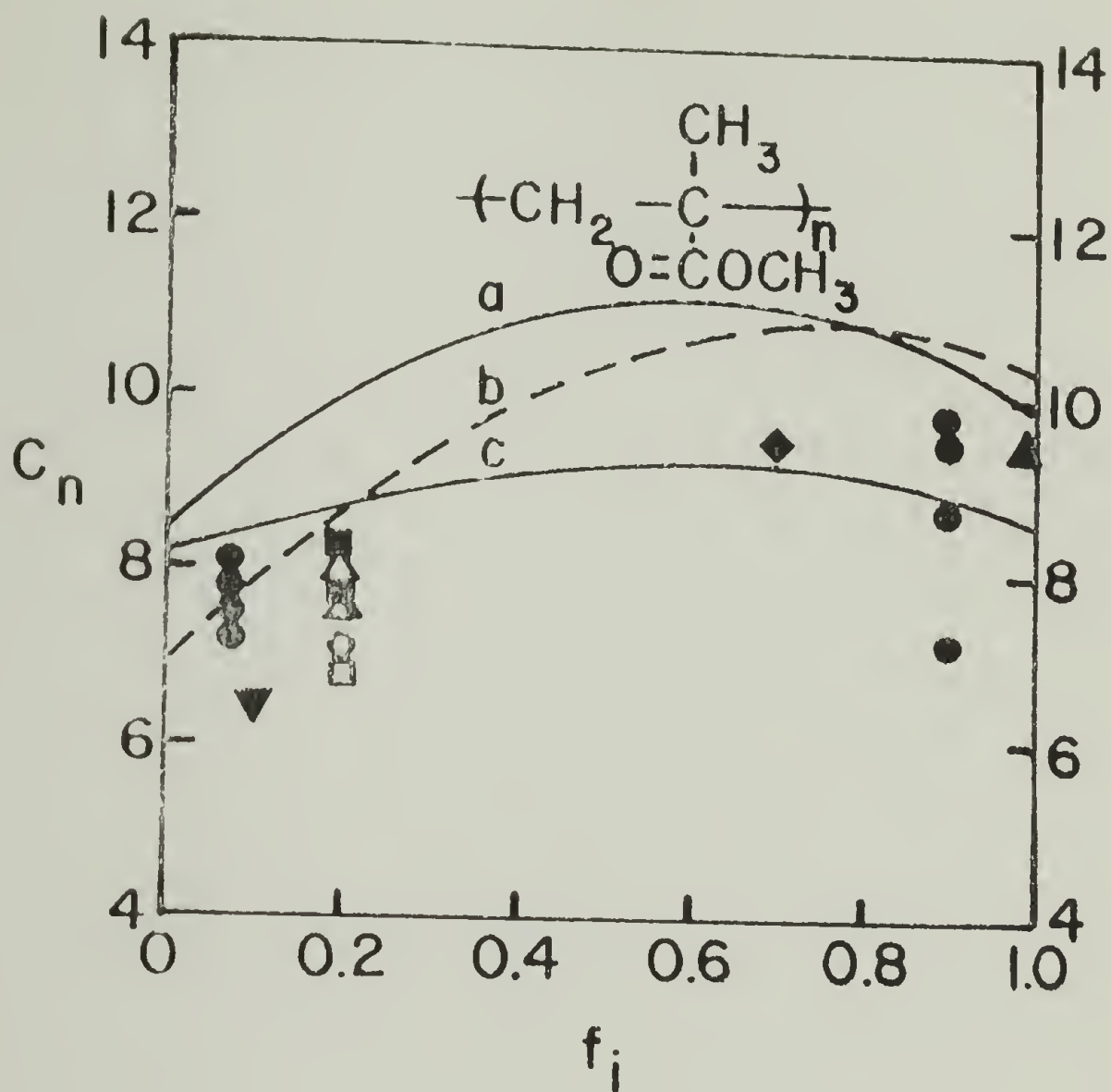


Figure 1.11. The characteristic ratios for Monte Carlo chains of 200 units each as a function of F_i , the fraction of meso dyads in the chain. Curves are shown for (a) $E_\alpha = 1.0$, $E_\beta = -0.6$, and $\theta = 58^\circ$; (b) $E_\alpha = 1.2$, $E_\beta = -0.6$, and $\theta' = 58^\circ$; (c) $E_\alpha = 1.2$, $E_\beta = -0.2$, and $\theta' = 56^\circ$, energies being Kcal. mol.⁻¹. The experimental results of various authors are represented by points as follows: Katime et al. (\blacktriangle) (75), Katime and Roig (\blacktriangledown) (74), Sakurada et al. (\bullet) (70), Fox (\blacksquare) (68), Drause and Cohn-Ginsburg (\blacklozenge) (76), Chinae and Valles (\triangle) (89), Vasudevan and Santappa (\square) (69). From Ref. 44.

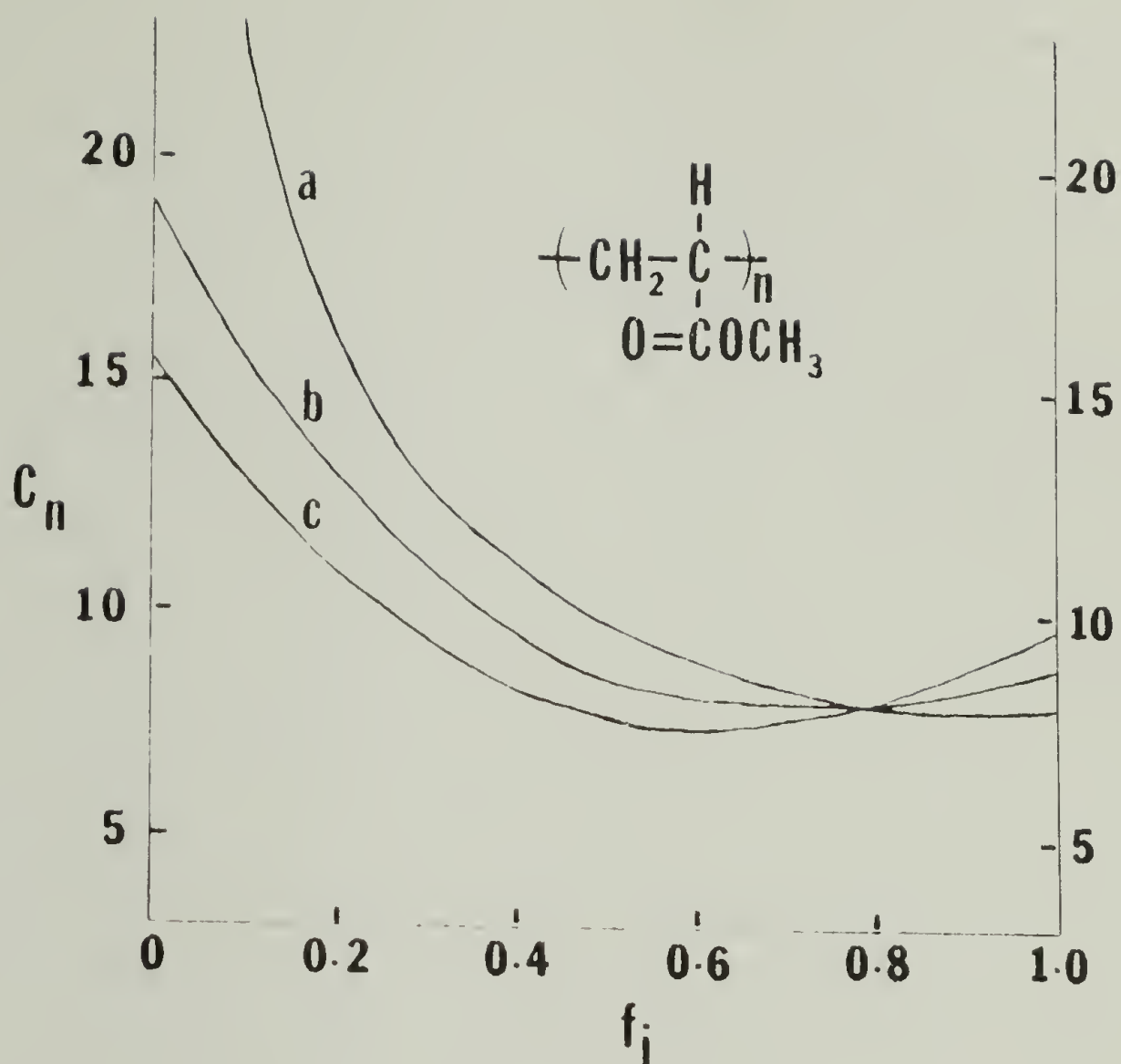


Figure 1.12. The characteristic ratios for Monte Carlo chains of 200 units each, plotted as a function of f_i , the fraction of meso dyads. Curve (a) $E = -0.5$; curve (b) $E = -0.3$; and curve (c) $E = -0.1$. $E_w = 2.8$; $E_{w,i} = 2.2$; $E_{w''i} = 1.6$; $E_{w''d} = 1.0$; $E_p = 0.3$; $T = 300$ K. All energies are in kcal mol⁻¹. The experimental values for atactic PMA given in Table 8 are estimated to correspond to 49-56% isotactic dyads, as estimated from the work of Matsuzaki et al. (94).

methods to generate chains of 200 units with random sequencing of meso and racemic dyads. The plots consist of C_n , the characteristic ratio for a chain of length n , versus f_i , the fraction of meso dyads. Where experimental data are available, the results are also shown on the appropriate plot. It is obvious however that the data available for polymers of known stereoregularity is insufficient to offer a sensitive test of these theoretical results. However, one interesting feature, as pointed out by Flory et al.⁽⁴⁴⁾, is the fact that for all vinyl polymers ($-\text{CH}_2 - \text{CHR}-$), the theoretical curve has a convex shape, whereas for all vinylidene polymers ($-\text{CH}_2 - \text{CR}_1\text{R}_2-$), where $\text{R}_1 \neq \text{R}_2$, the theoretical curve has a concave shape. This indicates that for the vinylidene polymers a few percent stereoirregularity results in an extension of the chain, whereas for the less sterically hindered vinyl chain a few percent stereoirregularity results in a decrease in the dimensions.

Discussion

Much has been learned from both theoretical and experimental studies of the conformations of polymer chains. It is obvious however that one cannot advance without the other. That is, good sound theoretical studies depend entirely on good experimental studies, and vice versa. In the case of the effect of stereoregularity on the unperturbed dimensions, it is obvious that considerable experimental work is needed in order to substantiate the theoretical results. However, advancements in both synthesis and characterization should result in a considerable improvement in our understanding in this area.

REFERENCES

1. G. Natta, J. Polym. Sci., 16, 143 (1955).
2. F. Danusso and G. Moraglio, J. Polym. Sci., 24, 161 (1957).
3. G. Natta, F. Danusso, and G. Moraglio, Makromol. Chem., 20, 37 (1956).
4. F.W. Peaker, J. Polym. Sci., 22, 25 (1956).
5. L. Trossarelli, E. Campi and G. Saini, J. Polym. Sci., 35, 205 (1959).
6. F. Ang, J. Polym. Sci., 25, 126 (1957).
7. F. Ang and H. Mark, Montash. Chem., 88, 427 (1957).
8. W.R. Krigbaum, D.K. Carpenter and S. Newman, J. Phys. Chem., 62, 1586 (1958).
9. W.R. Krigbaum and D.K. Carpenter, J. Phys. Chem., 59, 1166 (1955).
10. P. Outer, C.I. Carr and B.H. Zimm, J. Chem. Phys., 18, 830 (1950).
11. S.N. Chinai, P.C. Scherer, C.W. Boundurant and D.W. Levi, J. Polym. Sci., 22, 257 (1956).
12. N.T. Notley and P.J.W. Debye, J. Polym. Sci., 17, 99 (1955).
13. F. Danusso and G. Moraglio, Makromol. Chem., 28, 250 (1958).
14. J.B. Kinsinger and R.E. Hughes, J. Phys. Chem., 63, 2002 (1959).
15. P. Parrini, F. Sebastiano and G. Messina, Makromol. Chem., 38, 27 (1960).
16. H. Inagaki, T. Miyamota and S. Ohta, J. Phys. Chem., 70, 3420 (1966).
17. J.B. Kinsinger and R.E. Hughes, J. Phys. Chem., 67, 1922 (1963).
18. R. Chiang, J. Polym. Sci., 28, 235 (1958).
19. W.R. Krigbaum and J.D. Woods, J. Polym. Sci., A-2, 2, 3075 (1964).
20. S. Krause and E. Cohn-Ginsberg, Polymer, 3, 365 (1962).

21. S.H. Chinai and R.A. Guzzi, J. Polym. Sci., 21, 417 (1956).
22. S.N. Chinai, J.D. Matlock, A.L. Resnick and R.J. Samuels, J. Polym. Sci., 17, 391 (1955).
23. V.M. Tsvetkov, V.S. Skazka and N.M. Krinoruchko, Vysokomol. Soedin., 2, 1045 (1960).
24. R.A. Wessling, J.E. Mark and R.E. Hughes, J. Phys. Chem., 70, 1903 (1966).
25. J.E. Mark, R.A. Wessling and R.E. Hughes, J. Phys. Chem., 70, 1895 (1966).
26. W.R. Krigbaum, J.E. Kurz and P. Smith, J. Phys. Chem., 65, 1984 (1961).
27. P.J. Flory, Principles of Polymer Chemistry, Cornell Univ. Press (1975).
28. B. Zimm, J. Chem. Phys., 16, 1093 (1948).
29. S.N. Chinai and C.W. Bondurant, Jr., J. Polym. Sci., 22, 555 (1956).
30. T. Kato, K. Miyaso, I. Noda, T. Fujimoto and M. Nagasawa, Macromolecules, 3, 777 (1970).
- 30a. H. Matsuda, K. Yamano and H. Inagaki, J. Polym. Sci., A-2, 7, 609 (1969).
31. P.J. Flory and T.G. Fox, J. Amer. Chem. Soc., 73, 1904 (1951).
32. J.M.G. Cowie, J. Polym. Sci., C, 23, 267 (1968).
33. O.B. Ptitsyn and Y.Y. Eisner, J. Phys. Chem., U.S.S.R., 32, 2464 (1958).
34. M. Kurata and W.H. Stockmayer, Fortschr. Hochpolym. Forsch., 3, 196 (1963).
- 34a. W. Burchard, Makromol. Chemie, 50, 20 (1961).
35. T. Tsuruta and K.F. O'Driscoll, Structure and Mechanism in Vinyl Polymerization, Marcel Dekker, Inc., New York (1969).
36. T.A. Orofino and J.W. Mickey, Jr., J. Chem. Phys., 38, 2512 (1963).
37. A. Dondos and H. Benoit, Macromol., 4, 279 (1971).

38. G. Moraglio and G. Gianotti, *Europ. Polym. J.*, 5, 781 (1969).
- 38a. A. Bazuaye and M.B. Huglin, *Polymer*, 20, 44 (1979).
39. S. Lifson and I. Oppenheim, *J. Chem. Phys.*, 33, 109 (1960).
40. T.W. Bates and K.J. Ivin, *Polymer*, 8, 263 (1967).
41. K.J. Ivin, H.A. Ende and G. Meyerhoff, *Polymer*, 3, 129 (1962).
42. P.J. Flory, V. Crescenzi and J.E. Mark, *J. Amer. Soc.*, 86, 146 (1964).
43. U. Bianchi, *J. Polym. Sci., A*, 2, 3083 (1964).
44. P.R. Sundararajan and P.J. Flory, *J. Amer. Chem. Soc.*, 96, 5025 (1974).
45. D. Lath and M. Bohdanecky, *J. Polym. Sci., P.L.*, 15, 559 (1977).
46. P.J. Flory, C.A.J. Hoeve and A. Ciferri, *J. Polym. Sci.*, 34, 337 (1959).
47. A. Ciferri, *J. Polym. Sci., A*, 2, 3089 (1964).
48. J.M.G. Cowie, *Polymer*, 7, 487 (1966).
49. T.V.R. Roa and K.N. Swamy, *Z. Phys. Chemie*, 257, 17 (1976).
50. P.J. Flory, *J. Chem. Phys.*, 17, 303 (1949).
51. W.H. Stockmayer and M.J. Fixman, *J. Polym. Sci., C*, 1, 137 (1963).
52. G.C. Berry, *J. Chem. Phys.*, 46, 1338 (1967).
53. H. Yamakawa and G. Tanaka, *J. Chem. Phys.*, 47, 3991 (1967).
54. Z. Alexandrowicz, *J. Polym. Sci., C*, 23, 301 (1968).
55. T. Norisuye, K. Kawahara, A. Teramoto and H. Fujita, *J. Chem. Phys.*, 49, 4330 (1968).
56. T.A. Orofino and P.J. Flory, *J. Chem. Phys.*, 26, 1067 (1957).
57. F.C. Lin, S.S. Stivala and J.A. Biesenberger, *J. Appl. Polym. Sci.*, 17, 3465 (1973).
58. I.A. Katime Amashta and G. Sanchez, *Eur. Polym. J.*, 11, 223 (1975).
59. N. Hadjichristidis, M. Devaleriola and V. Desreux, *Eur. Polym. J.*, 8, 1193 (1972).

60. P.J. Flory, Statistical Mechanics of Chain Molecules, Interscience (1969).
61. P.J. Flory, P.R. Sundararajan and L.C. DeBolt, J. Amer. Chem. Soc., 96, 5015 (1974).
62. D.Y. Yoon, V.W. Suter, P.R. Sundararajan and P.J. Flory, Macromolecules, 8, 784 (1975).
- 62a. E.A. Ojalvo, E. Saiz, R.M. Masegosa, and I. Hernandez-Fuentes, Macromolecules, 12, 865 (1979).
63. Akihiro Abe, Polym. J., 1, 232 (1970).
64. D.Y. Yoon, P.R. Sundararajan and P.J. Flory, Macromolecules, 8, 776 (1975).
65. U.W. Suter and P.J. Flory, Macromolecules, 8, 765 (1975).
66. U. Biskup and H.J. Cantow, Macromolecules, 5, 546 (1972).
67. P.R. Sundararajan, Macromolecules, 10, 623 (1977).
68. T.G. Fox, Polymer, 3, 111 (1962).
69. P. Vasudevan and M. Santappa, J. Polym. Sci., A-2, 9, 483 (1971).
70. I. Sakurada, A. Nakajima, D. Yoshizaki and K. Nakamae, Kolloid-Zeitschrift A. Polym., 186, 41 (1962).
71. S. Gundiah, R.B. Mohite and S.L. Kapur, Makromol. Chem., 123, 151 (1969).
72. E. Hamori, L.R. Pusinowski, P.G. Sparks, and R.E. Hughes, J. Phys. Chem., 69, 1101 (1965).
73. G.V. Schulz, W. Wunderlich and R. Kriste, Makromol. Chem., 75, 22 (1964).
74. I.W. Katime and A. Roig, Ann. De Quimica, 69, 1217 (1973).
75. I.A. Katime, A. Roig, L.M. Leon and S. Montero, Eur. Polym. J., 13, 59 (1977).
76. S. Krause and E. Cohn-Ginsburg, J. Phys. Chem., 67, 1479 (1963).
77. J. Brandrup and E.H. Immergut, Polymer Handbook, Interscience (1966).
78. W.R. Krigbaum and P.J. Flory, J. Polym. Sci., A, 2, 4533 (1951).

79. T.G. Fox, Jr., and P.J. Flory, J. Phys. Chem., 73, 1915 (1951).
80. I. Noda, K. Mizutani, T. Kato, T. Fujimoto and M. Nagasawa, Macromolecules, 3, 787 (1970).
81. J.M.G. Cowie and S. Bywater, J. Polym. Sci., A-2, 6, 499 (1968).
82. S. Okamura, T. Higashimura and Y. Imanishi, Chem. High Polym., 16, 244 (1959).
83. G. Moraglio, G. Gianotti and F. Danusso, Eur. Polym. J., 3, 251 (1967).
84. K. Satyanarayana Sastry and R.D. Patel, Eur. Polym. J., 5, 79 (1969).
85. F. Heatley, R. Salovey and F.A. Bovey, Macromolecules, 2, 619 (1969).
86. A. Nakajima and A. Saijo, J. Polym. Sci., A-2, 6, 735 (1968).
87. G. Moraglio and J. Brzinski, J. Polym. Sci., B, 2, 1105 (1964).
88. J.E. Mark and P.J. Flory, J. Amer. Chem. Soc., 87, 1423 (1965).
89. S.N. Chinai and R.J. Valles, J. Polym. Sci., 39, 363 (1959).
90. W.R. Moore and R.F. Fort, J. Polym. Sci., Part A, 1, 929 (1963).
91. G. Moraglio, G. Gianotti and U. Bonicelli, Eur. Polym. J., 9, 623 (1973).
92. K. Karunakarn and M. Santappa, J. Polym. Sci., A-2, 6, 713 (1968).
93. A. Takahashi, T. Kawai, and I. Kagawa, Nippon Kagaku Zasshi, 83, 14 (1962).
94. K. Matsuzaki, T. Uryu, A. Ishida, M. Takeuchi, and T. Ohki, J. Polym. Sci., A-1, 5, 2167 (1967).

CHAPTER I I

SYNTHESIS AND CHARACTERIZATION OF STEREOREGULAR POLY (METHYL METHACRYLATE)

Introduction

Discussion of the preparation and characterization of the stereoregular poly (methyl methacrylate) samples used throughout the rest of this dissertation is the purpose of this chapter. Eight different samples of poly (methyl methacrylate) were used in this work. Three of these were obtained commercially, and the remaining samples were synthesized according to the procedures outlined in this chapter.

Characterization of all samples included infrared analysis, and ^{13}C -NMR for tacticity determination; molecular weight analysis by gel permeation chromatography coupled with on-line low angle laser light scattering photometry; and thermal analysis for the effect of tacticity on the glass transition temperature using differential scanning calorimetry.

Preparation of Stereoregular Poly- (Methyl Methacrylate)

The preparation of different stereoregular forms of "vinyl" polymers is a subject which has received considerable attention.⁽¹⁾ Consequently there are often several different methods for producing a

desired stereoregular form of a polymer. In particular, poly (methyl methacrylate) is one polymer which has been studied extensively and numerous synthetic methods have been proposed for obtaining different stereoregular forms.^(1,2,3) Table 2.1 describes briefly the methods used in this work in order to obtain a series of poly (methyl methacrylate) samples of varying degrees of stereoregular perfection. Three of the eight stereoregular PMMA samples listed in Table 2.1 are available commercially. Sample 1 is a syndiotactic polymer available from Polysciences Corporation, Warrington, Pennsylvania. Samples 2 and 3 are conventional "atactic" polymers available from Cellomer Associates, Webster, New York. The remaining five samples were prepared in this laboratory using the procedures described in this chapter.

Monomer preparation. As normally supplied, acrylic esters are inhibited to enhance their storage stability. In the case of the methyl methacrylate monomer used in this work, Aldrich Chemicals Inc., Milwaukee, Wisconsin, 65 ppm of hydroquinine monomethyl ether is incorporated as an inhibitor. The removal of this inhibitor is necessary before polymerization can be carried out and is readily accomplished by alkaline extraction. Since the monomer is inhibited with very small amounts of inhibitor, 65 ppm, three extractions with equal volumes of 10% aqueous sodium hydroxide was usually found satisfactory. In the case of the hydroquinone inhibitor used in MMA, the progress of the extraction is readily followed since the solution of the sodium salt of hydroquinone is intensely colored. Therefore, caustic extractions are simply continued until the aqueous layer is colorless. The monomer is then washed

Table 2.1. Synthesis and Characterization of Stereoregular PMMA

Sample No.	Initiator	Solvent	Temp. (°C.)	NMR (triads)			NMR (dyads)		Ref.
				i	h	s	I	S	
1	*	*	*	5	20	75	15	85	--
2	**	**	**	5	37	58	23	77	--
3	**	**	**	5	37	58	23	77	--
4	Thermal	None	210	15	42	43	36	54	7
5	9-Fluorenyl Lithium	Toluene	-40	76	16	8	83	17	8
6	n-Butyl Lithium	Toluene	30	76	16	8	83	17	2
7	LiAlH ₄	Diethyl Ether	30	90	4	6	92	8	3
8	PhMgBr	Toluene	0	100	0	0	100	0	1

* Syndiotactic PMMA (Polysciences)
 ** Conventional PMMA (Cellomer Assoc.)

with water until the water layer has the pH of normal water. Finally, the monomer is dried over magnesium sulfate and filtered. To insure that the monomer was totally free from moisture it was then stored over calcium hydride, CaH_2 , overnight. Distillation from CaH_2 was then carried out under vacuum, about 20mm, and the pure monomer collected at 40-41°C. The monomer was then used directly in the polymerization and was not stored for any length of time.

Preparation of samples 4, 5, 6, 7, & 8.

Sample 4. It has often been noted ^(2,4) that PMMA prepared by conventional free-radical techniques, at 50-100°C, and generally referred to as "atactic," contains appreciable amounts of syndiotactic sequences. Consequently, there have been several attempts to prepare a truly "atactic" PMMA in which the sequence placement is random. These have included free radical polymerization at elevated temperatures, ^(2,5) esterification of cyclopolymerized poly(methacrylic anhydride), ⁽⁶⁾ and anionic polymerization in solvating media with initiators less effective in producing stereoregular PMMA. ⁽⁷⁾ The method used in this work involves free-radical polymerization initiated thermally at high temperatures. ⁽⁷⁾

Methyl methacrylate of high purity (see section on monomer) was deaerated by successively freezing and thawing. The MMA monomer was then polymerized thermally in evacuated sealed ampoules in a constant temperature silicone bath at 210°C for 4 hours. The tube was then cooled rapidly by placing it in an ice bath and then opened and precipitated in

hexane. The precipitate was then washed with methanol to remove monomer and oligomers.

Sample 5. Steric interactions along the PMMA chain result in a preference in stereo placement in the polymer chain. That is, MMA inherently exhibits a preference for syndiotactic placement. This preference is inversely proportional to temperature since at low temperatures the process becomes less random. This is apparent in the room temperature free radical polymerization of MMA which has been shown^(2,4) to yield predominately syndiotactic sequences. In addition, one method often used⁽²⁾ to produce highly syndiotactic PMMA involves photoinitiation at very low temperatures. As a result of the inherent preference for syndiotactic placement, some means of coordination are necessary in order to obtain an increase in the isotactic content.

Several solvent-initiator systems have been proposed for the preparation of isotactic PMMA. A primary difference in these systems concerns the degree of isotactic placement. The system chosen for sample 5 was toluene-9-fluorenyl lithium which is known⁽⁸⁾ to produce a moderately isotactic sample (83% isotactic dyads).

9-fluorenyl lithium. Toluene was refluxed over CaH_2 for four hours and then distilled. Two hundred ml of the dried toluene was added to a three neck flask and nitrogen bubbled through for one hour. Next 8.5 gms. (.051 moles) of fluorene was added followed by 31 ml. (.049 moles) of a 1.6M solution of n-butyllithium in hexane. The reaction mixture was then refluxed for one hour and 9-fluorenyllithium separated as an orange powder. The initiator was then used in subsequent reactions as a slurry in toluene (.245 M).

Polymer preparation. Nitrogen was bubbled through a mixture of 300 ml. dry toluene and 25 ml. purified MMA (.228 moles) for two hours to remove dissolved oxygen. The contents were then cooled to -40°C and 7 ml. of the .245 M suspension of 9-fluorenyllithium in toluene was added. After five minutes the reaction mixture turned to an extremely viscous mass and stirring was continued for one hour. Next the reaction mixture was precipitated into 2500 ml. of methanol. The precipitate was then purified by dissolving in 800 ml. of tetrahydrofuran followed by precipitation in Petroleum Ether (B).

Sample 6. Another solvent-initiator system which is also known to yield moderately isotactic PMMA involves n-butyl lithium in toluene at 25°C .⁽²⁾ The n-butyl lithium was obtained as a 1.6 M solution in hexane from Aldrich Chemicals.

Nitrogen was bubbled through a mixture of 300 ml. of toluene and 30 ml. (.28 moles) of MMA for two hours to remove dissolved oxygen. Then 1.7 ml (.0027 moles) of n-butyl lithium was slowly added to the system. The reaction mixture was then stirred for six hours at room temperature. The polymer was recovered by precipitation into a large volume of methanol and purified by reprecipitation.

Sample 7. It is well known that solvent plays a very important role in stereoregulation. That is, in highly polar media coordination catalysts have been shown^(1,3) to yield syndiotactic polymers whereas in hydrocarbon solvents the same catalyst will yield isotactic polymers. This concept was applied by Tsuruta et al.⁽³⁾ who showed that in hydrocarbon solvents LiAlH_4 produced a 100% isotactic polymer whereas in more polar solvents the degree of isotactic placement was reduced.

We used this same method to obtain sample 7 which contained 92% isotactic dyads.

Lithium aluminum hydride, LiAlH_4 , was used after purification by dissolution, decantation and filtration in diethyl ether. Nitrogen was bubbled through a mixture of 200 ml of diethyl ether (anhydrous) and 30 ml (.28 moles) of MMA for two hours to remove dissolved oxygen. Then 1 mole % LiAlH_4 was added and the reaction mixture stirred for six hours. The reaction was quenched by adding a small amount of methanol-hydrochloric and to the reaction mixture. The polymer was then recovered by precipitation into a large volume of methanol and purified by subsequent dissolution and reprecipitation.

Sample 8. There are several proposed methods^(1,2,3) to obtain a highly isotactic PMMA. One method which is particularly simple involves using a Grignard reagent, PhMgBr , in toluene at 0°C . This method has been shown^(1,2,9,10,11) to yield 100% isotactic polymer with no measurable syndiotactic sequences.

Nitrogen was bubbled through 300 ml of toluene for three hours. The flask was then cooled to 0°C . and 2 ml of 2.9 M (.0058 moles) PhMgBr was added with stirring. Next 15 ml (.15 moles) of MMA was added dropwise from an addition funnel. The reaction mixture turned a milky yellow and was mixed for a total of four hours at 0°C . The contents were then poured into three liters of petroleum ether (B) and the precipitate collected by filtration.

Analysis of the product by gel permeation chromatography revealed a polymer with a trimodal distribution. It is believed that the trimodal distribution was a result of the fact that both homogeneous and

heterogeneous initiation occurred as well as the production of cyclic oligomers. The polymer was therefore fractionated by precipitation methods.

Stereoregularity Determination

Carbon-13 nuclear magnetic resonance spectroscopy. Carbon-13 NMR is a particularly useful tool in the study of stereoregular structures of polymers. Interpretation of chain tacticity is based on the original work of Bovey and Tiers⁽²⁾. The three possible steric configurations of PMMA are shown in Figure 2.1 where R is the group $-\text{COOCH}_3$. Three consecutive monomer units in a chain are considered to define a configuration called a triad. In the structures shown, the α -methyl carbon will absorb radiation at a certain frequency, however, this frequency will be different for each of the three kinds of triad because the environment of the α -methyl group in each is different. For PMMA, we observe resonances at $\rho = 22.06, 19.01$ and 16.55 ppm, which were assigned to the isotactic, heterotactic, and syndiotactic triads respectively. Figure 2.2 shows ^{13}C -NMR results for the α -methyl resonance of PMMA for six different stereoregular forms. The differences between the samples is immediately obvious from the intensity of the three resonances. The values reported on the right in Figure 2.2 are dyad tacticities, that is, the percent of isotactic dyads, I, in the chain where:

$$I = i + 1/2 h$$

and i is the fraction of isotactic triads and h , is the fraction of heterotactic triads. We also may then define the fraction of

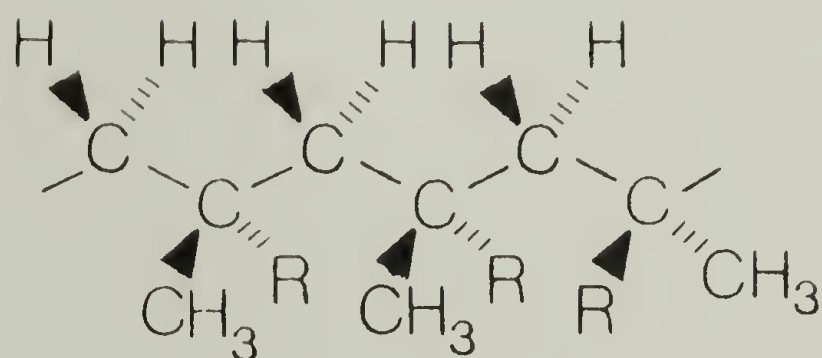
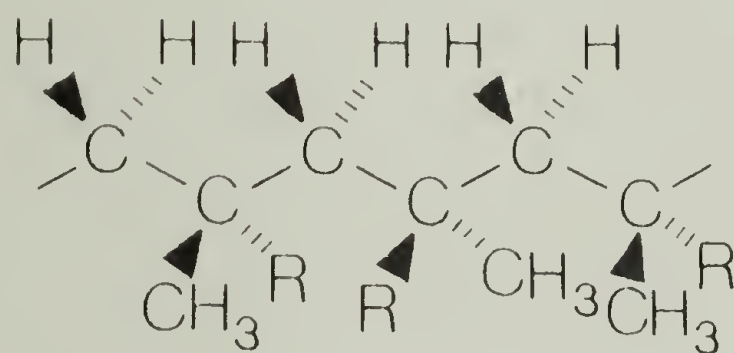
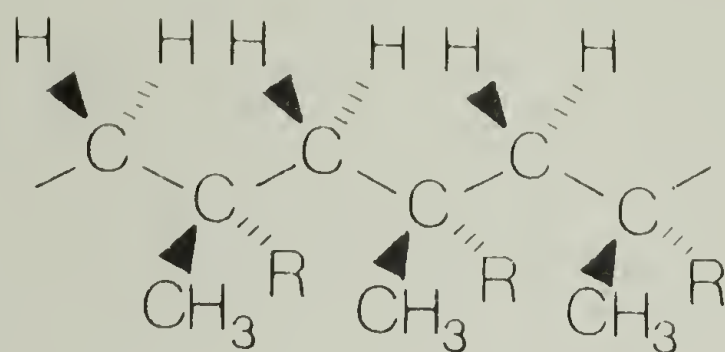


Figure 2.1. Stereoregular triads for poly(methyl methacrylate) where $R = -COOCH_3$.

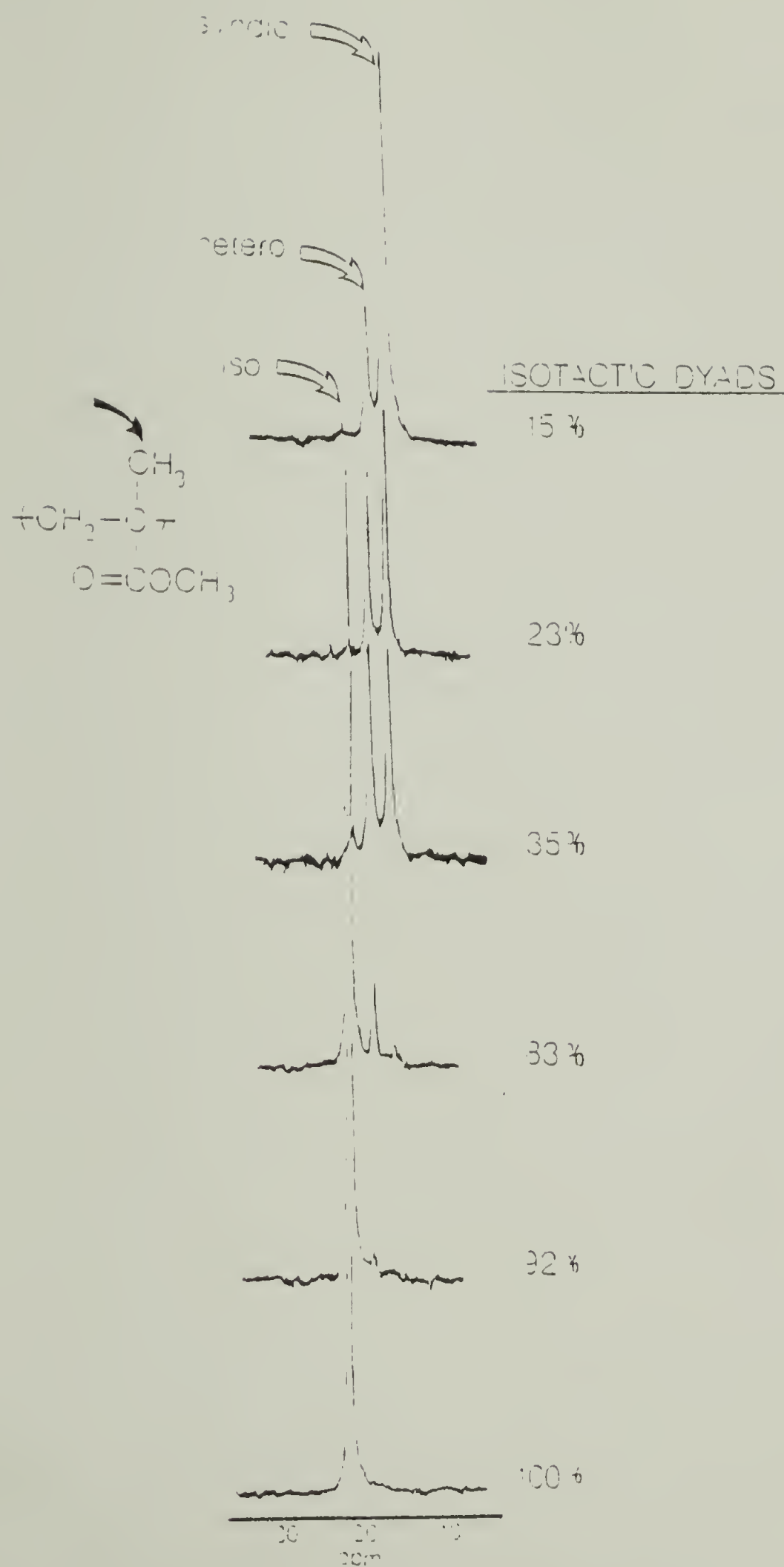


Figure 2.2. ^{13}C -NMR analysis of stereoregular poly(methyl methacrylate).

syndiotactic dyads as:

$$S = s + 1/2 h$$

Spectra were obtained on 25% (w/v) solutions of polymers in deuteriochloroform, 2 ml of solution being placed in 8 mm tubes. A Varian CFT-20 spectrograph was employed fitted with a ^{13}C probe. Tetramethylsilane was used as an internal reference.

Infrared analysis. In addition to NMR, infrared spectroscopy is also a useful method for characterizing the degree of stereoregular perfection. Years before NMR was used on a routine basis tacticity measurements were performed using J values as measures of tacticity. Basically a J value between 25 and 30 indicated an isotactic sample and a value between 110 and 115 indicated a syndiotactic polymer. Unfortunately IR has never been able to give the quantitative assignments of tacticity available from NMR.

The infrared spectra of the different stereoregular forms of PMMA are similar, but the differences are significant and are related to the differences in stereoregularity. Two frequencies which have been used to determine tacticity are the bands at 1063 cm^{-1} and 1377 cm^{-1} (12, 13). Figure 2.3 shows the IR absorbance spectra of two different stereoregular forms of PMMA. The ratio of the absorbance of the two peak as a function of tacticity is shown in Figure 2.4 (Table 3.2), where the exact tacticities were determined by ^{13}C -NMR as described in the previous section. The absorbance was determined by drawing a baseline from the minimum on either side of the peak in question, and measuring the vertical distance from the peak maximum. Having determined the

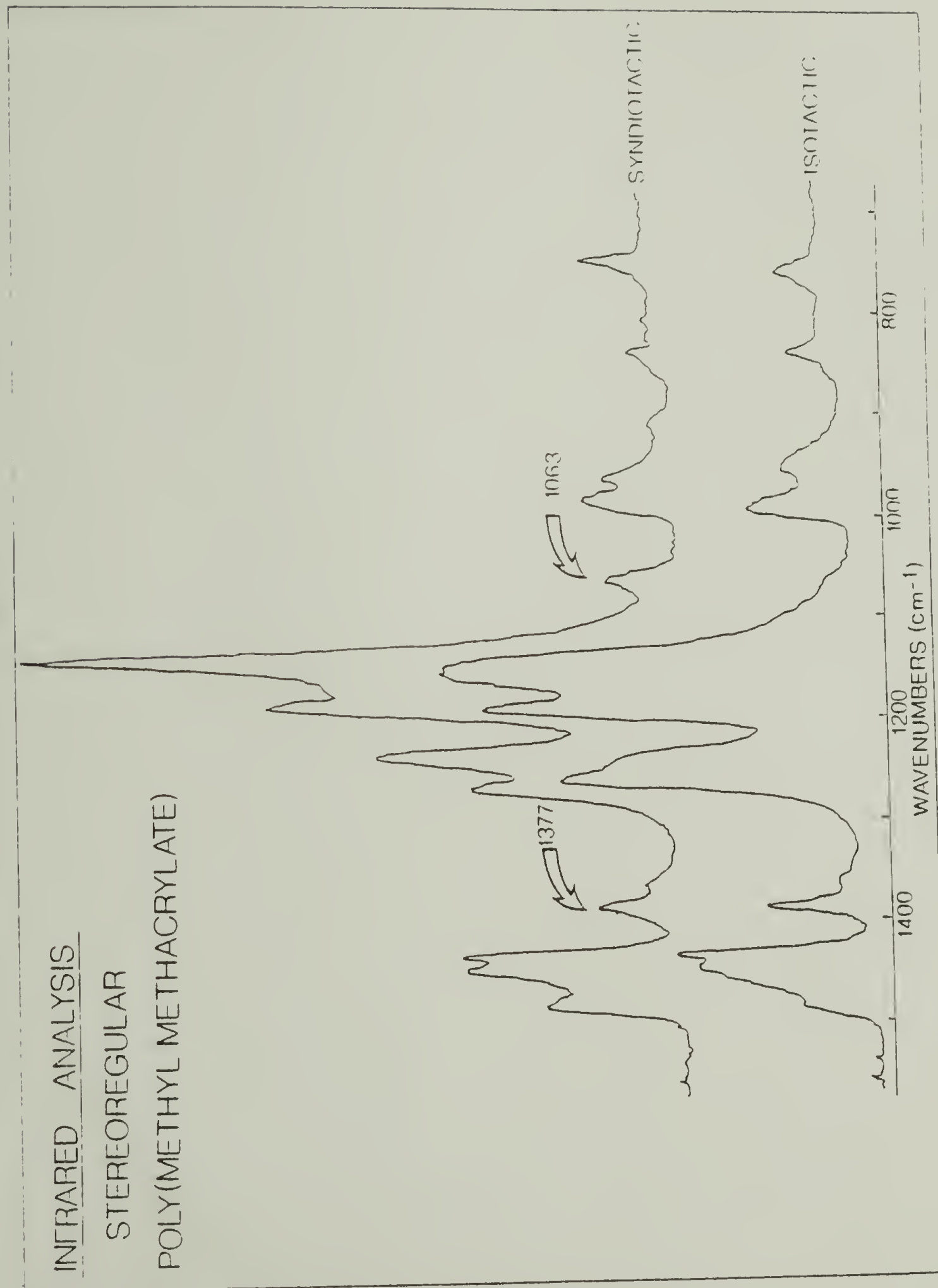


Figure 2.3. Infrared absorbance spectra for stereoregular PMMA.

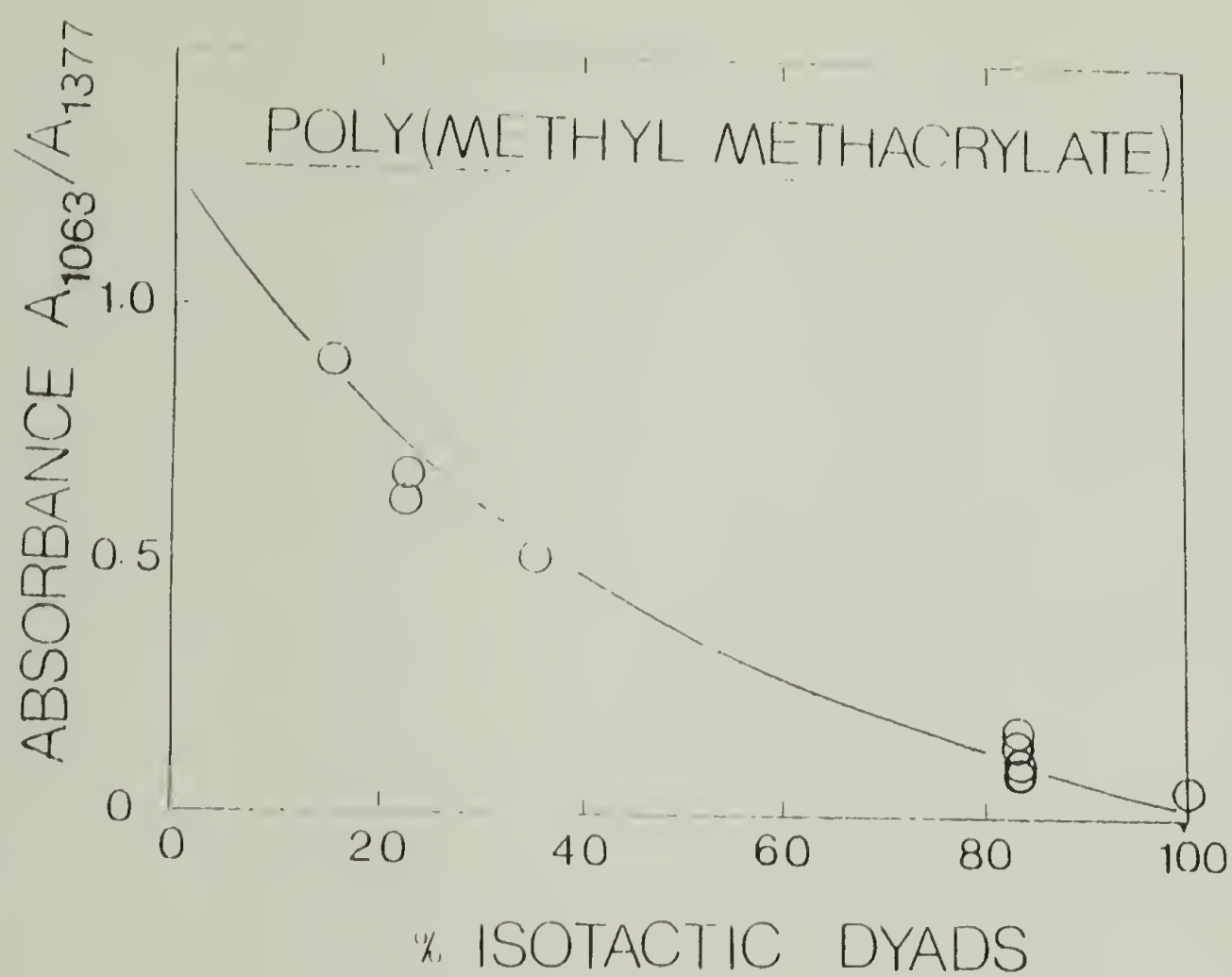


Figure 2.4. Infrared absorbance as a function of stereoregular composition.

Table 2.2. Infrared Analysis of Stereoregular PMMA.

Sample No.	Dyad Tacticity		A_{1063}/A_{1377}	J_1	J_2	J	MW
	I	S					
8b	100	0	.05	40.8	15.4	28.0	7.0×10^5
5a	83	17	.14	53.3	29.4	41.3	4.2×10^4
6b	83	17	.13	45.8	39.0	42.4	5.4×10^4
6a	83	17	.17	53.0	40.3	40.3	2.7×10^4
5b	83	17	.12	63.2	25.5	44.4	3.2×10^5
4a	35	65	.50	110.7	88.5	94.6	1.8×10^5
2	23	77	.62	134.4	94.4	114.4	1.1×10^5
3	23	77	.67	133.6	96.5	115.1	3.5×10^5
1	15	85	.89	137.2	97.8	117.5	3.2×10^5

relation between the absorbances and tacticity, the tacticity can then be determined simply by IR analysis and the calibration curve, Figure 2.4.

An alternate method using an empirical parameter called a J value has also been used as described earlier. The J value is simply the arithmetic average of the parameters J_1 and J_2 which in turn are defined as:

$$J_1 = [179 (A_{1075}/A_{990})] + 27$$

$$J_2 = [81.4 (A_{1481}/A_{1389})] - 43$$

The J value as a function of tacticity is shown in Figure 2.5 (Table 2.2), where the exact tacticities again were determined by ^{13}C -NMR as described in the previous section.

It should be noted that in the sample numbers used in Table 2.2, i.e., 6a, 6b and 8a, 8b, etc., the number, in this case 6 or 8, refers to the sample described in Table 2.1 and therefore describes the method of synthesis and the tacticity. The subscript a or b refers to a different fraction which will differ only in molecular weight and not in tacticity. The last column in Table 2.2 shows the exact molecular weight as determined by GPC/LALLS.

Thermal Analysis

Since the development of techniques for the synthesis of stereoregular vinyl polymers, there has been interest in studying the effect of stereoregularity on the physical properties of these polymers. It was first noted by Shetter⁽¹⁴⁾ that the glass transition temperature, T_g , was dependent on the tactic content for PMMA. Later, Karasz and

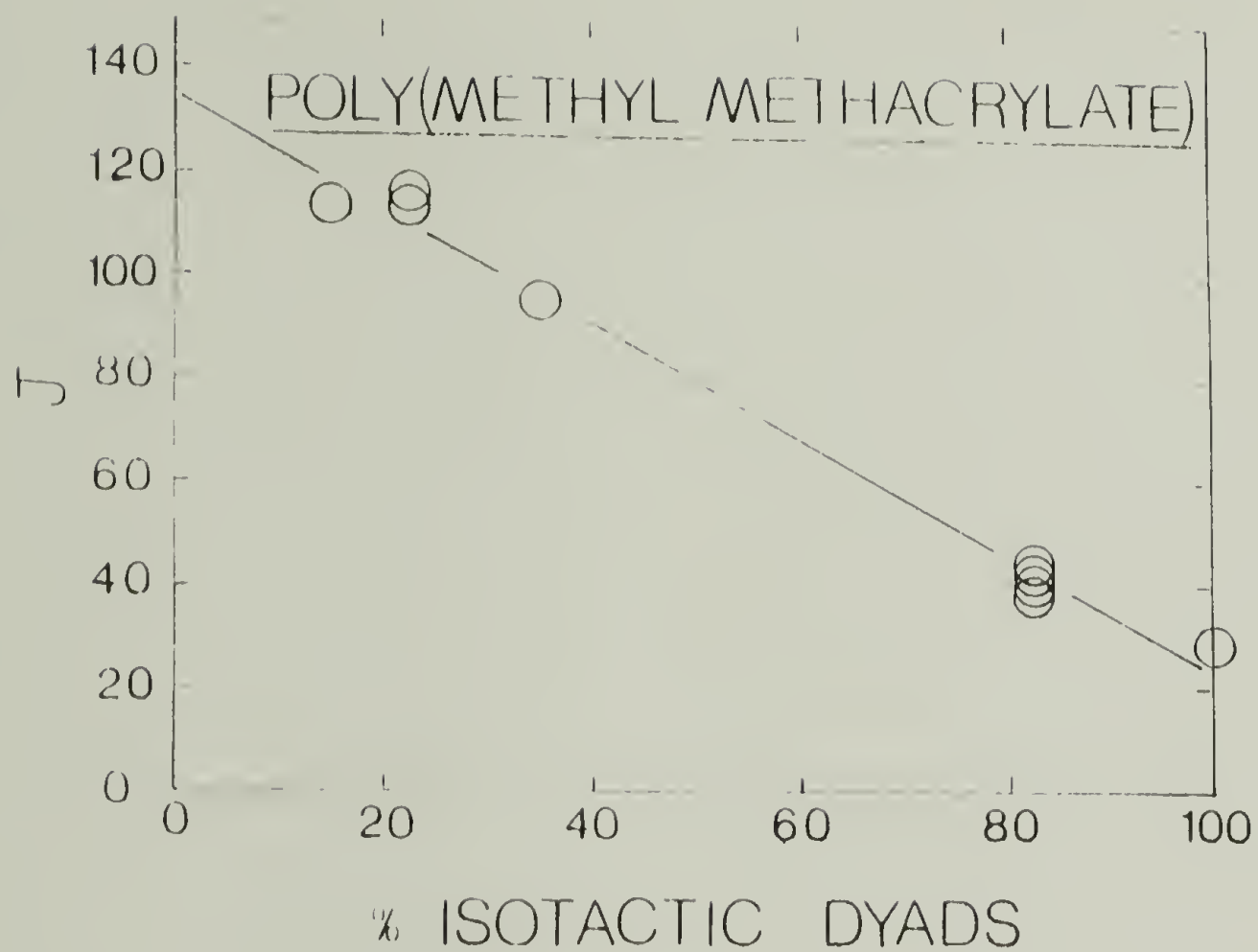


Figure 2.5. Infrared determination of tacticity using the J value.

MacKnight⁽¹⁵⁾ showed that this was a general trend for vinyl polymers of the type $(-\text{CH}_2\text{CXY}-)_n$ where neither X or Y is hydrogen. This is in sharp contrast to monosubstituted vinyl polymers where either X or Y is hydrogen, and tacticity has essentially no effect of T_g .

In light of this, measurements were made on the T_g of all polymers used in this dissertation. Figure 2.6 shows a plot of T_g versus the percent isotactic dyads in the chain as measured by ^{13}C -NMR. The solid circles represent the midpoint of the transition and the brackets on either side represent the beginning and end of the transition. It is immediately obvious that the highly isotactic samples have narrower transitions than the syndiotactic polymers indicating a higher degree of stereoregular perfection.

All measurements were made using a Perkin-Elmer DSC-2. The heating rate was $20^\circ\text{C}/\text{ml}$ for all samples. 10-20 mg samples were used in each case.

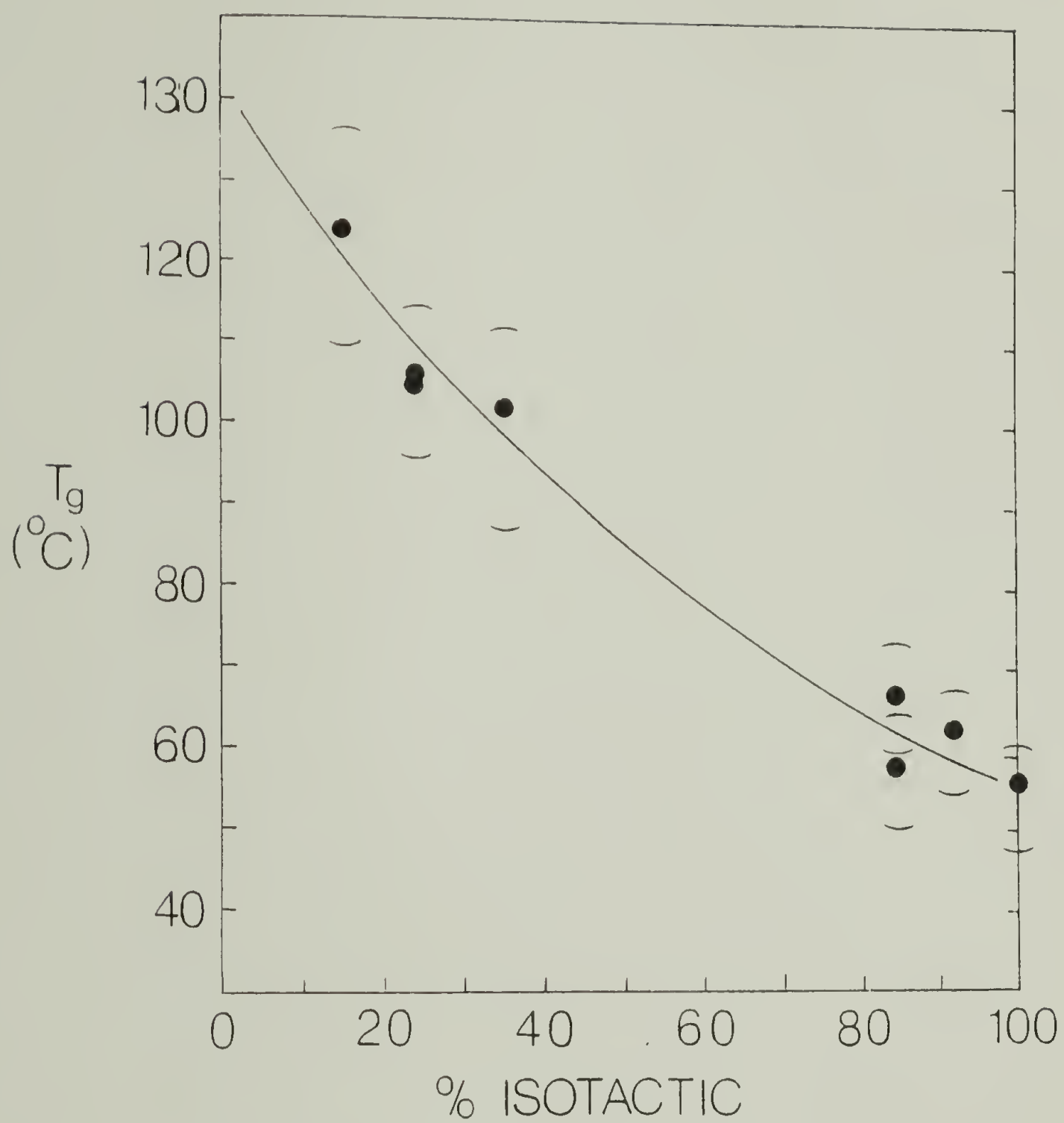


Figure 2.6. The effect of tacticity on the glass transition temperature.

REFERENCES

1. Polymer Synthesis, Vol. I, S.R. Sandler, and W. Kara, Academic Press, New York (1974).
2. F.A. Bovey, and G.V.D. Tiers, J. Polym. Sci., 44, 173 (1960).
3. T. Tsuruta, T. Makimoto, and Y. Nakayama, Makrom. Chem. 90, 12 (1966).
4. T.G. Fox, W.E. Goode, S. Gratch, C.M. Huggett, J.F. Kincaid, A. Spell, and J.D. Stroupe, J. Polym. Sci., 31, 173 (1958).
5. F.A. Bovey, J. Polym. Sci., 46, 59 (1960).
6. G.V.D. Tiers, and F.A. Bovey, J. Polym. Sci., 47, 479 (1960).
7. R.F. Graham, D.L. Dunkelberger, J.R. Panchak, J. Polym. Sci., 59, 543 (1962).
8. W.E. Goode, F.H. Owens, R.P. Fellman, W.H. Snyder, and J.E. Moore, J. Polym. Sci., 46, 317 (1960).
9. I. Katime, A. Roig, L.M. Leon, S. Montero, Eur. Polym. Journal, 13, 59 (1977).
10. S. Bywater, P.M. Toporowski, Polymer, 13, 94 (1972).
11. R. Iwamoto, K. Ohta, and S. Mima, J. Polym. Sci., PL, 17, 441 (1979).
12. A.H. Nishioka, H. Watanabe, K. Abe, and Y. Sono, J. Polym. Sci., 48, 241 (1960).
13. U. Baumann, H. Schreiber, and K. Tessmar, Makromol. Chem., 36, 81 (1960).
14. J.A. Shetter, J. Polym. Sci., PL, 1, 209 (1963).
15. F.E. Karasz, W.J. MacKnight, Macromolecules, 1, 537 (1968).

CHAPTER III

MEASUREMENT OF THE SPECIFIC REFRACTIVE INDEX INCREMENT

Introduction

The specific refractive index increment of a polymer in a given solvent and at a particular temperature is a parameter which must be known in order to measure the molecular weight by light scattering methods. Equation 3.1 shows the relation used to calculate molecular weight from light scattering measurements.

$$\frac{Kc}{R_{\theta}} = \frac{1}{M_w} + 2A_2c \quad (3.1)$$

Here c is the concentration, A_2 is the second virial coefficient, R_{θ} is the Rayleigh ratio, M_w is the weight average molecular weight and K is the optical constant which includes the specific refractive index increment.

$$K = (2\pi n^2/\lambda^4 N)(dn/dc)^2(1+\cos^2\theta) \quad (3.2)$$

where, n is the refractive index of the solvent, λ is the wavelength of the light, N is Avogadro's number, θ is the angle of measurement and dn/dc is the specific refractive index increment.

The purpose of this chapter is to present measurements of dn/dc for the polymers used throughout this dissertation. This includes measurements on three different polymers; polystyrene, PS, poly-(methyl methacrylate), PMMA, and poly(vinyl acetate), PVAc. In the

section on PS the effect of molecular weight on dn/dc is assessed. For PMMA we include a study concerning the effect of tacticity on dn/dc , and for PVAc we investigate the effect of branching on dn/dc .

Background

The determination of the differential refractive index is accomplished by measuring the deviation of a light beam passing through a divided cell composed of adjacent solvent and solution compartments. The beam deviation is proportional to the difference in refractive index, Δn , between the solvent and the solution. To calculate Δn , the beam deviation is multiplied by a calibration constant. The calibration constant is determined from measurements of standardized solutions of known solute concentration for which Δn values are known (see next section on Calibration).

The quantity required for light scattering molecular weight determinations is the differential change of solution refractive index with solute concentration, c , at infinite dilution, $\{dn/dc\}_{c=0}$. The dn/dc of a sample is the result of determining Δn for a series of solutions of different concentrations and then plotting $\Delta n/c$ versus c . Extrapolation to $c=0$ yields the value of dn/dc to be used for the calculation of molecular weight.

Calibration

To permit calculation of the change in refractive index from the angular deviation measured, the KMX-16 must be calibrated. This was carried out using aqueous solutions of sodium chloride at 25°C,

since Kruis⁽¹⁾ has previously measured the refractive indices for this system at a number of wavelengths. The data of Kruis was used by the manufacturer, Chromatix, Sunnyvale, California, extrapolated to 633 nm and rearranged to yield Equation 3.3 from which Δn can be obtained from knowledge of the concentration, c , where c is in units of gms NaCl/100 gms H_2O ,

$$\Delta n = [1740 + (1.63c - 30.85)c]c \quad (3.3)$$

and Δn is given in units of 10^{-6} R.I.

The calibration constant, K , for the instrument is found by dividing the Δn value for a given NaCl concentration by the deviation, Δx , measured for that concentration. The K values obtained for the

$$K = \Delta n / \Delta x \quad (3.4)$$

different NaCl concentrations were the averaged. Table 3.1 shows the data obtained for eight different concentrations of NaCl ranging from .4 to 2 gms/100 ml H_2O . The average value obtained was 1.3787×10^{-7} .

Specific Refractive Index Increments for Polystyrene as a Function of Molecular Weight

The specific refractive index increment, like many properties of polymers, is expected to reach an asymptotic limit at a certain molecular weight. Before work could be performed with certainty on PMMA and PVAc it was necessary to first determine at what molecular weight dn/dc reached its limiting value. Polystyrene was chosen for this study since it is available in well characterized samples for a

Table 3.1. Calibration of KMX-16 Using Sodium Chloride

Concentration (gms/100gms H ₂ O)	Difference (L-R) _c	Δn ($\times 10^6$)	Δx	\bar{K} ($\times 10^7$)
0.42992	5716.3	742.49	5296.5	1.4018
0.69156	9004.2	1189.09	8584.4	1.3852
1.03762	13232.7	1774.06	12812.9	1.3846
1.43662	18159.8	2440.88	17740.0	1.3759
1.55643	19823.0	2639.60	19403.2	1.3604
1.66019	20940.2	2811.16	20520.4	1.3699
1.69476	21221.3	2868.21	20801.0	1.3789
2.07524	25868.1	3492.63	25448.3	1.3724

$$\Delta x = (L-R)_{\bar{c}} - (L-R)_0$$

$$\Delta n = [1740.0 + (1.63c - 30.85)c]c$$

$$\bar{K} = 1.3787 \times 10^{-7}$$

wide range of molecular weights.

All measurements were made using the Chromatix KMX-16 laser differential refractometer, using Tetrahydrofuran, Fisher Certified, at a temperature of 25°C. Sample concentration ranged from 2 to 5 gms/liter. All samples were narrow distribution PS samples available from Pressure Chemical Co.

Table 3.2 lists the data obtained on eight PS samples ranging in molecular weight from 6.0×10^2 to 1.8×10^6 . Each value for dn/dc given in column 3 is an average of ten measurements at the particular concentration. Figure 3.1 shows the same data plotted as dn/dc versus concentration. It is immediately obvious that dn/dc is independent of concentration in the range of interest. As a result, we chose to use the arithmetic average rather than extrapolate to $c=0$. Column 4, in Table 3.2 lists the average values obtained for the eight PS samples. These average values are shown plotted as dn/dc versus $\log MW$ in Figure 3.2. It is obvious that dn/dc reaches its limiting value at a molecular weight of approximately 2.0×10^4 . Figure 3.3 shows the same data plotted as dn/dc versus the reciprocal of molecular weight. The linear dependence (Figure 3.3) expected for any relation which reaches a limiting value (Figure 3.2) is obtained.

Specific Refractive Index Increments for Stereoregular Poly(Methyl Methacrylate)

In this section the results of dn/dc measurements for the stereoregular PMMA samples listed in Table 2.1, Chapter II are discussed. Importantly, we have found a measurable change in dn/dc with tactic

Table 3.2. Specific Refractive Index Increments for Polystyrene

Polystyrene Molecular Weight	Concentration (gms/ml) $\times 10^3$	$\Delta n/c$ (ml/gm)	$\Delta n/c$ (ml/gm) Average
6.0×10^2	2.6560	.1691	.1689
	3.9860	.1691	
	5.3142	.1686	
2.1×10^3	2.1160	.1808	.1799
	2.2250	.1795	
	3.0900	.1798	
	3.6391	.1794	
	3.6480	.1806	
	5.3990	.1790	
1.0×10^4	2.3540	.1832	.1831
	2.5160	.1831	
	3.8490	.1820	
	4.0240	.1839	
	5.2260	.1832	
2.0×10^4	2.5200	.1852	.1845
	3.0720	.1845	
	6.1450	.1845	
1.1×10^5	3.5035	.1848	.1845
	3.7140	.1839	
	7.0070	.1849	
2.33×10^5	2.3100	.1840	.1839
	4.8360	.1838	
	4.8360	.1838	
	5.6670	.1841	
4.98×10^5	3.0120	.1845	.1844
	3.8420	.1845	
	5.5640	.1842	
1.8×10^6	1.6680	.1855	.1848
	2.5500	.1842	
	4.1530	.1848	
	4.9120	.1845	

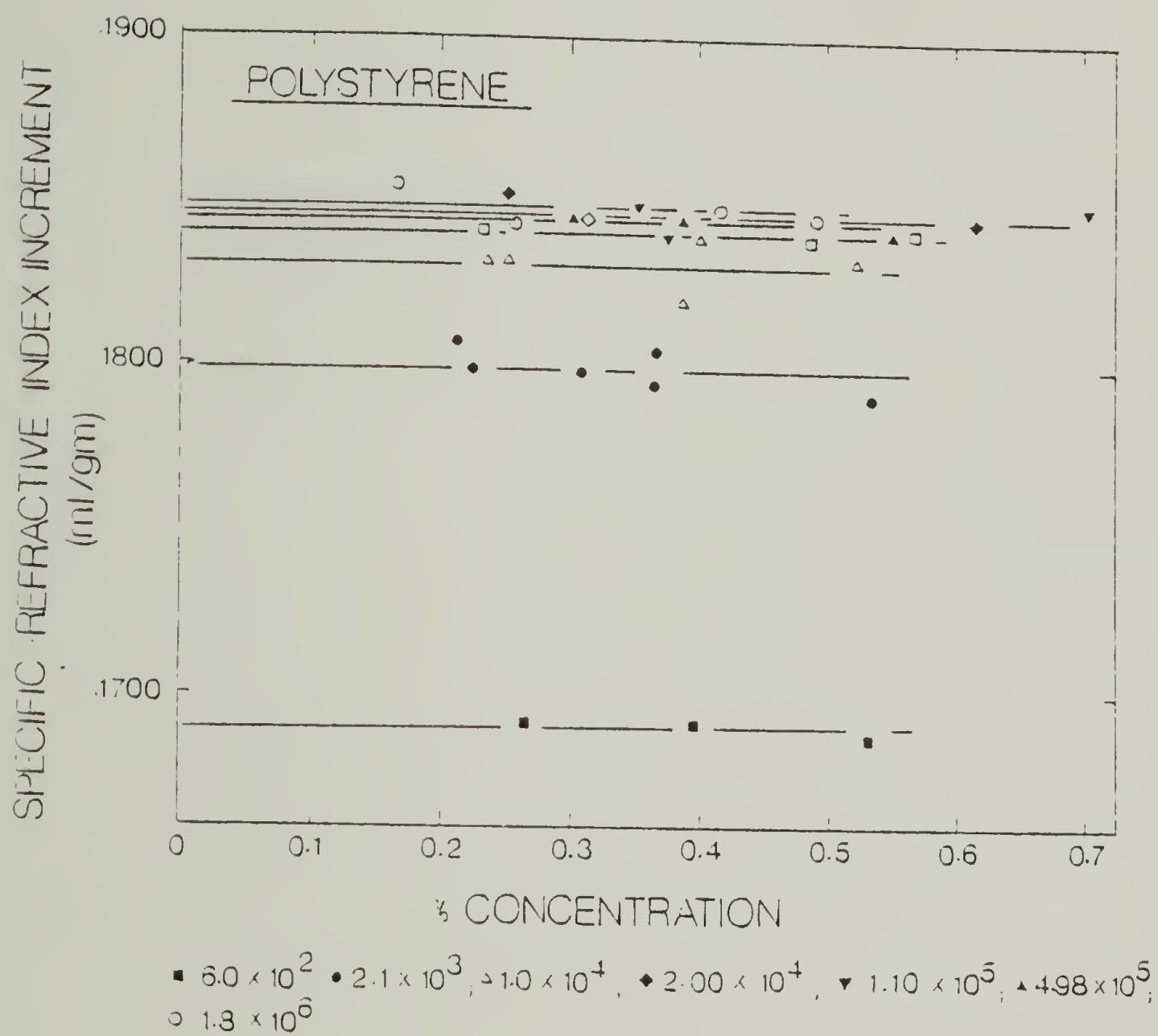


Figure 3.1. The specific refractive index increment as a function of concentration for several different molecular weight samples.

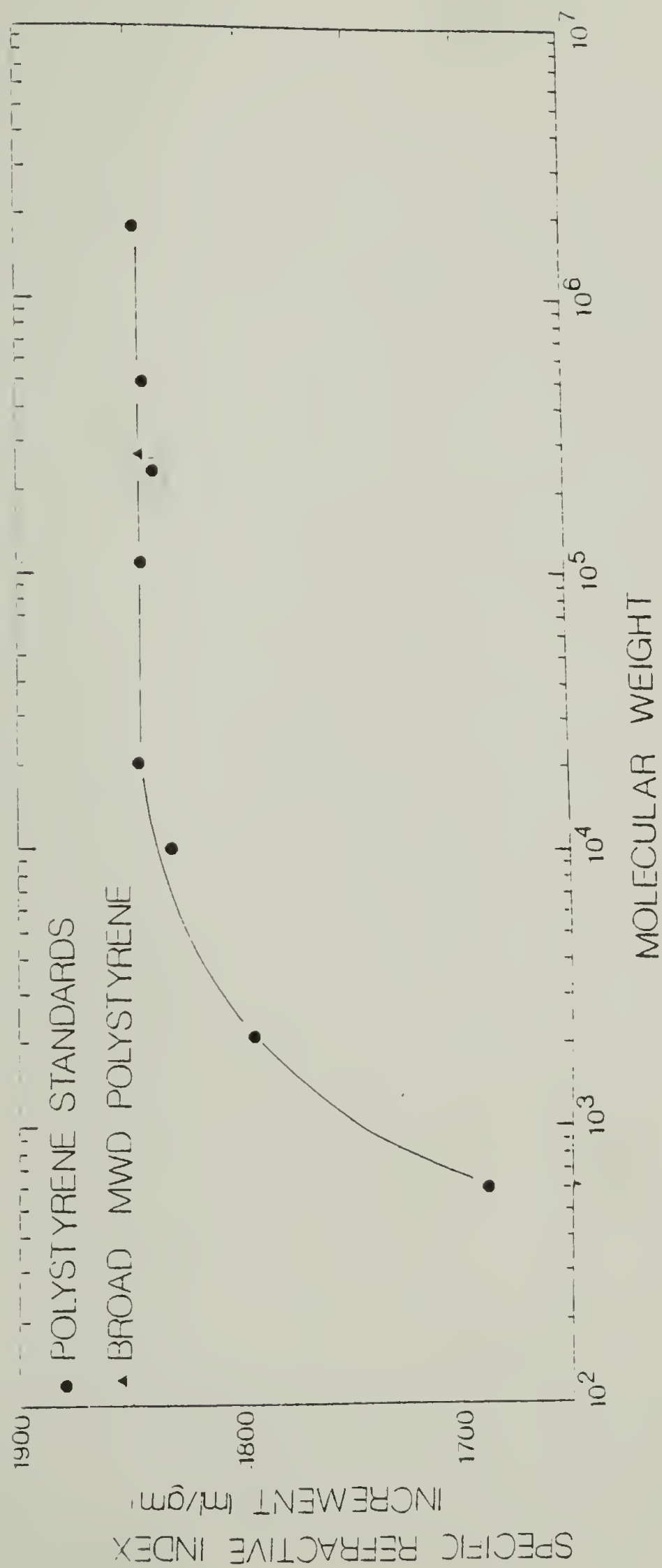


Figure 3.2. The effect of molecular weight on the specific refractive index increment, dn/dc .

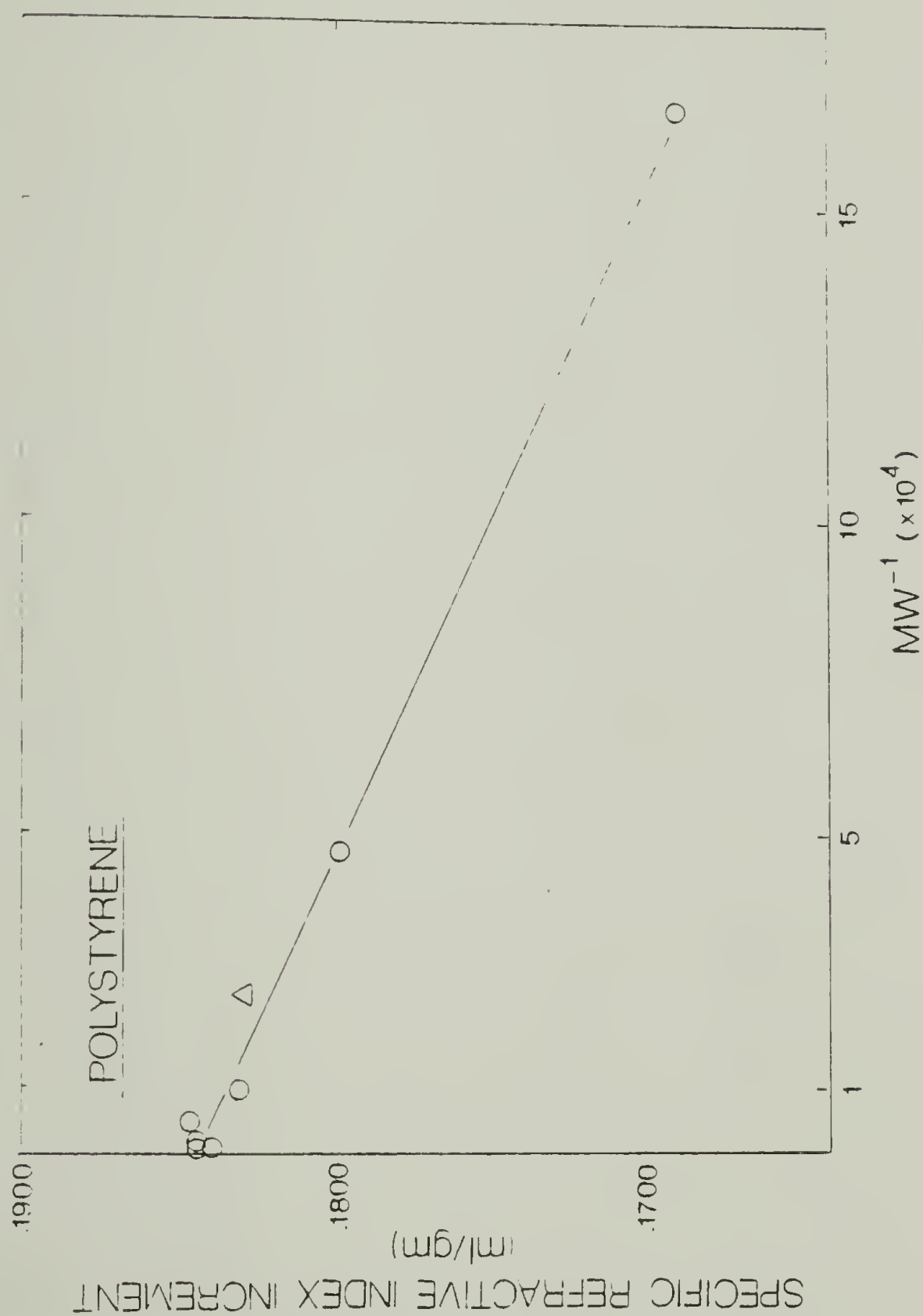


Figure 3.3. The specific refractive index increment versus the reciprocal of molecular weight. A linear dependence is indicated.

content of the chain.

A Chromatix KMX-16 differential refractometer, which uses a He-Ne laser operating at a wavelength of 633 nm, was used. All measurements were made at 25°C in tetrahydrofuran, Fisher Certified. The refractometer was calibrated at 25°C by aqueous solutions of NaCl as described in the section on calibration.

Table 3.3 contains the data obtained on eight stereoregular PMMA samples which represent six different tactic forms for this polymer. Column 2 in the table lists the dyad tacticities as calculated from triad tacticity using the α -methyl resonance as described in Chapter II. Concentrations ranged from 2 to 5 gms/liter and are given in column 3, Table 3.3. Again, each of the dn/dc values listed for a specific concentration in column 4 is an average of at least 10 measurements. All the measured values of dn/dc for the various stereoregular compositions of PMMA were found to be independent of concentration, within experimental error, as Figure 3.4 shows. As a result, we chose to use the arithmetic average rather than extrapolate to $c=0$.

Figure 3.5 shows the results graphically, plotted as dn/dc versus the percent isotactic dyads in the chain. The difference in dn/dc is shown to be up to about 5% over the limits of the two stereoregular forms; .0841 for the entirely syndiotactic chain to .0885 for the isotactic polymer. Moreover, this difference is believed to be significant since the square of this term is used in the optical constant, K , (Equation 3.2) required for the calculation of molecular weight. This change can thus result in an error as high as 10% in the calculated

TABLE 3.3: Specific Refractive Index Increments for Stereoregular Poly(Methyl Methacrylate)

Sample No.	Tacticity (dyads)		Concentration ₃ (gms/ml) × 10 ³	$\Delta n/c$ (ml/gm)	Average
	I	S			
1	15	85	4.2784	.0845	.0844
			2.8522	.0849	
			2.1392	.0840	
			1.4261	.0842	
2	23	77	5.1032	.0842	.0845
			5.0550	.0849	
			4.7780	.0842	
			3.82740	.0840	
			3.6110	.0845	
			3.3700	.0843	
			2.5516	.0849	
			2.5270	.0849	
			2.3890	.0837	
3	23	77	5.1872	.0858	.0855
			5.1404	.0857	
			3.8904	.0857	
			3.8553	.0854	
			3.4581	.0856	
			2.5936	.0848	
			2.5702	.0859	
4 a	35	65	3.6936	.0858	.0862
			2.7702	.0856	
			1.8468	.0869	
5b	83	17	6.7390	.0882	.0885
			6.0728	.0894	
			4.6970	.0888	
			4.5546	.0900	
			3.0364	.0901	
			1.9490	.0863	
6b	83	17	5.7946	.0879	.0882
			5.7642	.0879	
			4.6114	.0883	
			3.8428	.0881	
			2.8973	.0887	
			2.8821	.0876	
			1.9315	.0887	

TABLE 3.3 (continued)

Sample No.	Tacticity (dyads)		Concentration ₃ (gms/ml) x 10 ³	$\Delta n/c$ (ml/gm)	Average
	I	S			
7	98	8	4.1504	.0877	.0876
			3.4587	.0876	
			2.0752	.0874	
			1.1858	.0878	
8b	100	0	5.0684	.0877	.0884
			4.0298	.0891	
			3.8013	.0887	
			3.0220	.0881	
			2.6865	.0886	
			2.5342	.0879	
			2.0149	.0887	

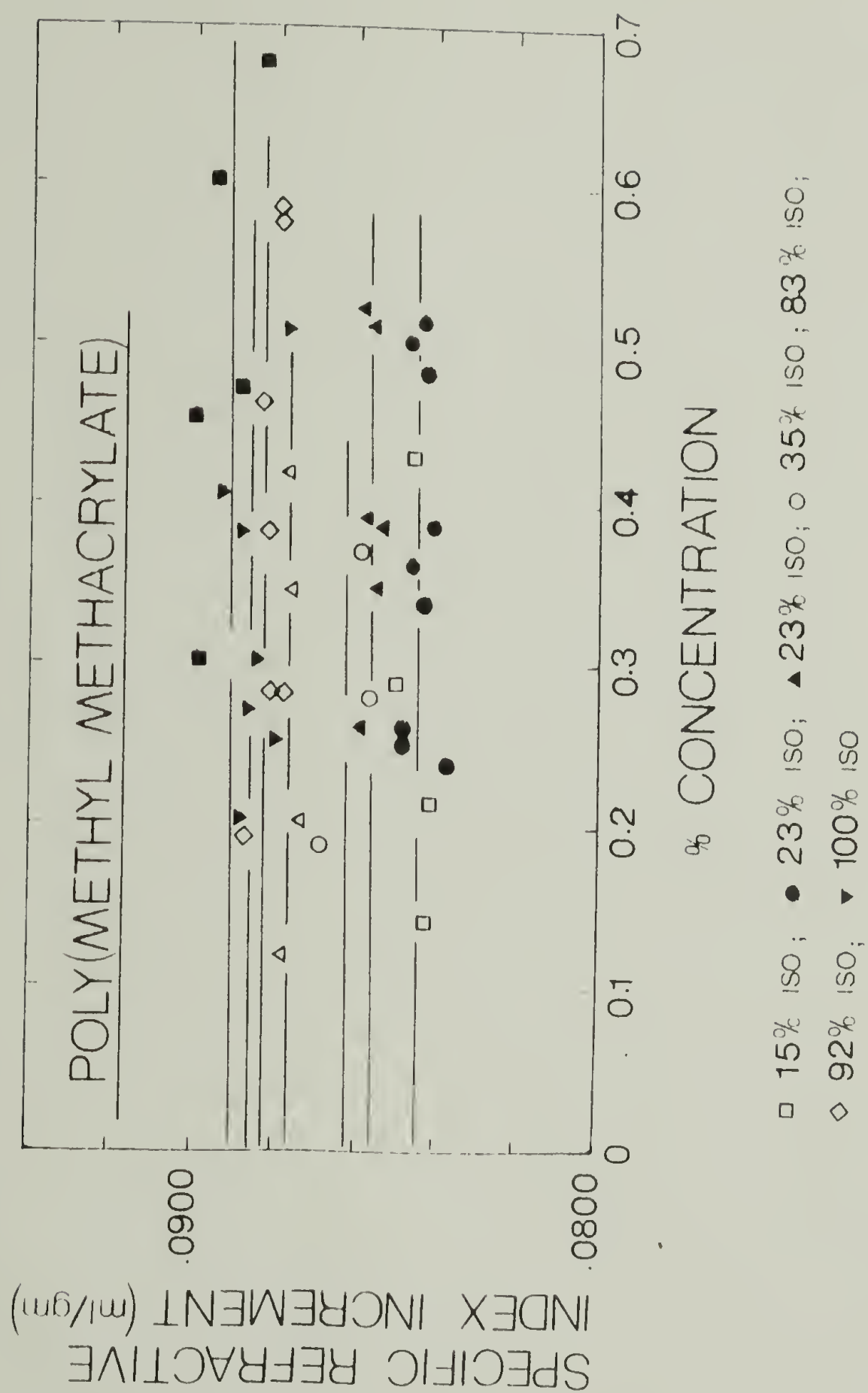


Figure 3.4. The specific refractive index increment as a function of concentration for several different stereoregular forms of poly(methyl methacrylate).

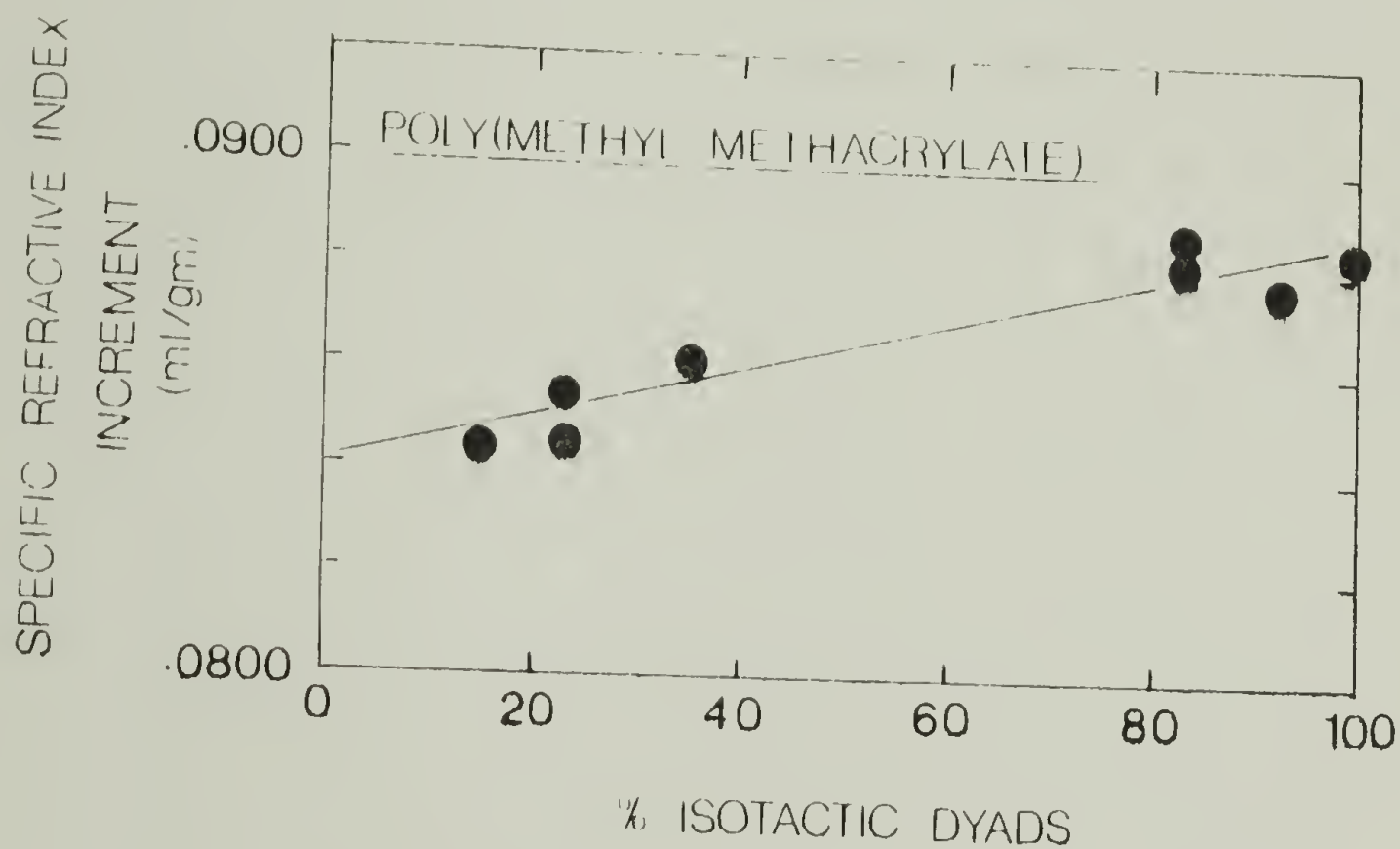


Figure 3.5. The effect of tacticity on the specific refractive index increment for Poly(methyl methacrylate).

weight average molecular weight if the correct dn/dc is not used for a particular stereoregular composition.

Discussion

It is believed that this may be the first reported study which encompasses a wide range of stereoregular polymers and shows a significant and systematic change in dn/dc with stereoregularity. Previous studies in different solvents and at different temperatures have nonetheless inferred the possibility of a dependence of dn/dc on stereoregularity. However, previous data is somewhat limited as well as contradictory. For example, the same value of dn/dc is reported for atactic and isotactic poly(isopropyl acrylate) in 2, 2, 3, 3-Tetrafluoropropanol,⁽²⁾ whereas significant differences among the values for atactic, isotactic and syndiotactic forms of PMMA have been found.^(3,4) For example, Schulz et al⁽³⁾ report a decrease in dn/dc with increasing isotactic content for solutions of PMMA in n-butyl chloride at both 25 and 50°C. Whereas, Bello and Guzman⁽⁴⁾ report an increase in dn/dc with increasing isotactic content for PMMA in toluene at 25°C (see Table 3.4).

Calculation of the specific volume. In a polymer solution, the specific refractive index increment, dn/dc is related, according to Outer, Carr and Zimm⁽⁵⁾, to the specific volume of the polymer, V_s , and the difference in refractive index between the polymer, n_2 and the solvent, n_1 , (see Equation 3.5).

TABLE 3.4: Specific Refractive Index Increments for Stereoregular Poly(Methyl Methacrylate)

Sample No.	Tacticity		dn/dc	Solvent	Temp °C	λ (nm)	Ref.
	I	S					
1	15	85	.0844	THF	25	633	this work
2	23	77	.0845	THF	25	633	"
3	23	77	.0855	THF	25	633	"
4a	36	54	.0862	THF	25	633	"
5b	85	15	.0885	THF	25	633	"
6b	85	15	.0882	THF	25	633	"
7	91	9	.0870	THF	25	633	"
8b	100	0	.0884	THF	25	633	"
-	Syndiotactic		.1001	n-butyl chloride	50	436	8
-	Atactic		.1021	n-butyl chloride	50	436	8
-	Isotactic		.0965	n-butyl chloride	50	436	8
-	Atactic		.0931	n-butyl chloride	50	436	8
-	Isotactic		.0902	n-butyl chloride	50	436	8
-	Syndiotactic		.007	Toluene	25	436	9
-	Atactic		.010	Toluene	25	436	9
-	Isotactic		.014	Toluene	25	436	9

$$dn/dc = V_s (n_2 - n_1) \quad (3.5)$$

Indeed, this relation has been shown⁽⁶⁾ to yield useful estimates of dn/dc from the refractive indices of the solvent and the specific volume and refractive index of the polymer. Others^(4,7,8) have shown the method useful in estimating the partial specific volumes of polymers from measurements of dn/dc and n_2 . However, Huglin⁽⁶⁾ has suggested that values obtained from this relation are generally in poor agreement with experiment since one is essentially estimating a solution parameter, dn/dc , from measurement of parameters in the solid state, that is, refractive index and specific volume.

As a check on the relation, and to see if our measured change in dn/dc with tacticity could be interpreted in terms of the parameters in Equation 3.5, we measured n_2 for our stereoregular PMMA samples. This was accomplished quite simply by using a microscope, and a set of immersion oils. Basically, when a polymer and the surrounding medium have exactly the same refractive index, no line of demarcation will be observable, and the object will appear invisible.⁽⁹⁾ The immersion oils used in our measurements were obtained from Cargille Laboratories, New Jersey. For these oils the refractive index at three different wavelengths, 589, 486, and 656 nm, are supplied by the manufacturer. These values were then extrapolated to 633 nm using a Cauchy equation of the following order:

$$n = A + B/\lambda^2 \quad (3.6)$$

where n is the refractive index of the solution, λ is the wavelength

of light and A and B are constants. The n_2 values obtained ranged from 1.490 for the 15% isotactic polymer, sample 1, to 1.500 for the 100% isotactic polymer, sample 8. Table 3.5 lists the n_2 values obtained for each of the stereoregular PMMA samples. No value was obtained for sample 4 because sufficient quantity of this polymer was not available to press a film for refractive index measurement. In addition, Figure 3.6 shows graphically the change in n_2 with tactic content of the chain.

Using the refractive index values listed in Table 3.5 along with our dn/dc values, and the refractive index of THF as 1.405, we predict values for the specific volume ranging from 0.931 for sample 1 to 0.993 for sample 8. These V_s values, (see Table 3.5) are in sharp contrast to those reported by Bywater and Toporowski⁽¹⁰⁾, who found values ranging from 0.810 to 0.843 gm/ml (Table 3.4, Column 6). Figure 3.7 shows a comparison of the specific volumes calculated according to Equation 3.6, open circles, and those measured experimentally, solid circles.

The primary reason for the disagreement between the V_s values calculated from Equation 3.5 and those measured experimentally lies in the use of quantities pertaining to the bulk polymer rather than the more appropriate values in solution. That is the partial specific volume, and the refractive index of the solute in solution. The basic premise of Equation 3.5 is believed to be correct. While quantitative agreement is not obtained for the reasons discussed, qualitative agreement for the change in specific volume with tacticity

TABLE 3.5: Estimation of the Specific Volume

Sample No.	Tacticity		dn/dc (ml/gm)	n_2	V_s (ml/gm)	V_s (ml/gm)
	I	S			(predicted)	(From Ref. 10)
8b	100	0	.0884	1.500	.931	.810
7	92	8	.0876	1.498	.942	.817
5b	83	17	.0882	1.498	.948	.820
4a	35	65	.0862	*	*	.836
2	23	77	.0845	1.490	.994	.840
1	15	85	.0844	1.490	.993	.843

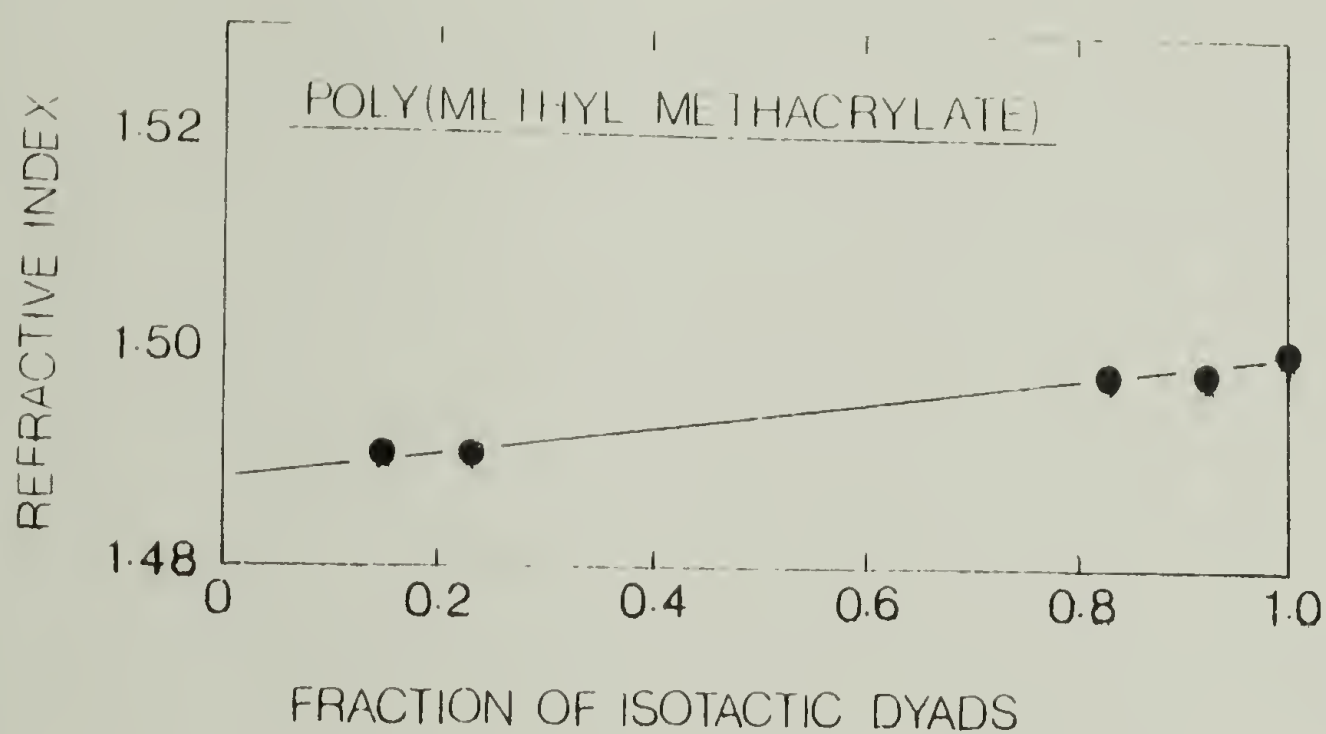


Figure 3.6. The effect of tacticity on the refractive index for poly(methyl methacrylate).

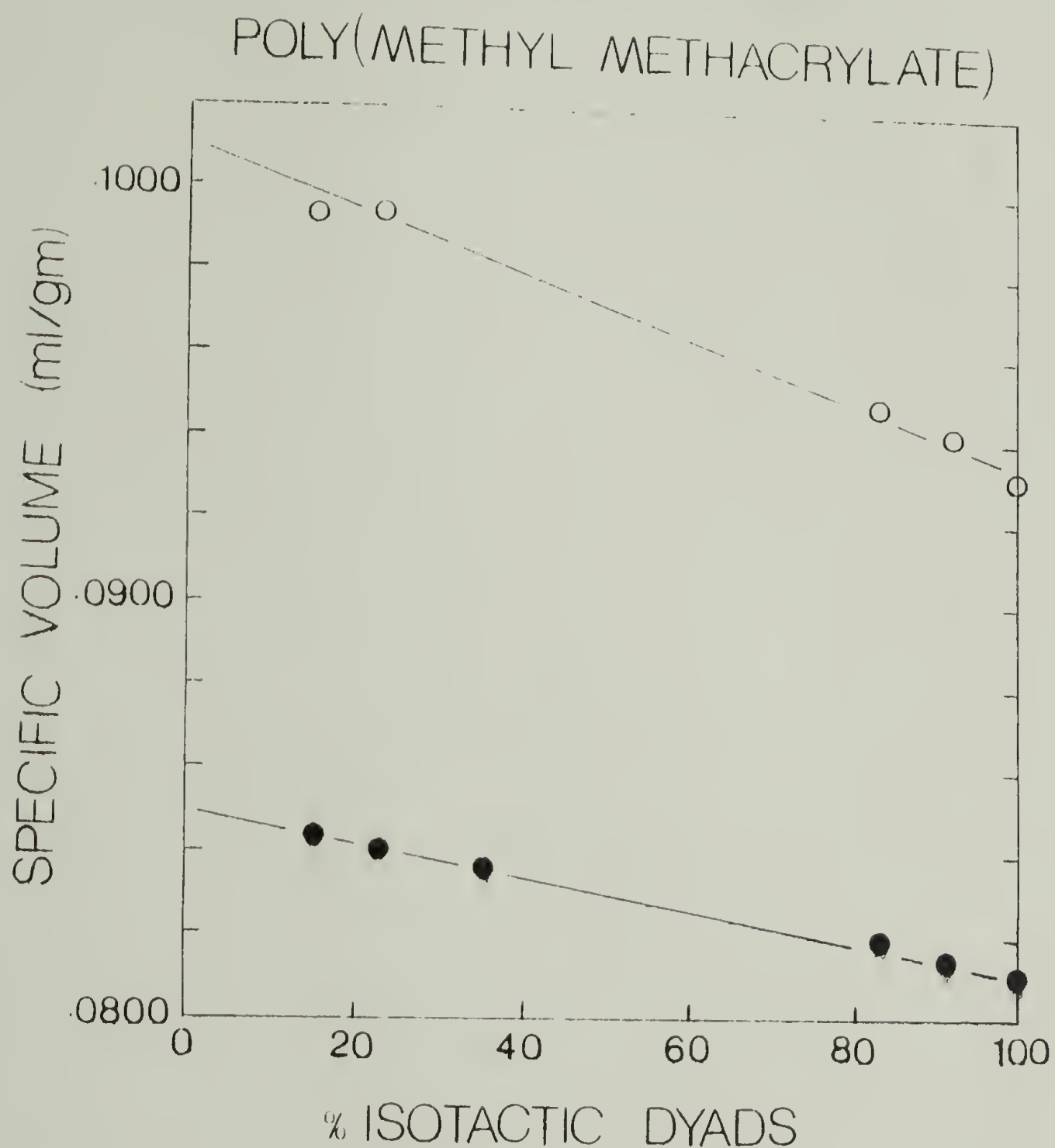


Figure 3.7. A comparison of the specific volumes calculated according to Equation 3.6, open symbols, and those measured experimentally, solid symbols, for various stereoregular forms of poly-(methyl methacrylate).

is apparent.

The quantity dn/dc which has the dimensions of $\text{cm}^3\text{gm}^{-1}$ is a measure of the specific volume, (or more appropriately as demonstrated here of the partial specific volume), of a solute. The same applies to the intrinsic viscosity, $[\eta]$, which has the same dimensions. The information obtained from dn/dc and $[\eta]$ is, however, both numerically and phenomenologically different; the latter is a measure of the hydrodynamically effective volume, and the former is a measure of the optically effective volume. Whereas the two quantities cannot be readily compared the information obtained from them can be complementary. For instance, in Chapters IV and V we have shown that the intrinsic viscosity, a measure of the hydrodynamic volume, for an isotactic sample is higher than for a syndiotactic sample of the same molecular weight. This is qualitatively reflected in the increase in dn/dc , the optically effective volume, which also is higher for the isotactic PMMA. However, the actual value will also depend on the difference in refractive indices between the solute in solution and the solvent, a parameter which will depend on the functional groups present in both the polymer and the solvent.

Specific Refractive Index Increments for Branched Poly(vinyl acetate)

In this section the results of dn/dc measurements for the branched PVAc samples used in Chapter VI are discussed. Importantly, we have found a small but measurable change in dn/dc with branching density.

As in all the work discussed in this chapter a Chromatix KMX-16 differential refractometer was used. All measurements were made at 25°C in tetrahydrofuran, and the refractometer was calibrated as described in the section on Calibration.

Table 3.6 contains the data obtained on 4 different PVAc samples, labeled A, B, C & D. Chapter VI describes the preparation and characterization of these samples. It suffices here to note that samples A and B are more highly branched than C and D. Column 1 in this table lists briefly the preparation of each sample. Column 2 lists the concentrations used in this work. In general, concentrations ranged from 2 to 5 gms/liter except for sample D where concentrations ranged from 0.4 to 1.5 gms/liter because of the limited availability of this sample. Each of the dn/dc values listed in column 3 is the result of at least 10 measurements. As in the case of PS and PMMA dn/dc was again found to be independent of concentration. Consequently, the arithmetic average was used rather than extrapolate to $c=0$. The average values obtained are listed in column 4.

Figure 3.8 shows the results graphically plotted as dn/dc versus concentration. The open symbols have been used for the less branched samples and the filled in symbols for the more highly branched samples. It is apparent that dn/dc is affected by the degree of branching in PVAc. Whereas no measurable difference exists between samples A and B or between samples C and D it is obvious that the more highly branched samples exhibit lower dn/dc values.

These results are in qualitative agreement with those obtained for stereoregular PMMA. That is, for PMMA, the tactic form which ex-

TABLE 3.6: Specific Refractive Index Increments for Poly(Vinyl Acetate)

Sample	Concentration ₃ (gms/ml) x 10 ³	$\Delta n/c$ (ml/gm)	$\Delta n/c$ Average (ml/gm)
Original PVAc	5.4769	.0544	
A	4.10768	.0544	
	3.65127	.0544	
	2.73845	.0546	.0544
Sheared PVAc	5.6632	.0545	
B	4.2474	.0542	
	3.7754	.0549	
	2.8316	.0549	.0546
Saponified and	3.9972	.0556	
Reacetylated	2.9979	.0564	
C	2.6648	.0557	
	1.9986	.0558	.0559
Sheared and Saponi-	1.3142	.0561	
fied and Reacety-	0.8123	.0557	
lated	0.3877	.0562	.0560
D			

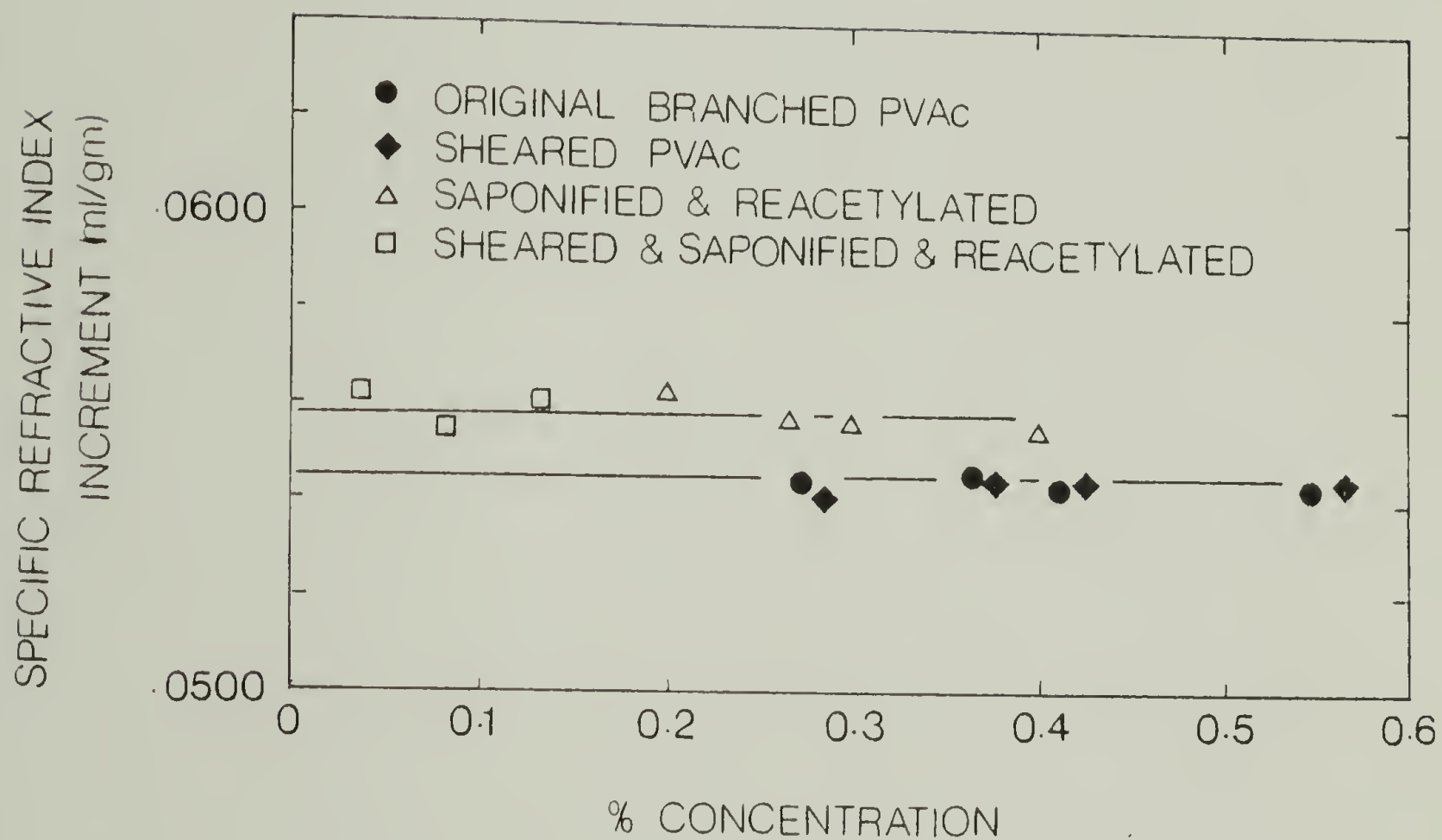


Figure 3.8. The specific refractive index increment as a function of concentration for branched poly(vinyl acetate).

hibited the larger intrinsic viscosity also exhibited the larger dn/dc value. For branched PVAc samples it is known⁽¹¹⁾ that branched samples exhibit smaller dimensions, and consequently a lower intrinsic viscosity, than linear samples of the same molecular weight. This fact is also exhibited in the dn/dc values which are also lower for the more highly branched samples, sample A and B. The difference is however small, less than 2% between the samples used in this study.

Conclusions

In this chapter we have presented several important results which are of primary concern to the remainder of the work in this dissertation. In the first section we studied PS standards and determined that dn/dc reached a limiting value at a molecular weight of about 2.0×10^4 . This data is of prime concern since from it we can be assured that for all the polymers used in this work dn/dc will be independent of molecular weight. In the second section we investigated the dependence of dn/dc on the tactic content of the chain for PMMA. It was observed that dn/dc changed by as much as 5% over the limits of the stereoregular forms. This was deemed as being significant since the square of this term is used in the optical constant, K , used in the calculation of molecular weight. In the third section we showed that dn/dc was measurably affected by the degree of branching in PVAc. The change in dn/dc for the four samples studied was however small, less than 2%.

hibited the larger intrinsic viscosity also exhibited the larger dn/dc value. For branched PVAc samples it is known⁽¹¹⁾ that branched samples exhibit smaller dimensions, and consequently a lower intrinsic viscosity, than linear samples of the same molecular weight. This fact is also exhibited in the dn/dc values which are also lower for the more highly branched samples, sample A and B. The difference is however small, less than 2% between the samples used in this study.

Conclusions

In this chapter we have presented several important results which are of primary concern to the remainder of the work in this dissertation. In the first section we studied PS standards and determined that dn/dc reached a limiting value at a molecular weight of about 2.0×10^4 . This data is of prime concern since from it we can be assured that for all the polymers used in this work dn/dc will be independent of molecular weight. In the second section we investigated the dependence of dn/dc on the tactic content of the chain for PMMA. It was observed that dn/dc changed by as much as 5% over the limits of the stereoregular forms. This was deemed as being significant since the square of this term is used in the optical constant, K , used in the calculation of molecular weight. In the third section we showed that dn/dc was measurably affected by the degree of branching in PVAc. The change in dn/dc for the four samples studied was however small, less than 2%.

REFERENCES

1. A. Kruis, Z. Physik, Chem., B., 34, 13 (1936).
2. R.A. Wessling, J.E. Mark, E. Hamori, and R.E. Hughes, J. Phys. Chem., 70, 1903 (1966).
3. G.V. Schulz, W. Wunderlich, and R. Kriste, Makromol. Chem., 75, 22 (1964).
4. A. Bello, and G.M. Guzman, Europ. Polym. J., 2, 85 (1966).
5. P. Outer, C.I. Carr, and B.H. Zimm, J. Chem. Phys., 21, 581 (1950).
6. M.B. Huglin, Light Scattering from Polymer Solutions, Academic Press, New York (1972).
7. J. Horska, J. Stejskal, P. Kratochvil, J. Appl. Polym. Sci., 24, 1845 (1979).
8. W. Heller, J. Polym. Sci., A-2, 4, 209 (1966).
9. E. Chamot, C.W. Mason, Handbook of Chemical Microscopy, Wiley, New York (1944).
10. S. Bywater, and P.M. Toporowski, Polymer, 13, 94 (1972).
11. E.E. Drott, and R.A. Mendelson, J. Polym. Sci., A-2, 8, 1361 (1970).

C H A P T E R I V
MEASUREMENT OF THE UNPERTURBED DIMENSIONS USING
A GEL PERMEATION CHROMATOGRAPH COUPLED WITH A
LOW ANGLE LASER LIGHT SCATTERING PHOTOMETER

Introduction

In this chapter methods are developed whereby one can use the distribution of the polymer in order to generate a series of values for molecular weight, M_{w_i} , and intrinsic viscosity, $[\eta]_i$. After demonstrating the agreement between values generated by this method with those values determined by more conventional methods, (i.e., viscometry and light scattering), the values are used to obtain estimates of the polymers unperturbed dimensions. In this chapter the method is demonstrated with two stereoregular PMMA samples. In Chapter V these same techniques are applied to a complete set of stereoregular PMMA's, and the data evaluated using numerous extrapolation procedures. In Chapter VI these same methods will be used in order to obtain a measure of the degree of branching in PVAc.

Experimental

The basic experimental apparatus used throughout the rest of this dissertation consisted of a Gel Permeation Chromatograph coupled with an on-line Low Angle Laser Light Scattering Photometer, GPC/LALLS. A block diagram of the setup is shown in Figure 4.1. Here the LALLS

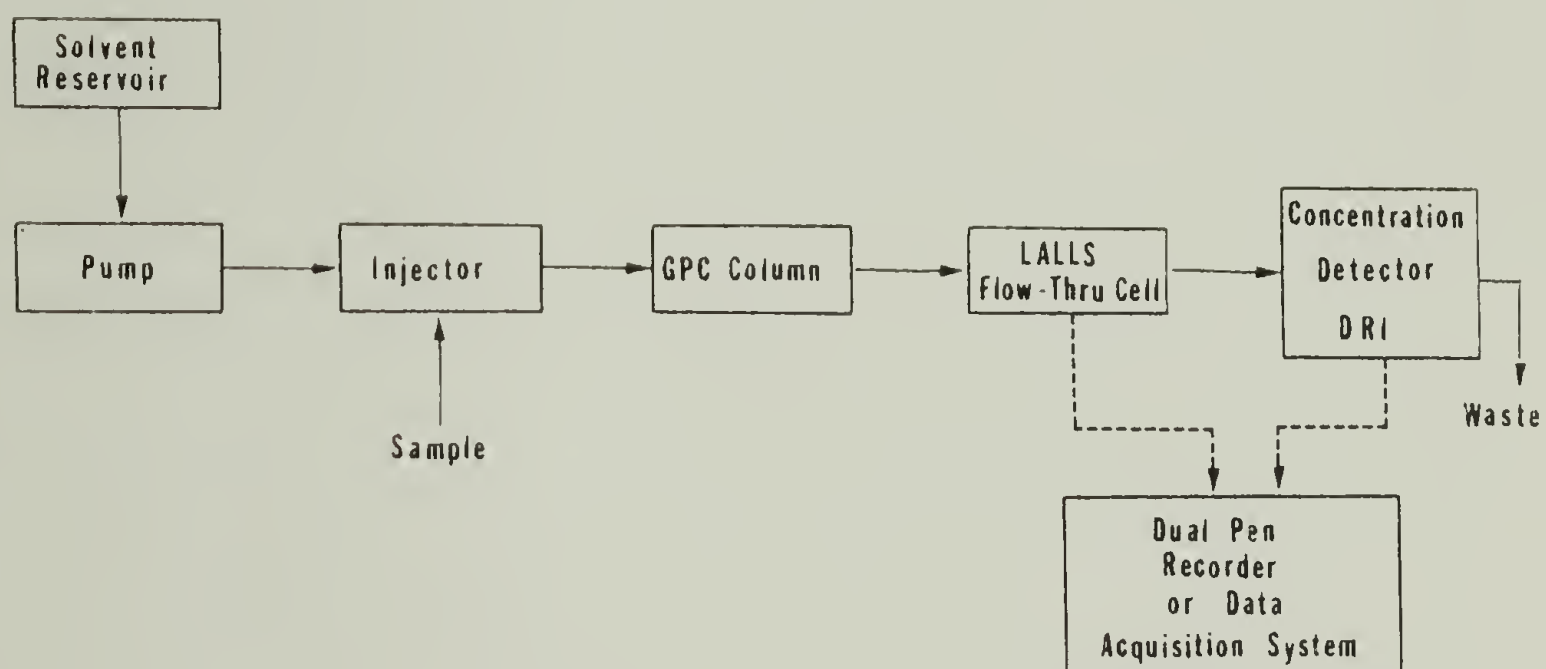


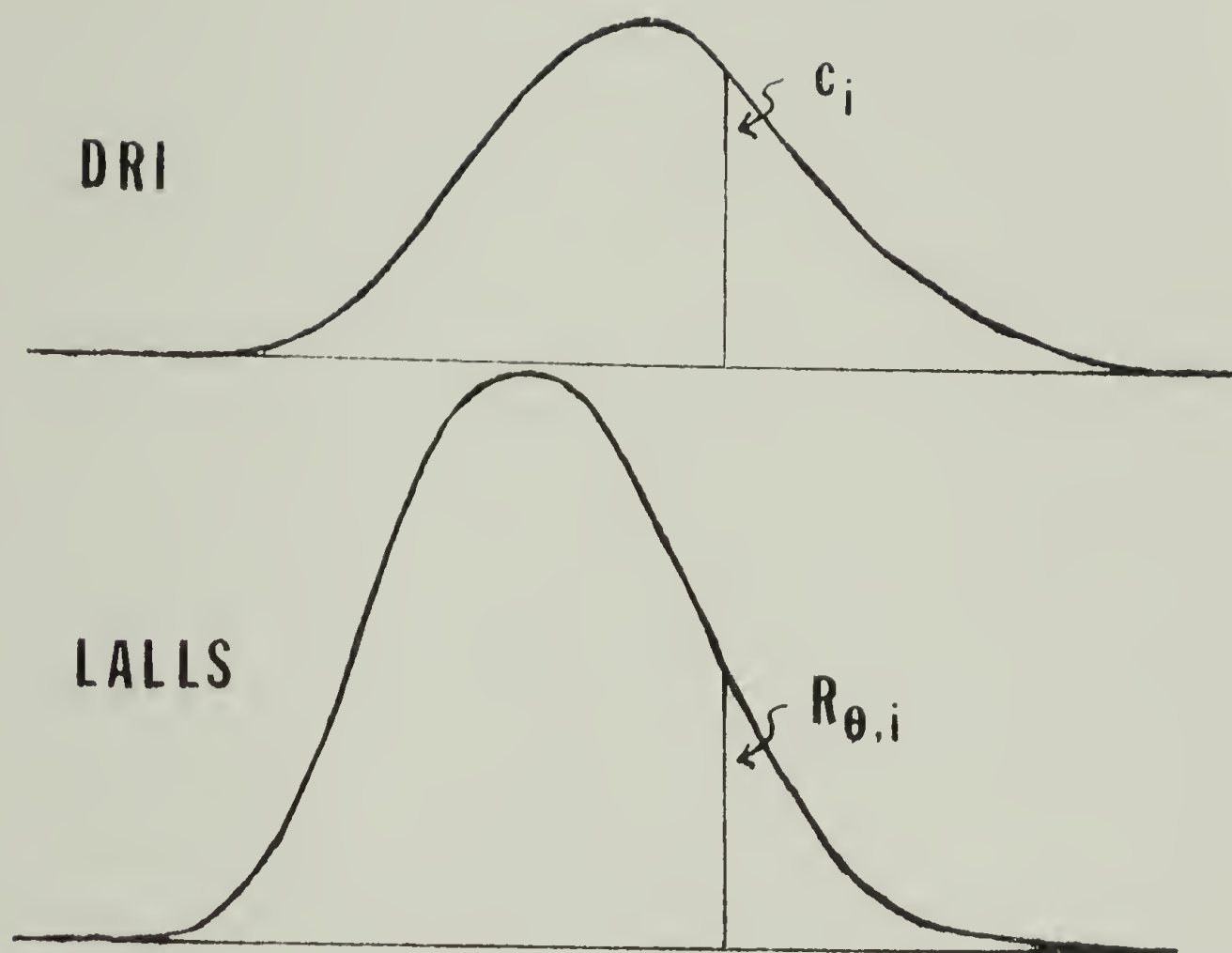
Figure 4.1. Block diagram of the combined GPC and LALLS units.

has been inserted between the columns and the conventional concentration detector. The GPC was a Waters model 201 equipped with 4 μ -Styragel columns of nominal pore size 10^3 , 10^4 , 10^5 , and 10^6 Å. The LALLS was a Chromatix KMX-6. A 0.5 μ fluoropore filter, Millipore Corporation Bedford, Mass., was placed between the columns and the LALLS, and appeared to give a clean signal relatively free from dust particles.

The output from the GPC/LALLS system consists of a dual response; that of the LALLS and the response from the differential refractometer. Figure 4.2 shows typical results obtained from a GPC/LALLS system. As indicated in Figure 4.2, the LALLS response, which is essentially a measure of the intensity of scattered light, yields a value from which the Rayleigh ratio, R_{θ_i} , may be obtained. The differential refractometer yields a value from which the concentration, c_i , may be determined.

It is interesting to note the effect of dust particles, long known to be a major cause of problems in conventional light scattering measurements, cause very little problems in a GPC/LALLS system. Figure 4.3 shows data obtained for a PS sample where the filter apparatus was not functioning properly. The effect of the particles is to produce a brief increase in the intensity of scattered light, whereas the actual scattering from the polymer solution is readily apparent as the baseline.

The detailed theory behind the analysis of light scattering data has been the subject of considerable work.⁽¹⁾ It suffices here to note that at the small forward scattering angles employed in the KMX-6,



$$\frac{K c_i}{R_{\theta,i}} = \frac{1}{M_{w,i}} + 2A_{2,i}c_i$$

Figure 4.2. Typical response from the differential refractometer and the light scattering detectors.

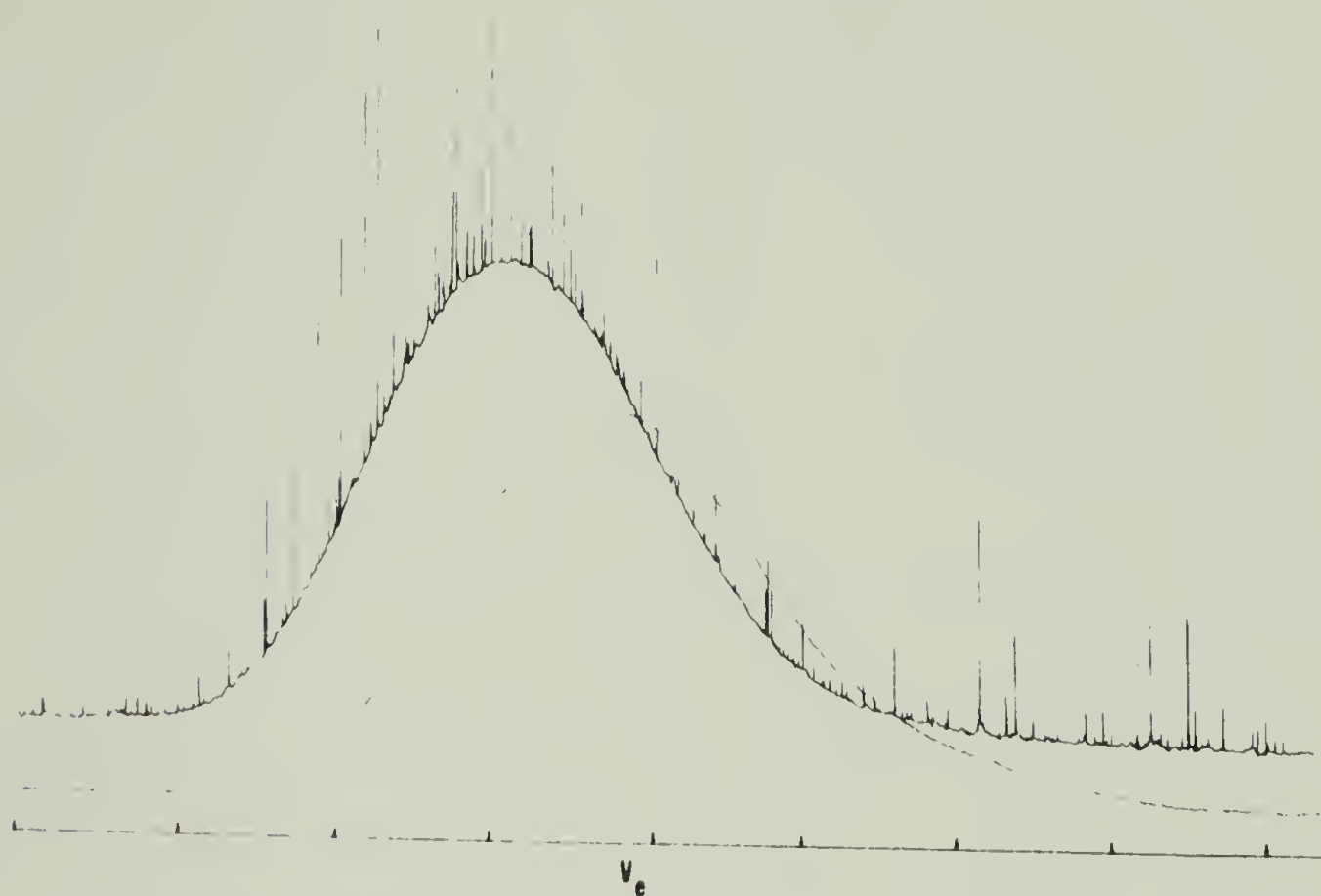


Figure 4.3. The effect of dust particles in the GPC/LALLS system.

and at the low solute concentrations used, the relationship between the Rayleigh factor and the weight average molecular weight is;⁽²⁾

$$\frac{Kc}{R_\theta} = \frac{1}{M_w} + 2A_2c \quad (4.1)$$

where c is the solute concentration in gms/ml and A_2 is the second virial coefficient. For measurements on line with a GPC the molecular weight at uniform intervals across the distribution curve is calculated from a modified form of Equation 4.1 (Equation 4.2)⁽³⁾.

$$Kc_i/R_{\theta_i} = 1/M_i + 2A_2c_i \quad (4.2)$$

The concentration, c_i , was then calculated by normalizing the detector response;

$$c_i = mx_i/v_i \sum x_i \quad (4.3)$$

where m is the mass injected, v_i is the effluent volume passing through the sample cell during the i th interval, and $\sum x_i$ is the sum of the x_i values for all the intervals within the peak.⁽²⁾

The second virial coefficient, A_2 , was obtained by static analysis of the sample from the slope of a plot of Kc/R_θ versus c . For all samples except polystyrene an average value of A_2 was used. For polystyrene analysis of narrow distribution standards in the static mode makes it possible to assess the dependence of A_2 on molecular weight, that is, to obtain the constants a and α in Equation 4.4.

$$A_i = aM_i^{-\alpha} \quad (4.4)$$

Equation 4.4 was then iteratively evaluated in conjunction with

Equation 4.2, to obtain M_i . The Newton-Raphson method of successive approximations was used for the iteration.

For polystyrene we used the data of Ouano⁽⁴⁾ who determined $a = .037$ and $\alpha = .187$ for narrow distribution polystyrene in THF. For PMMA and PVAc we used the static technique and determined an average value for each sample. For these samples no dependence of A_2 on molecular weight was incorporated into Equation 4.2, a procedure which has been shown to result in negligible errors.⁽³⁾ For PMMA it was determined that A_2 was slightly smaller for the isotactic samples, samples 5-8, than for the syndiotactic samples, samples 1-4. An average value of $5.01 \times 10^{-4} \text{ mole} \cdot \text{cm}^3/\text{g}^2$ was used for samples 5-8, whereas $6.15 \times 10^{-4} \text{ mole} \cdot \text{cm}^3/\text{g}^2$ was used for samples 1-4. For PVAc an average value of $5.0 \times 10^{-4} \text{ mole} \cdot \text{cm}^3/\text{g}^2$ was used for the second virial coefficient for all samples. In view of the relatively small magnitude of the term containing A_2 in the GPC/LALLS equation, Equation 4.2, uncertainty in M_w from this approximation is insignificant.

Once M_{w_i} has been calculated at uniform intervals on the elution curve by means of Equation 4.2, the molecular weight averages may be calculated in the conventional manner;

$$M_n = \Sigma c_i / \Sigma (c_i M_i) \quad (4.5)$$

$$M_w = \Sigma c_i M_i / \Sigma c_i \quad (4.6)$$

$$M_z = \Sigma c_i M_i^2 / \Sigma c_i M_i \quad (4.7)$$

Calculations of the Incremental Molecular Weights and Intrinsic Viscosities

Universal calibration. The method to be described in this chapter for

determining M_{w_i} and $[\eta]_i$ involves using the light scattering apparatus to determine the weight average molecular weight at incremental points across the polymers distribution and then using "Universal Calibration" to calculate the corresponding intrinsic viscosities. "Universal Calibration" as originally developed by Benoit et al.⁽⁵⁾ involves the concept of separation by hydrodynamic volume expressed as the product of intrinsic viscosity and molecular weight.

In order to construct the Universal Calibration curve a series of well characterized polystyrene standards was used. Measurements of the intrinsic viscosity of each sample was obtained in THF at 25°C, using an Ubbelholde viscometer. Measurement of the intrinsic viscosity for PS in THF is a procedure which has been carried out by numerous researchers. Table 4.1 lists just a few of the values of the Mark-Houwink constants, K and α , available in the literature. It is obvious that there is a wide variation in the constants reported. Values for the exponent α have been reported ranging from .64 to .768, whereas K values range from 2.84×10^{-4} to $.609 \times 10^{-4}$ dl/gm.

Spychaj et al.⁽⁶⁾ have shown that the wide variation in the Mark-Houwink constants reported in the literature may be a result of the variation in water content in the THF used, since THF is known to be a highly hydroscopic solvent. In their study they determined the Mark-Houwink constants for PS samples in THF while varying the concentration of water from 0% to 8.2% water. Their results were as follows;

TABLE 4.1 Mark-Houwink Constants For The System PS-THF

$K(\times 10^4)$ (dl/g)	α	Temperature (°C)
2.84	0.64	25
2.63	0.65	25
2.89	0.65	30
1.68	0.69	25
1.622	0.694	25
1.41	0.70	25
1.60	0.700	25
1.47*	0.70*	25
1.23	0.703	35
1.51	0.706	25
1.25	0.707	30
1.17	0.717	25
1.11	0.723	25
1.251	0.717	25
	0.72	25
1.14-1.22	0.72	25
1.09	0.723	25
1.112	0.723	30
1.11	0.725	25
1.17	0.725	25
1.01	0.729	25
0.99	0.730	35
1.16	0.730	25
1.05	0.731	40
	0.74	25
0.861	0.74	30
0.682	0.766	23
0.609	0.768	25

From ref. 6

THF	$[\eta] = 1.16 \times 10^{-4} M^{0.73}$
4.5% Water	$[\eta] = 1.32 \times 10^{-4} M^{0.70}$
7.7% Water	$[\eta] = 7.45 \times 10^{-4} M^{0.53}$
8.2% Water	$[\eta] = 11.9 \times 10^{-4} M^{0.48}$

The results of Spychaj et al⁽⁶⁾ point out the necessity for determining the Mark-Houwink relationship for the particular THF to be used. Using data reported in the literature will result in obvious errors. As a result every effort was made to use the THF as quickly as possible after it was opened.

Figure 4.4 shows the results of our intrinsic viscosity measurements using PS standards, Pressure Chemical Co., and THF, Fisher Certified. The Mark-Houwink constants, determined from the least-squares line through our data, are $K = 1.47 \times 10^{-4} (\text{dl/gm})$ and $\alpha = 0.70$. These values are also listed in Table 4.2 where they appear to be in good agreement with a majority of the data. These values were then used to calculate the hydrodynamic volume, $[\eta]M$, used in "Universal Calibration."

Determination of the spreading function. Column dispersion is a major factor that causes inaccuracy in quantitative GPC interpretations, because it distorts the elution curve and affects the calibration and the molecular weight calculations. Compensation for the dispersion effect is discussed in the next section. However, to account for column dispersion by using the methods discussed in the next section, one needs to know how much peak broadening has been imposed on the experimental GPC elution curve. There are two methods which can be

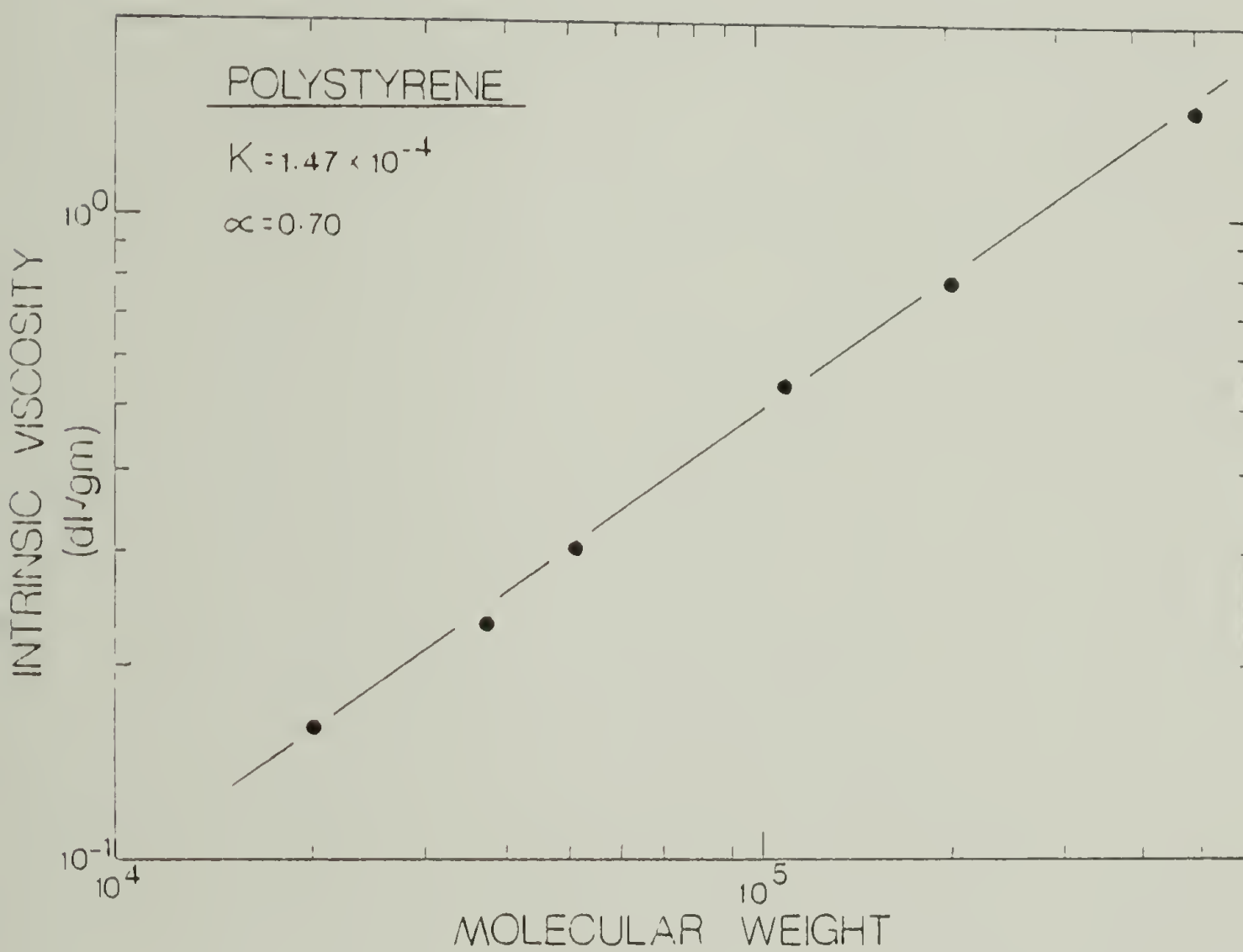


Figure 4.4. The intrinsic viscosity-molecular weight relationship for narrow distribution polystyrene in tetrahydrofuran, 25°C.

used to assess column broadening⁽⁷⁾, a reverse-flow experiment, and recycle GPC. We chose to use recycle GPC since this method allows determination of both axial dispersion parameters and accurate determination of the polydispersity.

Recycle GPC. The basic theory behind recycle GPC has been discussed in detail in several treatments.^(7,8) For our purpose it suffices to state that the variance of the total chromatographic curve width, σ_T^2 , is given by the sum of the variances of each of the contributors, i.e.,

$$\sigma_T^2 = \sigma_{inj}^2 + \sigma_{disp}^2 + \sigma_{MWD}^2 + \sigma_{ex.col.}^2 \quad (4.8)$$

where σ_{inj}^2 is that due to sample injection, σ_{disp}^2 is the chromatographic band dispersion, σ_{MWD}^2 is the spreading due to the actual MWD of the sample, and $\sigma_{ex.col.}^2$ consists of the spreading caused by all extracolumn sources.

In conventional GPC systems, σ_{inj}^2 is insignificant, and $\sigma_{ex.col.}^2$ has also been minimized to the extent that Equation 4.8 may be rewritten as;

$$\sigma_T^2 = \sigma_{disp}^2 + \sigma_{MWD}^2 \quad (4.9)$$

Since σ_{disp} is proportional to \sqrt{n} and σ_{MWD} is proportional to n , where n is the number of cycles,

$$\sigma_T^2 = n\sigma_{disp}^2 + n^2\sigma_{MWD}^2 \quad (4.10)$$

Dividing through by n we obtain:

$$\frac{\sigma_T^2}{n} = \sigma_{disp}^2 + n\sigma_{MWD}^2 \quad (4.11)$$

Thus plotting the experimental quantity σ_T^2/n as a function of n should yield a straight line. Its intercept gives the axial dispersion parameter, σ_{disp}^2 , and the slope gives the polydispersity of the sample if the calibration curve for the instrument is known.

Table 4.2 lists the data obtained by recycle GPC for 13 cycles of a narrow distribution PS standard of 51,000 molecular weight.

Figure 4.5 shows the data plotted according to Equation 4.11. From the slope we obtain $\sigma_{\text{MWD}}^2 = .079$ and from the intercept we obtain $\sigma_{\text{disp}}^2 = .386$. Since we know;

$$\sigma_{\text{MWD}}^2 = a^2 \delta^2 \quad (4.12)$$

where, $\delta^2 = \ln(M_w/M_N)$, and a is the slope of the calibration curve $V = a \ln M + b$, we can calculate precisely the polydispersity of the sample. For our system $a^2 = 5.43 \text{ ml}^2$ and $\sigma_{\text{MWD}}^2 = .079 \text{ ml}^2$ so that we obtain $\delta^2 = 1.45 \times 10^{-2}$ and $M_w/M_N = 1.015$.

Once we have determined the exact polydispersity of a sample by this method this data can then be used along with Equation 4.9 to calculate σ_{disp}^2 for any other chromatographic system. It is this value, σ_{disp} , which will be used in the next section in order to compensate for spreading.

Correction for spreading. Many of the parameters involved in GPC/LALLS systems have previously been discussed (9-12). It suffices here to note that from such a system one obtains M_{w_i} , that is, the weight average molecular weight at any measurable point across a polymer's distribution. Through the use of a universal calibration curve, which relates the hydrodynamic volume, $[\eta]M$, to the elution volume,

TABLE 4.2: Recycle GPC Data for Polystyrene, MW = 51,000

No. of Cycles n	1/n	σ_{chr} (ml)	σ_{chr}^2/n (ml ²)	$\sigma_{\text{chr}}^2/n^2$ (ml ²)
1	1	0.33	0.111	0.111
2	0.5	0.99	0.499	0.249
3	0.33	1.45	0.699	0.233
4	0.25	1.81	0.815	0.204
5	0.20	2.15	0.925	0.185
6	0.17	2.54	1.073	0.179
7	0.14	2.58	0.951	0.136
8	0.13	2.92	1.069	0.134
9	0.11	3.04	1.027	0.114
10	0.10	3.55	1.259	0.126
11	0.09	3.67	1.223	0.111
12	0.08	4.09	1.399	0.117
13	0.07	3.87	1.152	0.089

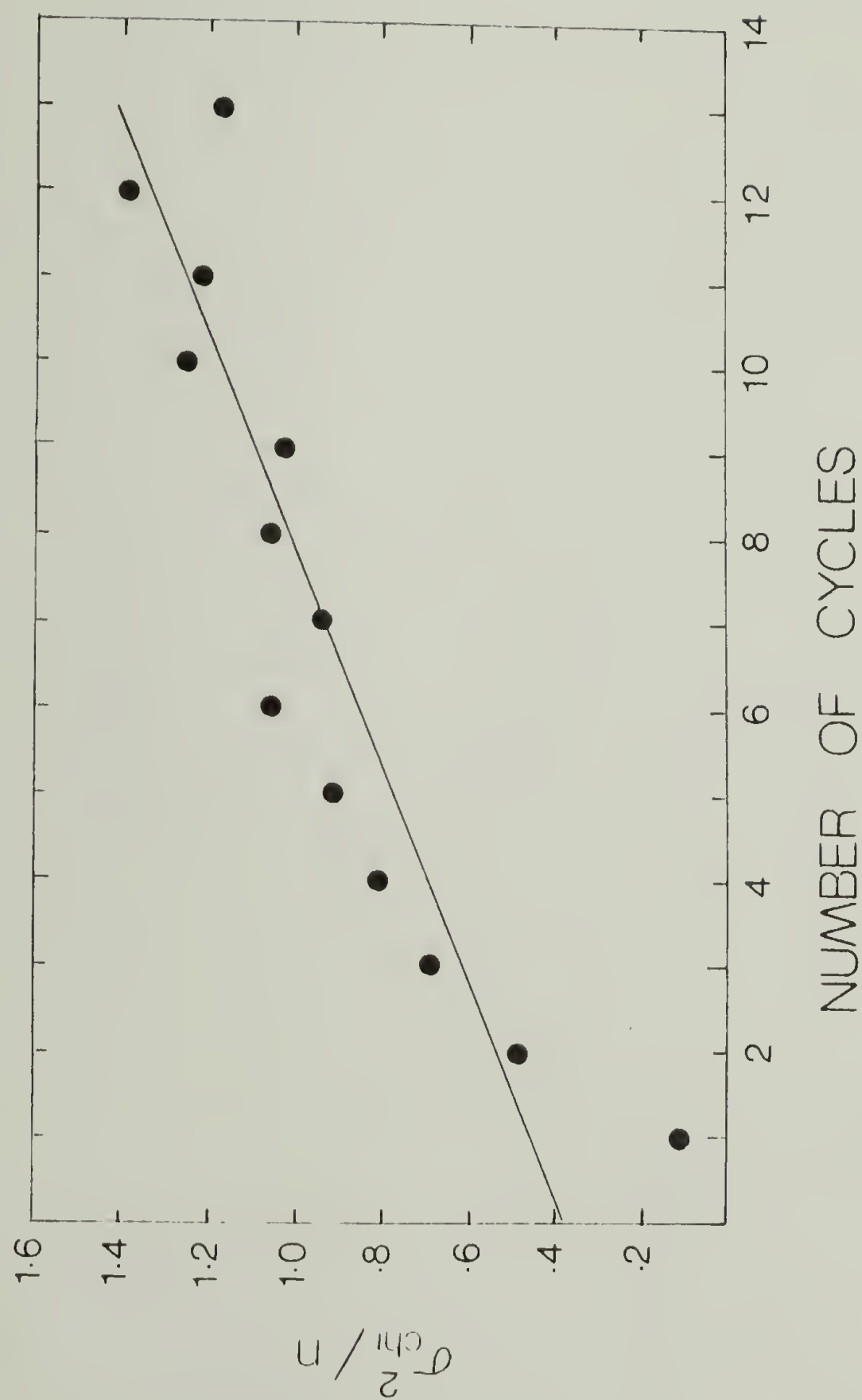


Figure 4.5. σ^2_{chr}/n versus the number of cycles, n , for a polystyrene sample of $M_w = 51,000$.

the corresponding values for the intrinsic viscosity, $[\eta]_i$, are obtained by dividing the hydrodynamic volume by the corresponding molecular weight.

A problem which needs to be considered here is which average of the molecular weight is correct for use in universal calibration. If it were M_n as a recently proposed (11), dividing $[\eta]M_n$ by M_w would result in an incorrect value for the intrinsic viscosity. We thus chose to avoid the problem by using the $1/(\alpha + 1)$ average of the hydrodynamic volume, ϕ , where $\phi = [\eta]M$, and α is the Mark-Houwink exponent. That is, it can simply be shown that:

$$\bar{M}_w = \frac{\sum c_i \left(\frac{\phi}{K}\right)^{1/(\alpha + 1)}}{\sum c_i} \quad (4.13)$$

Consequently, dividing the $1/(\alpha + 1)$ average of ϕ by M_w will result in a correct average of the intrinsic viscosity.

Since α is an unknown, some means of evaluating α must be available before it is possible to calculate the correct average of ϕ . In addition, some correction for axial dispersion should be applied. To resolve both, we chose to use the method of Benoit et al. (13) which was originally developed for on-line viscometry, and is particularly applicable to systems using dual detectors. The method is unique in that the overall chromatogram is treated by correcting incremental elution volumes for axial dispersion, i.e., spreading. It is important to note here that when using a GPC/LALLS system, it is the intrinsic viscosities, $[\eta]_i$, not the molecular weight values, that need to be corrected for spreading (see Figure 4.6). This is

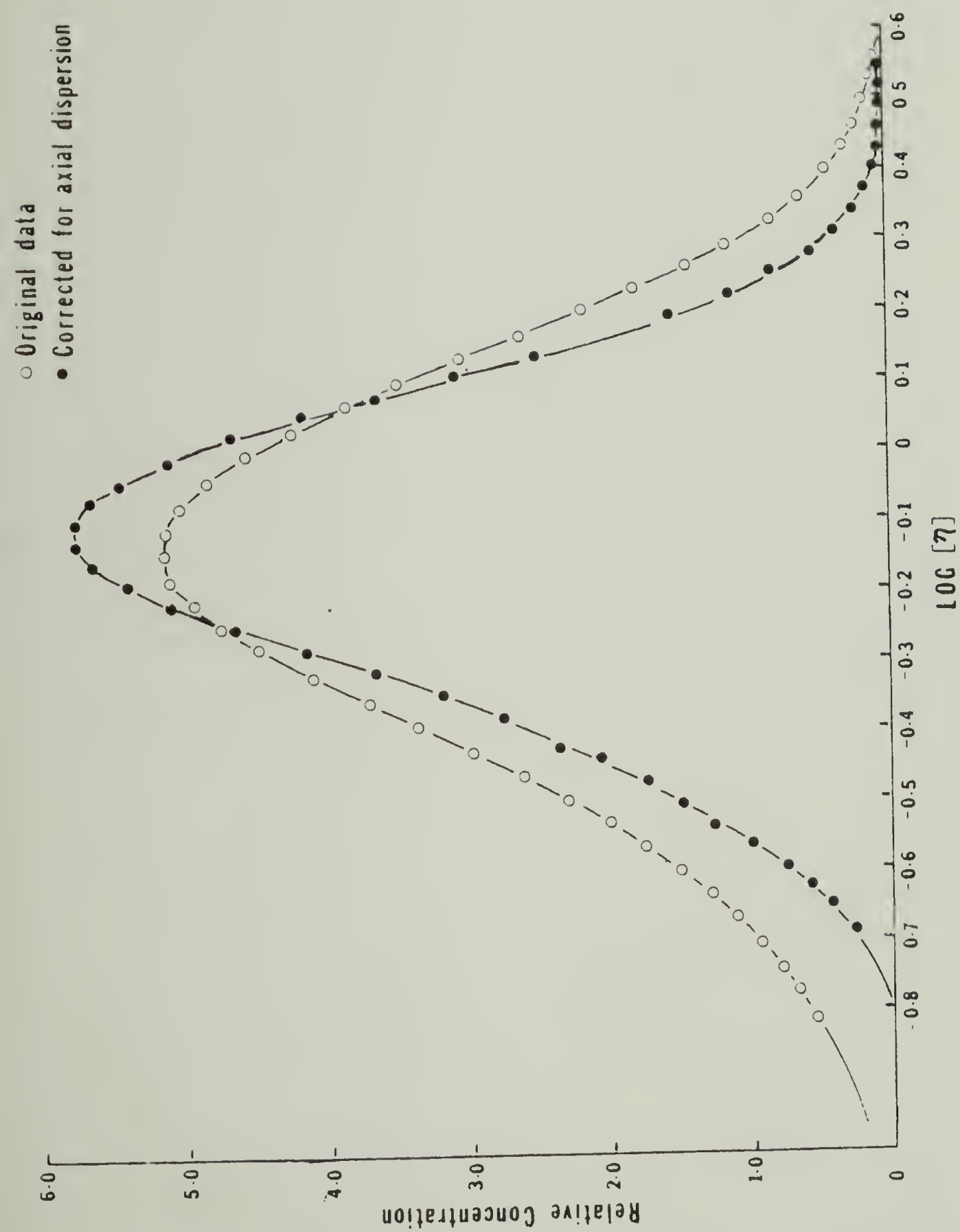


Figure 4.6. The effect of spreading on the incremental intrinsic viscosity values.

because, in spite of any "spreading" process, the light scattering detector will always measure the correct weight average molecular weight of the fraction in the cell at any given elution volume. The effect of "spreading" will thus be evident in the intrinsic viscosities which are calculated from the elution volume and a universal calibration curve.

In order to calculate α we use the relation:

$$\phi = KM^{\alpha} + 1 \quad (4.14)$$

from which, $\alpha + 1$ can be obtained from a plot of $\log \phi$ versus $\log M$. At this point no correction for axial dispersion has been applied and the results for atactic PMMA (See figure 4.7) for α are shown to be in poor agreement with those obtained by conventional viscometry. Figure 4.7 shows a plot of ϕ_e versus M_w , where ϕ_e is the uncorrected hydrodynamic volume. It can be seen that agreement between this method and conventional viscometry is obtained only at a point which corresponds to the peak in the molecular weight distribution. This is to be expected since the intrinsic viscosities and therefore the hydrodynamic volumes have not been corrected for spreading.

The 17 data points shown in Figure 4.7 represent data obtained from the portion of the distribution where adequate detector response was obtained from both the differential refractometer and the LALLS detectors. The scattered intensity, as measured by the LALLS, is a product of the concentration and the molecular weight, whereas the differential refractometer is sensitive only to concentration. As a result the LALLS is extremely sensitive to the high end of the MWD

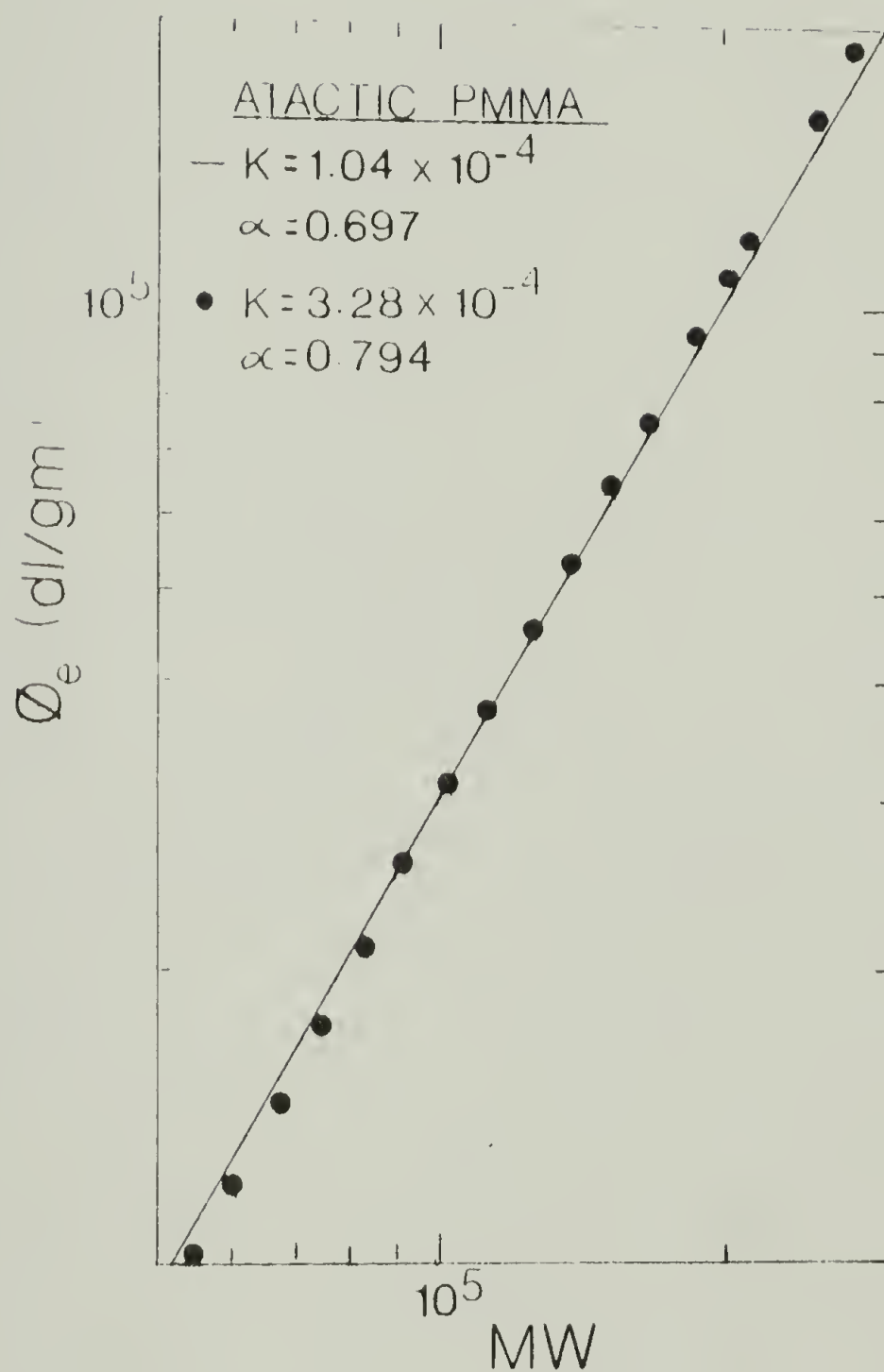


Figure 4.7. The uncorrected hydrodynamic volume, ϕ_e , versus molecular weight, MW, for atactic PMMA.

and correspondingly less sensitive to the low end. This results in an offset between the two detectors which increases with the MWD and makes calculation of the molecular weights of the sample at both ends of the chromatogram imprecise for broad MWD samples. Consequently, data acquisition is limited to a region where adequate response from the two detectors can be obtained.

To correct for axial dispersion we proceed as follows. The average we are interested in may be defined as:

$$\phi_{\beta} = \left[\frac{\sum c_i \phi_i^{\beta}}{\sum c_i} \right]^{1/\beta} \quad (4.15)$$

where, in our case, $\beta = 1/(\alpha+1)$. Going from summation to integration we use the function:

$$Y^*(\beta) = \int_0^{\infty} \phi^{\beta} C(\phi) d\phi \quad (4.16)$$

and the β average can then be written as:

$$\phi_{\beta} = \left[\frac{Y^*(\beta)}{Y^*(0)} \right]^{1/\beta} \quad (4.17)$$

The problem now lies in the evaluations of $Y^*(\beta)$. As a first approximation we use the simplest case, that of a polymer with a gaussian molecular weight distribution. For this case it has been shown that (13):

$$Y^*(\beta) = \phi_0^{\beta} \exp \left\{ \frac{-(v-v_0)^2}{2\sigma^2} \right\} \exp \left\{ \frac{(\beta + \frac{A(v-v_0)}{2})^2}{2(\frac{A^2}{\sigma^2} + \frac{1}{\delta^2})} \right\} \quad (4.18)$$

where:

ϕ_0 , is the peak hydrodynamic volume,

v_0 , is the peak elution volume,

v , is the elution volume at the increment being evaluated,

σ , is the axial dispersion parameter,

$A = a/(\alpha+1)$, where: a is the slope of the calibration curve,

$\gamma^* = \gamma(\alpha+1)$, and $\gamma^2 = \ln(M_w/M_n)$

Substituting Equation 4.18 into Equation 4.17 and evaluating for $\beta = 1/(\alpha+1)$ and $\beta=0$, we obtain:

$$\langle \phi \rangle^{1/(\alpha+1)} = \phi_0^\beta \exp \left\{ \frac{\beta^2 + 2\beta A(v-v_0)}{\sigma^2} \right\} \quad (4.19)$$

$$\left\{ \frac{2 \left(\frac{A^2}{\sigma^2} + \frac{1}{\gamma^{*2}} \right)}{\gamma^{*2}} \right\}$$

Using the fact that, $v-v_0 = A \log \frac{\phi_e}{\phi_0}$ and $\gamma^* = \sigma/A$ and rearranging, we

obtain:

$$\text{Log } \langle \phi \rangle^{1/(\alpha+1)} = c + \frac{1}{\alpha+1} \frac{1}{(1+\tau^{*2}/\gamma^{*2})} \text{Log } \phi_e \quad (4.20)$$

Since we know, $\bar{M}_w = \frac{\sum c_i \left(\frac{\phi}{K} \right)^{1/(\alpha+1)}}{\sum c_i}$

we can rearrange and obtain: $M_w K^{1/(\alpha+1)} = \langle \phi \rangle^{1/(\alpha+1)}$

Upon substitution and rearrangement we then obtain:

$$\text{Log } \phi_e = c + (\alpha+1)(1+\tau^{*2}/\gamma^{*2}) \text{Log } M_w \quad (4.21)$$

This relation implies that for the case of a Gaussian distribution, a plot of $\text{Log } \phi_e$ vs. $\text{Log } M$ will yield $(\alpha+1)(1+\tau^{*2}/\gamma^{*2})$ as the slope and not $(\alpha+1)$ as suggested in Equation 4.14. The term $(1+\tau^{*2}/\gamma^{*2})$

is simply a correction term for axial dispersion. Since both τ^* and γ^* are readily evaluated for the system, α can be obtained. As a check on this equation, we can see that in the case of no spreading, τ^* approaches 0, and the slope reduces to $(\alpha+1)$. Also, as the molecular weight distribution becomes broad, γ^* approaches ∞ and the slope again reduces to $(\alpha+1)$.

For the data shown in Figure 4.7 the slope is 1.794. Upon evaluating τ^* and γ^* for this system and substitution into Equation 4.21 we find that the actual value of α is 0.695. This is in excellent agreement with the value of 0.697 as determined by conventional viscometry (7).

Having determined the actual value of α for the polymer in question, we may now calculate the $1/(\alpha+1)$ average of ϕ . To do this we need to solve Equation 4.16 for the general case. Benoit (13) has shown that the equation can be expressed in terms of τ^* , ϕ_e , the chromatogram C , and its derivatives C' , C'' , etc. According to Benoit (13):

$$\phi_\beta = \left[\frac{\gamma^*(\beta)}{\gamma^*(0)} \right]^{1/\beta} = \phi_e \exp \left\{ \frac{\tau^{*2}\beta}{2} \right\} \left[1 + \tau^{*2} \frac{C'}{C} + \tau^{*4} \left(\frac{\beta}{2} \frac{C''}{C} + \frac{1}{2} \frac{C'''}{C} - \frac{(\beta-1)}{2} \frac{C'}{C^2} - \frac{1}{2} \frac{C'C''}{C^2} \right) \right] \quad (4.22)$$

where the expansion has been stopped after τ^{*4} .

When we apply Equation 4.22 using the value of α calculated from Equation 4.12, we obtain excellent agreement between ϕ and $[n]$ values calculated by this method and those obtained by conventional viscometry. Figure 4.8 shows the results of applying this correction. Essentially,

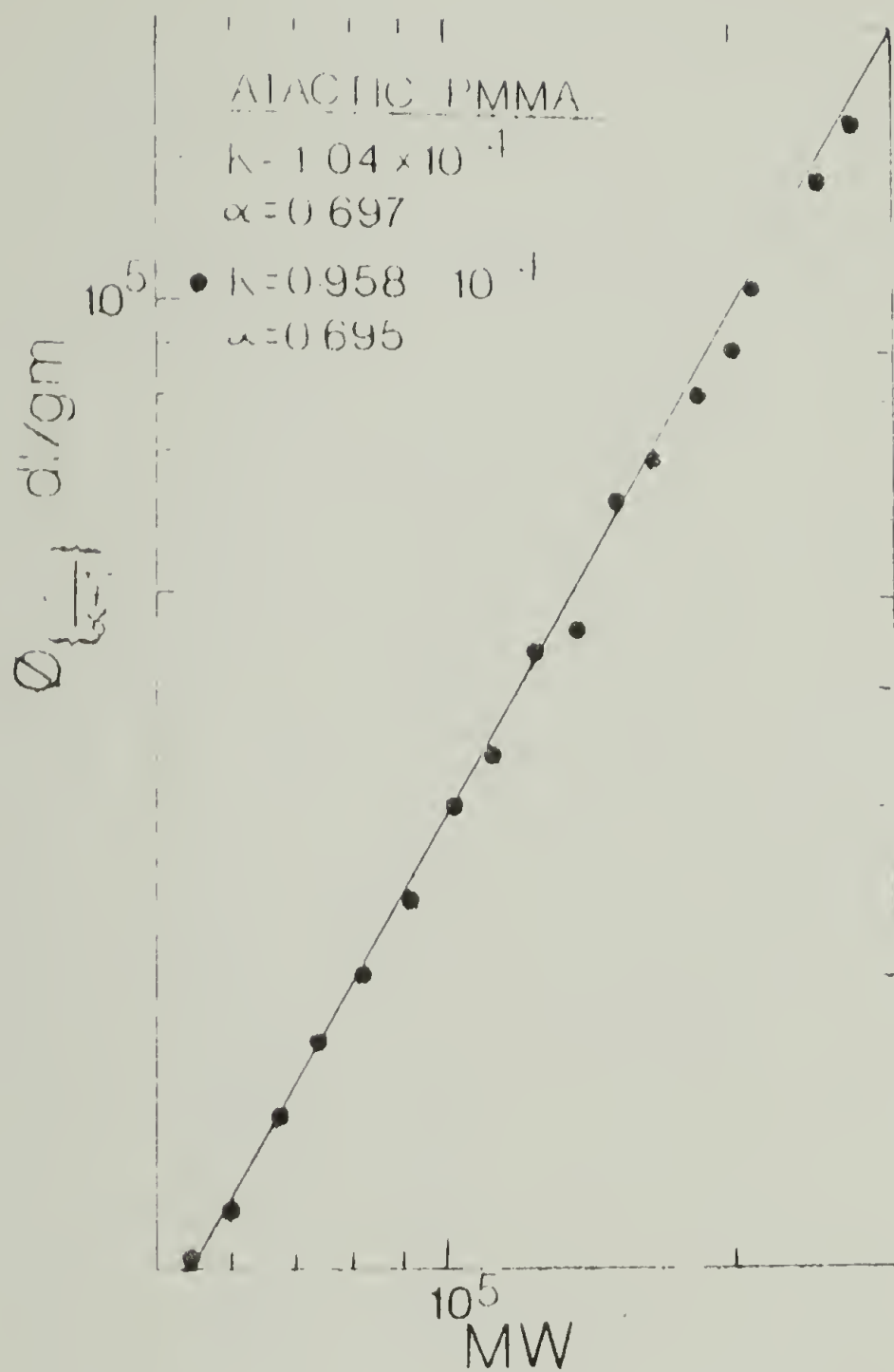


Figure 4.8. The corrected hydrodynamic volume, $\phi \left\{ \frac{1}{\alpha+1} \right\}$, versus molecular weight, MW, for atactic PMMA.

Equation 4.22 states that ϕ_β is equal to ϕ_e , the parameter we measure before correction, times a correction factor. An additional point is that Equation 4.22 is not very sensitive to β . Thus estimating the value of β from Equation 4.21 does not alter the usefulness of this method.

Intrinsic viscosities and molecular weights obtained by this method, and the resultant Mark-Houwink constants are found to be in good agreement with those obtained by conventional viscometry. For polystyrene we obtain, $K = 1.28 \times 10^{-4}$ and $\alpha = 0.70$ as compared to $K = 1.41 \times 10^{-4}$ and $\alpha = 0.70$ as obtained by conventional viscometry (5). For conventional atactic poly(methyl methacrylate) we obtain $K = 0.958 \times 10^{-4}$ and $\alpha = 0.695$ as compared to $K = 1.04 \times 10^{-4}$ and $\alpha = 0.697$ as obtained by conventional viscometry (7). For highly isotactic PMMA, 98% as determined by ^{13}C NMR, we obtain $K = 1.66 \times 10^{-4}$ and $\alpha = 0.66$. Unfortunately, no values are available for comparison.

It is interesting to compare the results of our GPC/LALLS method to those of Benoit et al.⁽¹⁴⁾ who originally developed this method for GPC coupled with on-line viscometry. Figure 4.9 shows schematically a comparison of the results obtained by the GPC/LALLS and the GPC/Viscometry technique for polystyrene in THF. Line A is the relation obtained from the GPC/LALLS system and yields a slope slightly higher than that obtained by conventional intrinsic viscosity and light scattering methods, line B. Line C is the relation obtained from the GPC/Viscometry system and gives a slope considerably lower than that obtained by conventional methods. Equation 4.21 which contains the term $(1 + \tau^2/\delta^2)$ has been used to explain the higher

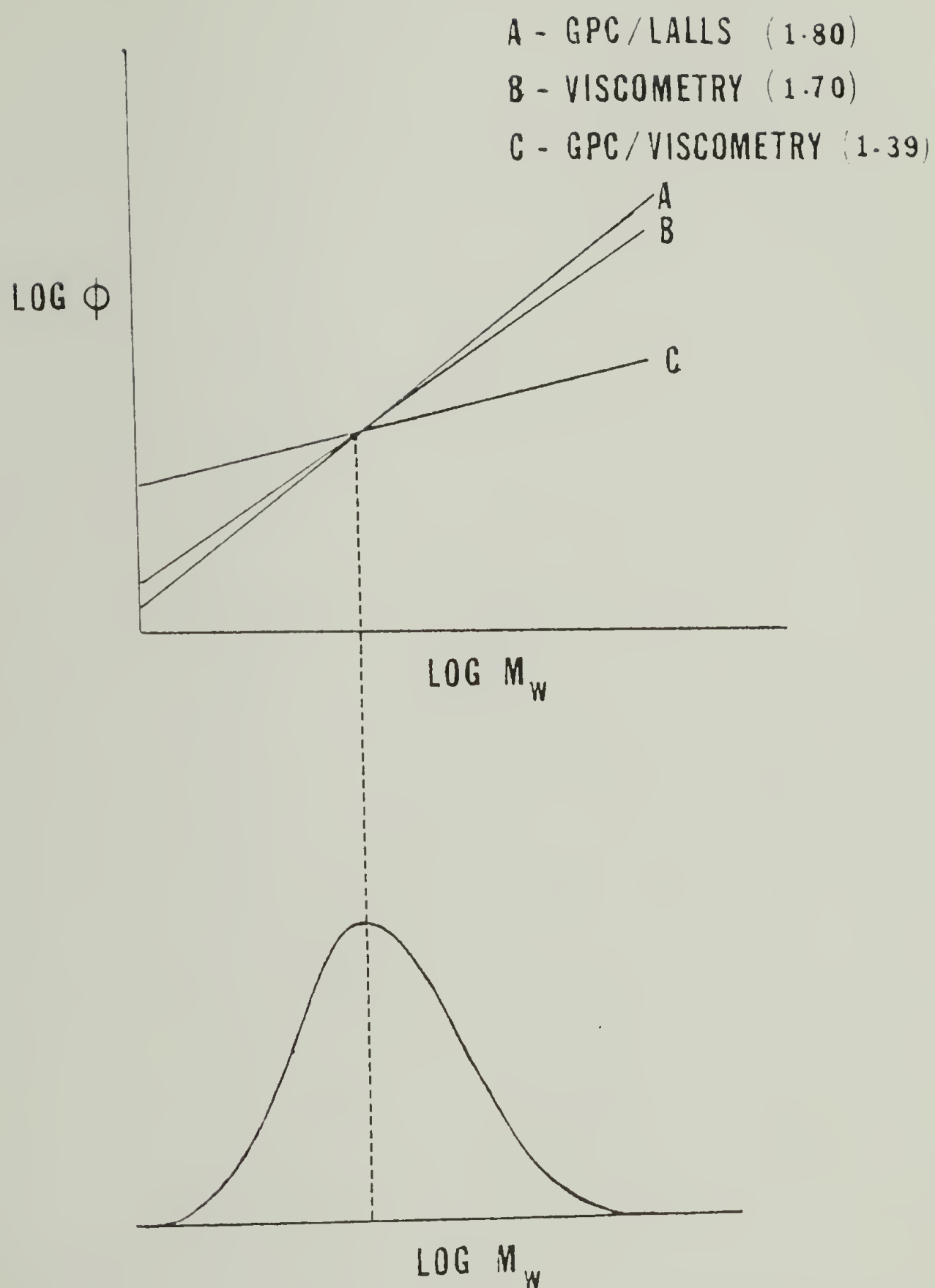


Figure 4.9. A comparison of the uncorrected hydrodynamic volume versus molecular weight as obtained by GPC/LALLS, GPC/viscometry, and conventional intrinsic viscosity measurements.

slope of the GPC/LALLS system. It is interesting to note that for the GPC/Viscometry system Equation 4.21 takes the form;

$$\text{Log } \phi_e = c + (\alpha+1)/(1+\tau^2/\delta^2) \text{ Log } M_w \quad (4.21a)$$

In Equation 4.21a the slope will therefore be lower than $\alpha+1$ by an amount which will depend on the degree of spreading in the system. The fact that the GPC/Viscometry results are in much poorer agreement with those obtained by conventional methods is indicative of the fact that the on-line viscometer has considerably more spreading, a problem which results from the large sample volumes used in the viscometric detector.

It is also interesting to note that lines A, B, and C intersect at a point which corresponds to the peak in the polymers' distribution. This result shows quite clearly the effect of spreading. That is, on one side of the peak spreading causes an overestimation of a value, either the intrinsic viscosity or the molecular weight depending on whether we are using GPC/LALLS or GPC/Viscometry, and on the other side an underestimation. At the peak the effect of spreading is compensated for by the opposing sides of the distribution and we obtain agreement between lines A, B, and C.

Calculation of the Unperturbed Dimensions

The unperturbed dimension is a characteristic parameter of a polymer which directly reflects the conformation of the chain. Knowledge of the conformation is important since it influences many of the properties of a polymer, both in the bulk state and in solution.

Properties such as rubber elasticity, the thermodynamics and hydrodynamics of polymer solutions and birefringence, are only several of the properties which may be related to the conformation. Measurement of the unperturbed dimension is, however, a task which has previously involved considerable time and effort. One method often used to obtain the unperturbed dimension involves measurements of the intrinsic viscosity of several narrow molecular weight fractions in thermodynamically good solvents. Several graphical procedures have been proposed for data treatment which require knowledge of the intrinsic viscosity of polymer fractions of known molecular weight. Those of Fox-Flory⁽¹⁵⁾ Equation 4.23, and Stockmayer-Fixman⁽¹⁶⁾, Equation 4.24, are among the best known.

$$[\eta]^{2/3}/M^{1/3} = K_{\theta}^{2/3} + K_{\theta}^{5/3} C_T (M/[\eta]) \quad (4.23)$$

$$[\eta]/M^{1/2} = K_{\theta} + 0.51\phi BM^{1/2} \quad (4.24)$$

$$\text{where: } K_{\theta} = \phi (\bar{r}_0^2/M)^{3/2} \quad (4.25)$$

$$C_T = 2\psi_1 C_M(1 - \theta/T) = (\alpha^5 - \alpha^3)/M^{1/2}$$

ψ_1 is an entropy parameter

and, $B = \beta/c_m^2$; where: c_m is the molar weight of a chain segment, and β is the binary cluster integral. In each case the unperturbed parameter, K_{θ} , is obtained from the intercept of the appropriate plot.

We have herewith shown that one may generate a series of values for the intrinsic viscosity, $[\eta]_i$, and the molecular weight, M_{w_i} , simply by injecting a polymer with a broad molecular weight distribution

into a gel permeation chromatograph, GPC, coupled with a low-angle laser light scattering photometer, LALLS. These values are then used in the appropriate relations to obtain measurements of the unperturbed dimensions. We have demonstrated this method with two stereoregular poly(methyl methacrylates).

The extrapolation method we chose to use to obtain the unperturbed dimensions was that of Benoit et al. (17) (see Equation 4.26). This is a modification of the Stockmayer-Fixman equation (Equation 4.24), and has the advantage of producing a linear plot, making extrapolation to the unperturbed dimensions less ambiguous:

$$[\eta]/M^{1/2} = K_0 + 0.51\phi\beta M^{1/2}(1 - DM^{1/2}) \quad (4.26)$$

where $D = 12 \times 10^{-4} (\alpha - 0.5)$.

Figure 4.10 shows typical data as obtained for two poly(methyl methacrylate) samples using the method of Benoit et al. (17). The value of K_0 obtained for atactic PMMA, 5.4×10^{-4} , is in excellent agreement with those obtained by conventional measurements, see Table 4.4. In addition, for isotactic poly(methyl methacrylate) we obtain $K_0 = 8.0 \times 10^{-4}$ which also is in very good agreement with values obtained by conventional viscometry (Table 4.3).

Conclusion

We believe this new approach for measurement of the unperturbed dimensions should be applicable to any polymer for which universal calibration is valid. The method has the advantage of producing valuable data concerning a polymer's unperturbed dimension from the

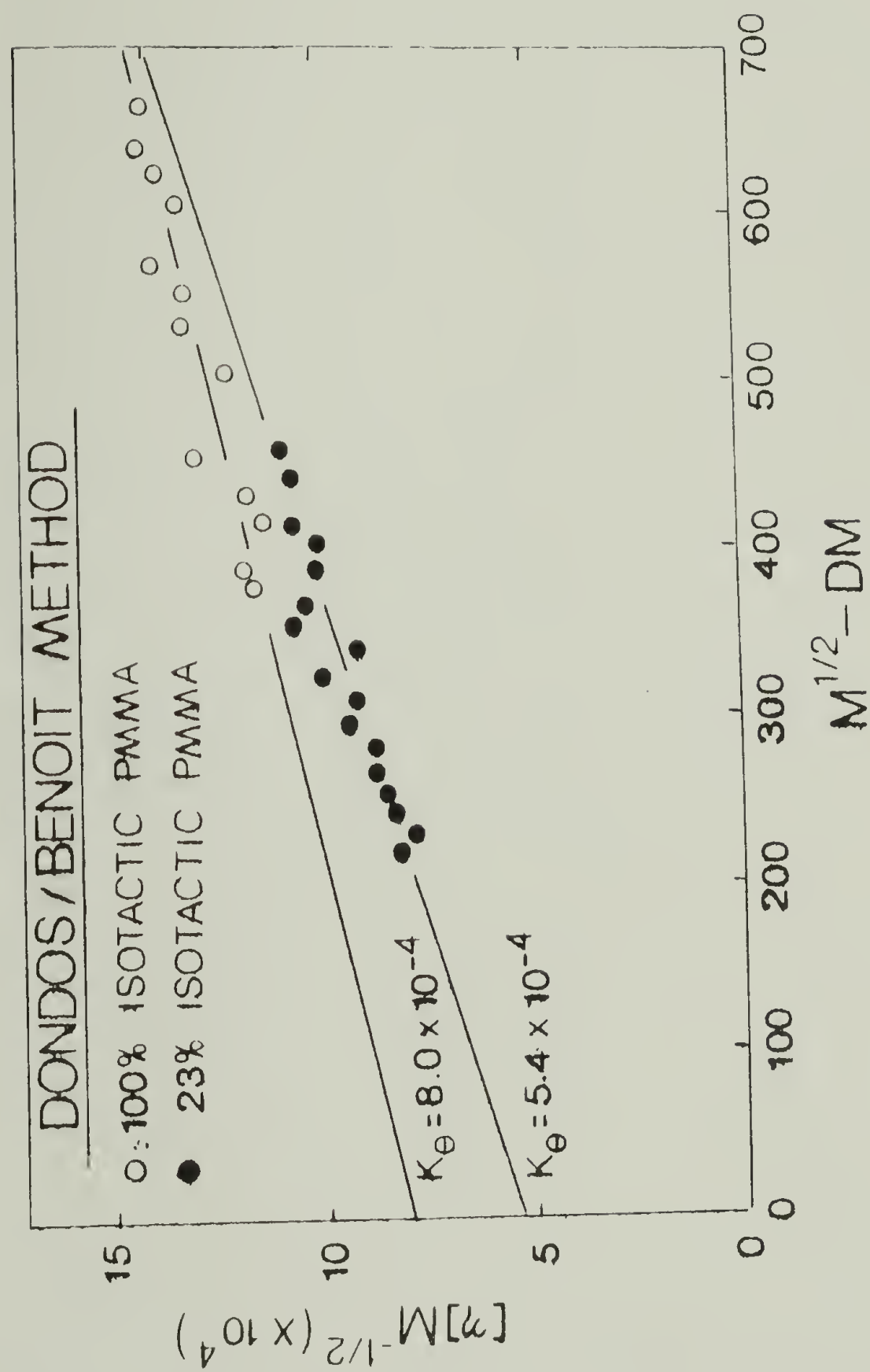


Figure 4.10. Estimation of the unperturbed dimensions for two different stereoregular forms of PMMA using the method of Dondos and Benoit.

TABLE 4.3 Comparison of K_θ values obtained by direct measurement in theta solvents, by the Fox-Flory method, the Stockmayer-Fixman method, and by the GPC/LALLS method.

PMMA	$K_\theta \times 10^4 \text{ (dl g}^{-1}\text{)}$				GPC/LALLS
	Direct Measurement		Fox-Flory	Stockmayer-Fixman	
77% Syndiotactic	5.7 ⁽¹⁹⁾	5.0 ⁽²⁰⁾	4.9 ⁽²¹⁾	4.6 ⁽²²⁾	5.4
98% Isotactic	8.7 ⁽¹⁹⁾	7.7 ⁽²³⁾	7.0 ⁽²⁴⁾	8.2 ⁽²⁵⁾	8.0

injection of a single sample of broad molecular weight distribution. A disadvantage is that it relies on the validity of semi-empirical relations, e.g., Equations 4.23 and 4.24. However, these relations have previously been shown to yield results which are generally within 8% of those determined by direct theta temperature measurements (18).

REFERENCES

1. M.B. Huglin, Light Scattering From Polymer Solutions, Academic Press, New York (1973).
2. Measurement of Molecular Parameters by Low Angle Light Scattering Methods, Chromatix Appl. Note LS-1, 1978.
3. A.C. Ouano, W. Kaye, J. Polym. Sci., P. Chem. Ed., 12, 1151 (1974).
4. A.C. Ouano, J. Chrom., 118, 303 (1976).
5. H. Benoit, Z. Grubisic, P. Rempp, D. Decker, and J.G. Zilliox, J. Chim. Phys., 11, 1507 (1966).
6. T. Spychaj, D. Lath, and D. Berek, Polymer, 20, 437 (1979).
7. W.W. Yau, J.J. Kirkland, and D.D. Bly, Modern Size Exclusion Chromatography, Wiley Interscience, New York (1979).
8. Z.G. Gallot, L. Marais, H. Benoit, J. Polym. Sci., P.Ph., 14, 959 (1976).
9. A.C. Ouano, J. Chrom., 118, 303 (1976).
10. A.C. Ouano, and W. Kaye, J. Polym. Sci., 12, 1151 (1974).
11. A.E. Hemelec., A.C. Ouano, and L.L. Nebenzahl, J. Liq. Chrom., 1 (4), 527 (1978).
12. T.B. MacRury, and M.L. McConnell, J. Appl. Polym. Sci., 24, 651 (1979).
13. L. Marais, and H. Benoit, J. Appl. Polym. Sci., 21, 1955 (1977).
14. L. Marais, Z. Gallot, and H. Benoit, Analysis, 4, 443 (1976).
15. P.J. Flory, and T.G. Fox, J. Amer. Chem. Soc., 73, 1904 (1951).
16. W.H. Stockmayer, and M.J. Fixman, J. Polym. Sci., c, 1, 137 (1963).
17. A. Dondos, and H. Benoit, Polymer, 19, 523 (1978).
18. J.M.G. Cowie, Polymer, 7, 487 (1966).

19. I. Sakurada, A. Nakajima, D. Yoshizaki, and K. Nakamae, *Kolloid-Z.Z. Plym.*, 186, 41 (1962).
20. T.G. Fox, *Polymer*, 3, 111 (1962).
21. S. Gundiah, R.B. Mohite, and S.L. Kapur, *MaKromol. Chem.*, 123, 151 (1969).
22. P. Vasudevan, and M. Santappa, *J. Polym. Sci., A-2*, 9, 483 (1971).
23. G.V. Schulz, W. Wunderlich, and G.V. Kirste, *MaKromol. Chem.*, 75, 22 (1964).
24. S. Krause, and E. Cohn-Ginsberg, *Polymer*, 3, 565 (1962).
25. E. Hamorie, L.R. Pusinowski, P.G. Sparks, and R.E. Hughes, *J. Phys. Chem.*, 69, 1101 (1965).

CHAPTER V

MEASUREMENT OF THE UNPERTURBED DIMENSIONS OF STEREOREGULAR POLY(METHYL METHACRYLATE)

Introduction

Chapter I presented a literature review encompassing information available on the unperturbed dimensions of stereoregular polymers. A method considered in Chapter I, and used in Chapter IV, involved measurement of intrinsic viscosity and molecular weight for a series of narrow molecular weights and extrapolation to the unperturbed dimension. In Chapter IV methods were developed whereby the necessary values can be obtained from a GPC/LALLS system and the MWD of a single polymer sample. Measurement of the unperturbed dimension was then made using the method of Dondos and Benoit⁽¹⁾ for two different stereoregular forms of PMMA.

This chapter reports on a set of six stereoregular PMMA samples, ranging from 15% to 100% isotactic dyad content. Data was generated by the GPC/LALLS technique described in Chapter IV and the dimensions obtained by six different extrapolation procedures.

Measurement of the Molecular Weights and Intrinsic Viscosities. The experimental conditions used for the six stereoregular PMMA samples were identical to those described in Chapter IV. The methods used to determine the incremental values of $[\eta]_i$, and M_{w_i} were also

described in Chapter IV. The samples used in this work were the stereoregular PMMA's prepared in Chapter II and characterized in Chapters II and III.

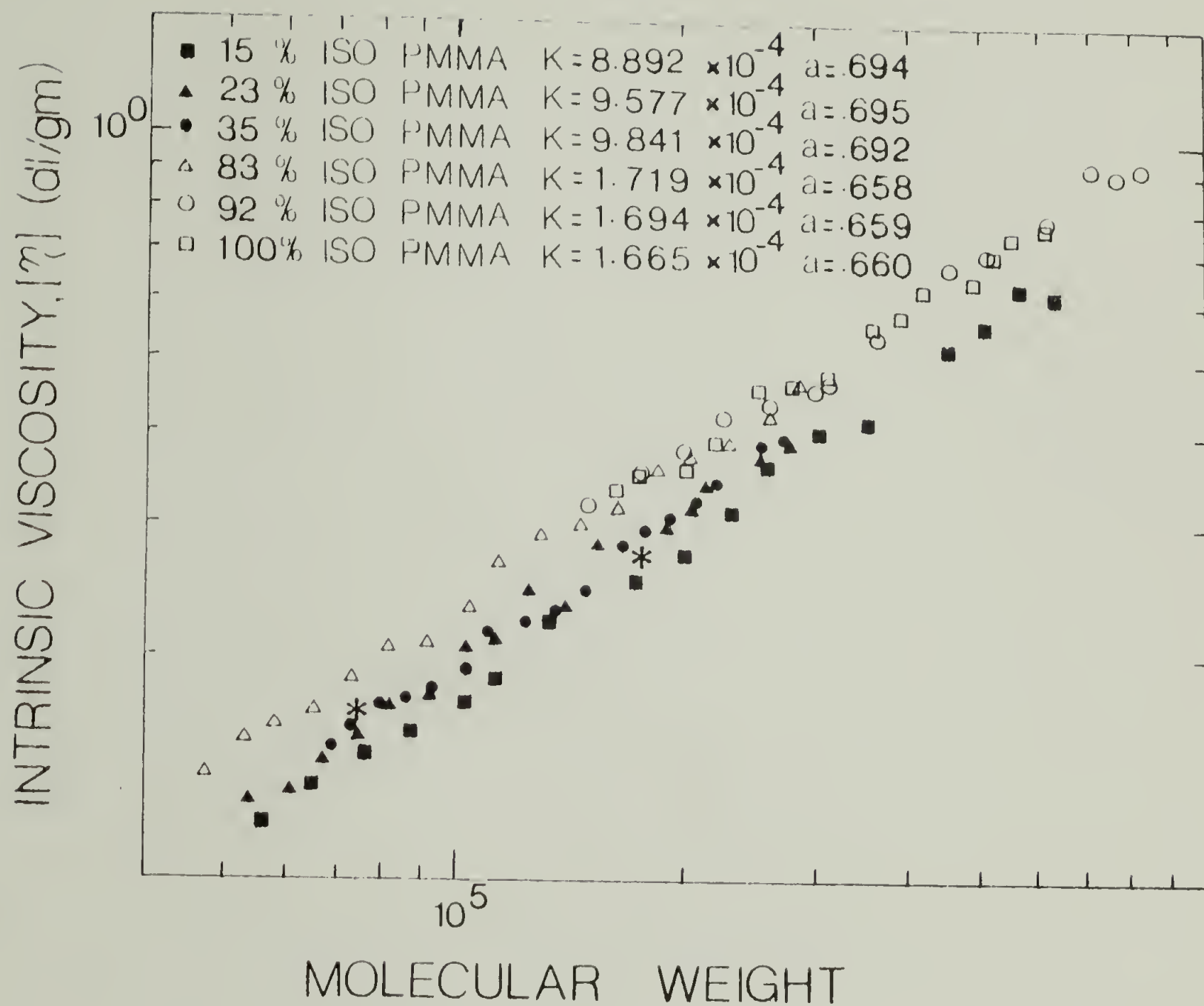
Table 5.1 lists the $[\eta]_i$ and M_i data obtained for six stereoregular forms of PMMA. As described in Chapter IV, the incremental values of $[\eta]_i$ and M_{w_i} were determined from the portion of the distribution where adequate response was obtained from the two detectors. Data was obtained at 0.25 ml increments. This procedure usually resulted in 14-17 usable data points for each sample. Outside this range, data scatter was excessive. In the lower portion of Table 5.1 the Mark-Houwink constants K and α are listed. The data suggests that there is very little measurable difference among the three isotactic samples, samples 5b, 7, and 8b, or among the three most syndiotactic samples, samples 1, 2, and 4a. Considerable difference is observed, however, between the three isotactic and the three syndiotactic samples. The isotactic samples exhibit Mark-Houwink exponents generally of the order of 0.66, whereas, an average value of 0.69 is obtained for the more syndiotactic set.

Figure 5.1 shows all the data in Table 5.1 plotted graphically as $[\eta]$ versus MW. The open symbols are the isotactic samples, samples 5b, 7 and 8b, and the filled symbols are the more syndiotactic samples, 1, 2, and 4a. The difference between the isotactic and syndiotactic sets is obvious. All the data points for the isotactic sets lie above those for the syndiotactic polymers, although at high molecular weight, 10^6 , the least squares lines through the data tend to converge.

Table 5.1. Intrinsic Viscosity--Molecular Weight Relationship for Stereoregular PMMA

Sample 8b 100% Iso [η] Mx10 ⁻⁵	Sample 7 92% Iso [η] Mx10 ⁻⁵	Sample 5h 83% Iso [η] Mx10 ⁻⁵	Sample 4a 35% Iso [η] Mx10 ⁻⁵	Sample 2 23% Iso [η] Mx10 ⁻⁵	Sample 1 15% Iso [η] Mx10 ⁻⁵
.472	.450	.204	.219	.190	.180
1.66	1.50	.48	.69	.54	.57
.492	.504	.228	.235	.192	.201
1.76	1.74	.54	.73	.60	.65
.512	.535	.238	.251	.215	.222
2.05	2.01	.59	.80	.67	.76
.551	.590	.244	.255	.232	.235
2.22	2.25	.66	.86	.74	.87
.654	.620	.274	.265	.251	.257
2.55	2.61	.74	.93	.82	1.03
.664	.650	.300	.281	.261	.274
2.85	2.98	.82	1.03	.92	1.12
.680	.661	.301	.315	.299	.330
3.16	3.05	.93	1.10	1.02	1.34
.793	.775	.338	.321	.305	.371
3.61	3.62	1.05	1.23	1.12	1.71
.821	.957	.389	.332	.355	.402
3.95	4.51	1.15	1.35	1.25	1.98
.896	.999	.423	.351	.337	.457
4.21	5.03	1.31	1.48	1.37	2.36
.921	1.10	.435	.407	.415	.531
4.87	6.10	1.47	1.65	1.52	2.61
.991	1.30	.459	.427	.419	.589
5.23	6.98	1.65	1.76	1.66	3.02
1.05	1.27	.521	.440	.435	.605
5.55	7.54	1.86	1.91	1.86	3.51
1.09	1.30	.530	.464	.451	.750
6.10	8.10	2.04	2.05	2.03	4.51
		.562	.499	.490	.805
		2.31	2.20	2.13	5.00
		.612	.552	.534	.920
		2.60	2.52	2.53	5.64
		.675	.569	.569	.890
		2.88	2.73	2.75	6.13
<hr/>					
$K = 1.665 \times 10^{-4}$	$K = 1.690 \times 10^{-4}$	$K = 1.719 \times 10^{-4}$	$K = 9.84 \times 10^{-5}$	$K = 9.577 \times 10^{-5}$	$K = 8.892 \times 10^{-5}$
$\alpha = 0.660$	$\alpha = 0.659$	$\alpha = 0.658$	$\alpha = 0.692$	$\alpha = 0.695$	$\alpha = 0.694$

$$[\eta] = K M^\alpha$$



* Data obtained by conventional viscometry

Figure 5.1. A comparison of the intrinsic viscosity-molecular weight relation for six different stereoregular forms of poly(methyl methacrylate).

Figure 5.1 also shows two data points as an asterisk, *. These two data points represent the results of conventional $[\eta]$ and MW measurements for two commercially available narrow MWD PMMA standards; Polysciences, Inc., Warrington PA. Good agreement is shown between the results obtained by conventional methods and those obtained by the GPC/LALLS method.

Calculation of unperturbed dimensions.

Measurement of K_θ . As discussed in Chapters I and IV there are several relations which have been previously proposed for the calculation of unperturbed dimensions from measurements of intrinsic viscosity and molecular weight. The theory behind these methods is discussed in Chapter I. It suffices here to note that none of the proposed method has been shown to give good results under all circumstances. As a result, it has been suggested⁽¹⁾ that the extrapolation procedures be used to complement one another.

In this chapter the intrinsic viscosity and molecular weight data obtained for the six stereoregular forms of PMMA is evaluated using six different extrapolation procedures. The methods proposed by Fox and Flory⁽²⁾, Equation 5.1; Stockmayer and Fixman⁽³⁾, Equation 5.2; and Berry⁽⁴⁾, Equation 5.3; were described in Chapter I. The method of Dondos and Benoit⁽⁵⁾, Equation 5.4, which is a modification of the Stockmayer-Fixman method was described in Chapter IV. In addition, we also use the methods of Cowie⁽⁶⁾ Equation 5.5, and Inagaki et al⁽⁶⁾, Equation 5.6. Cowie's method has the advantage of incorporating a solvent-dependent factor, $\phi(\epsilon)$, whereas the method of Inagaki et al, has been shown⁽⁶⁾ to yield accurate K_θ values even in thermodynamically good solvents.

$$[\eta]^{2/3}/M^{1/3} = K_{\theta}^{2/3} + K_{\theta}^{5/3} C_T (M/[\eta]) \quad (5.1)$$

$$[\eta]/M^{1/2} = K_{\theta} + .51\phi BM^{1/2} \quad (5.2)$$

$$([\eta]/M^{1/2})^{1/2} = K_{\theta}^{1/2} + .42K_{\theta}^{3/2} B (\bar{r}_0^2/M)^{-3/2} (M/[\eta]) \quad (5.3)$$

The terms C_T , ϕ , and B have been defined in Chapter 1.

$$[\eta]/M^{1/2} = K_{\theta} + .51 \phi BM^{1/2} (1-DM^{1/2}) \quad (5.4)$$

Where D has been described in Chapter IV.

$$[\eta]/M^{1/2} = (\phi(\epsilon)/\phi_0) K_{\theta} + 0.9166(\phi(\epsilon)/\phi_0) K_{\theta} k^{7/10} M^{7/20} \quad (5.5)$$

Here we have;

$$\epsilon = (2\alpha - 1)/3 \quad (5.5a)$$

where α is the Mark-Houwink exponent, and;

$$\phi(\epsilon) = \phi_0 (1 - 2.63\epsilon + 2.86 \epsilon^2) \quad (5.5b)$$

$$[\eta]^{4/5}/M^{-2/5} = 0.786K_{\theta}^{4/5} + 0.950K_{\theta}^{4/5} k^{2/3} M^{1/3} \quad (5.6)$$

where;

$$k = 0.33B[M/(\bar{r}_0^2)_0]^{3/2} \quad (5.6a)$$

In each of Equations 5.1-5.6, the unperturbed parameter, K_{θ} defined in Equation 5.7 is obtained from the intercept of the appropriate plot involving intrinsic viscosity and molecular weight values.

$$K_{\theta} = \phi(\bar{r}_0^2/M)^{3/2} \quad (5.7)$$

In addition, from the slope of each we may obtain several thermodynamic parameters characterizing the polymer-solvent interactions. These polymer-solvent interaction parameters will be discussed in a later section. Figures 5.2-5.7 show examples of each of Equations 5.1-5.6 graphically for two different tactic forms of PMMA, one highly isotactic, sample 8b, and the other syndiotactic, sample 2. In each figure a straight line is obtained with the unperturbed parameter K_{θ} as the intercept. Least squares analysis was used to obtain K_{θ} values,

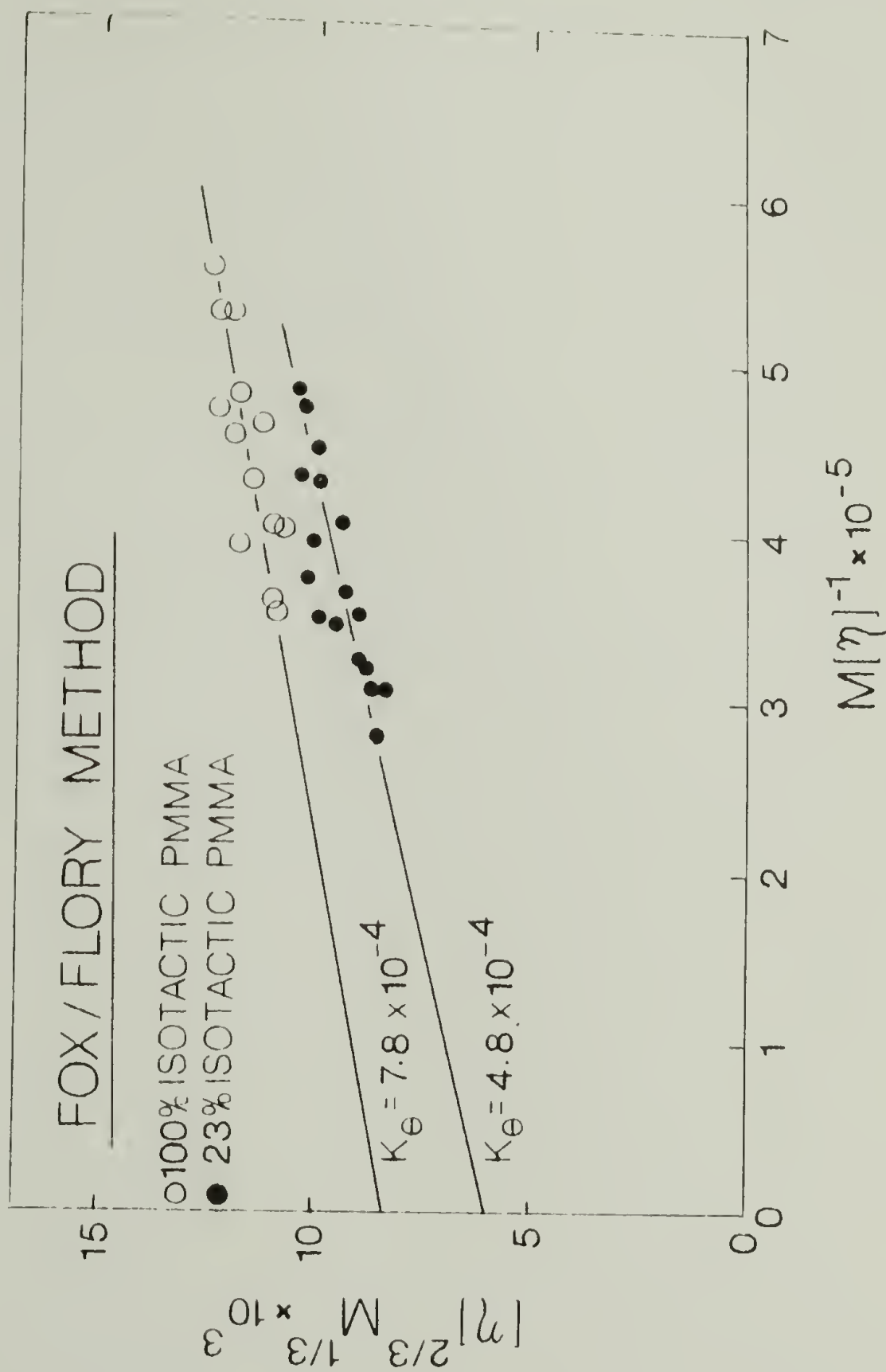


Figure 5.2. Estimation of the unperturbed dimensions for two different stereoregular forms of poly(methyl methacrylate), using the method of Fox and Flory.

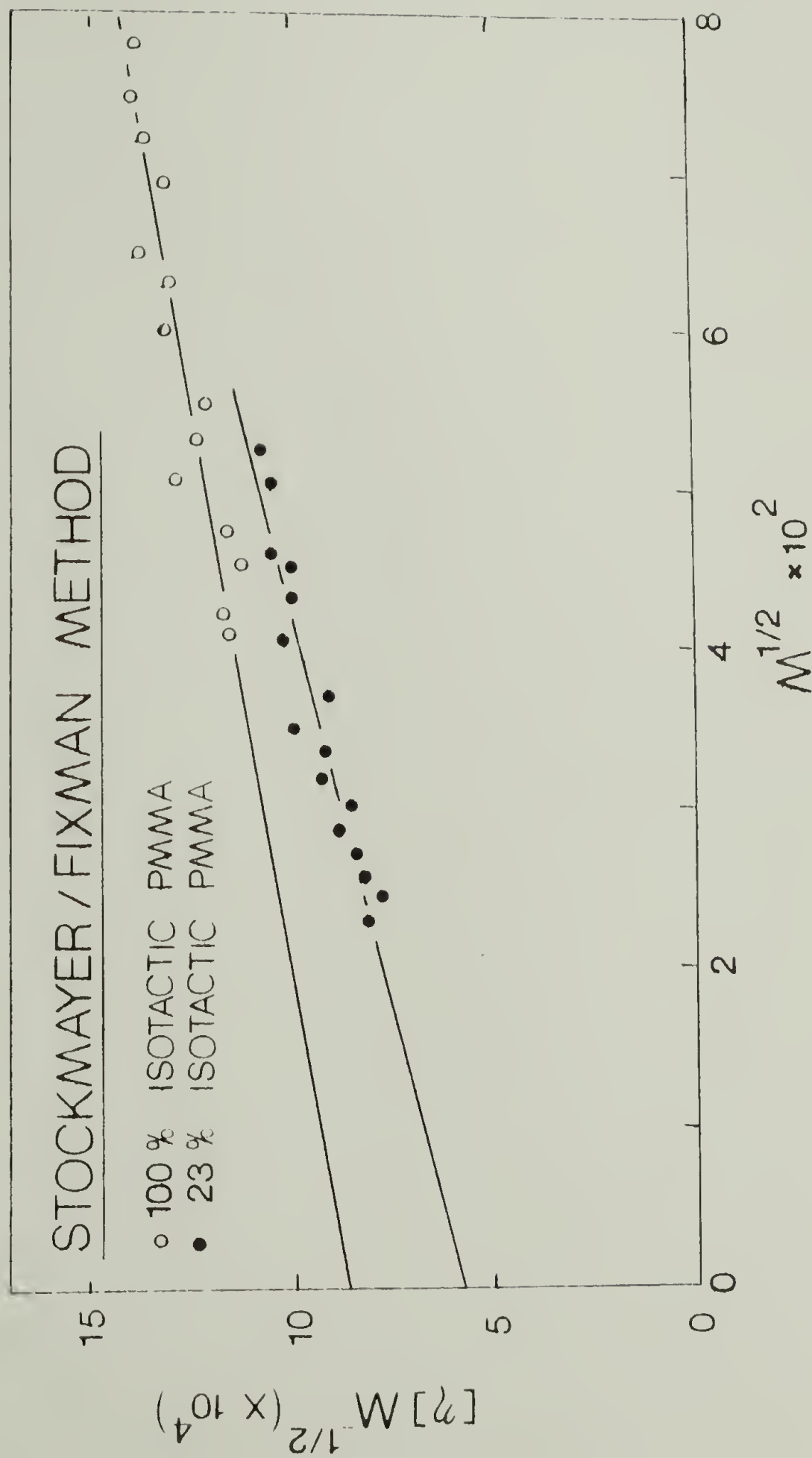


Figure 5.3. Estimation of the unperturbed dimensions for two different stereoregular forms of poly(methyl methacrylate) using the method of Stockmayer and Fixman.

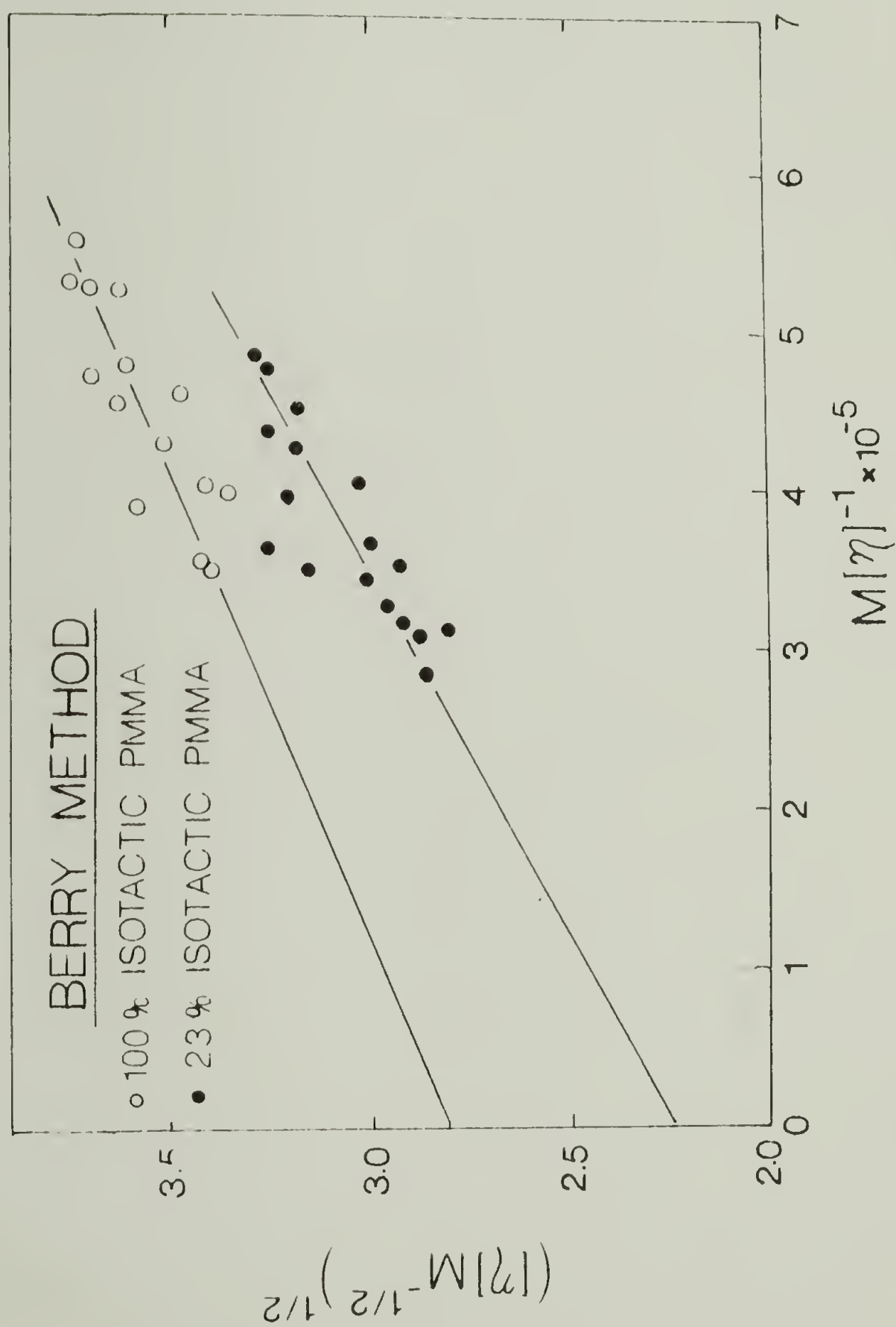


Figure 5.4. Estimation of the unperturbed dimensions for two different stereoregular forms of poly(methyl methacrylate) using the method of Berry.

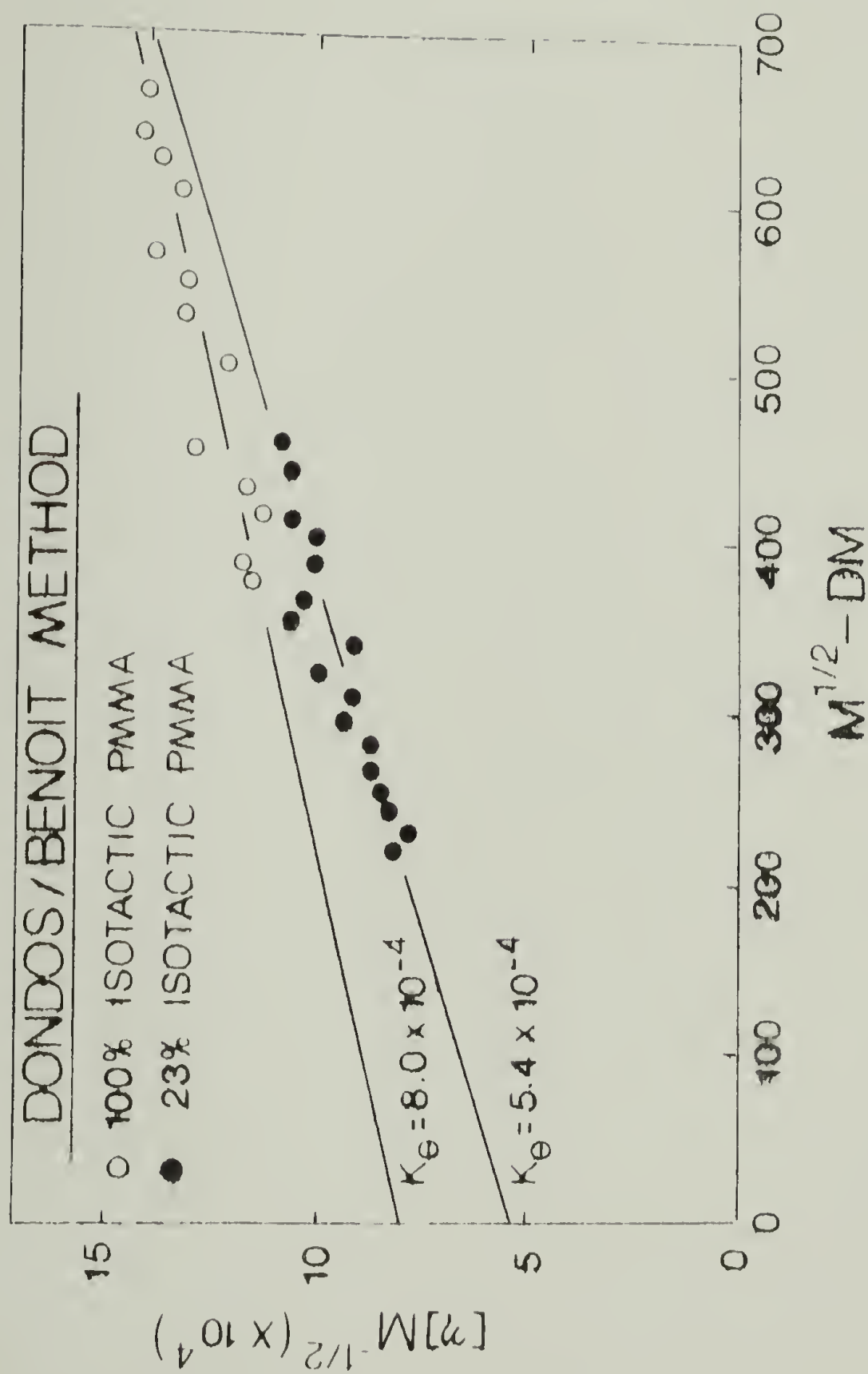


Figure 5.5. Estimation of the unperturbed dimensions for two different stereoregular forms of poly(methyl methacrylate) using the method of Dondos and Benoit.

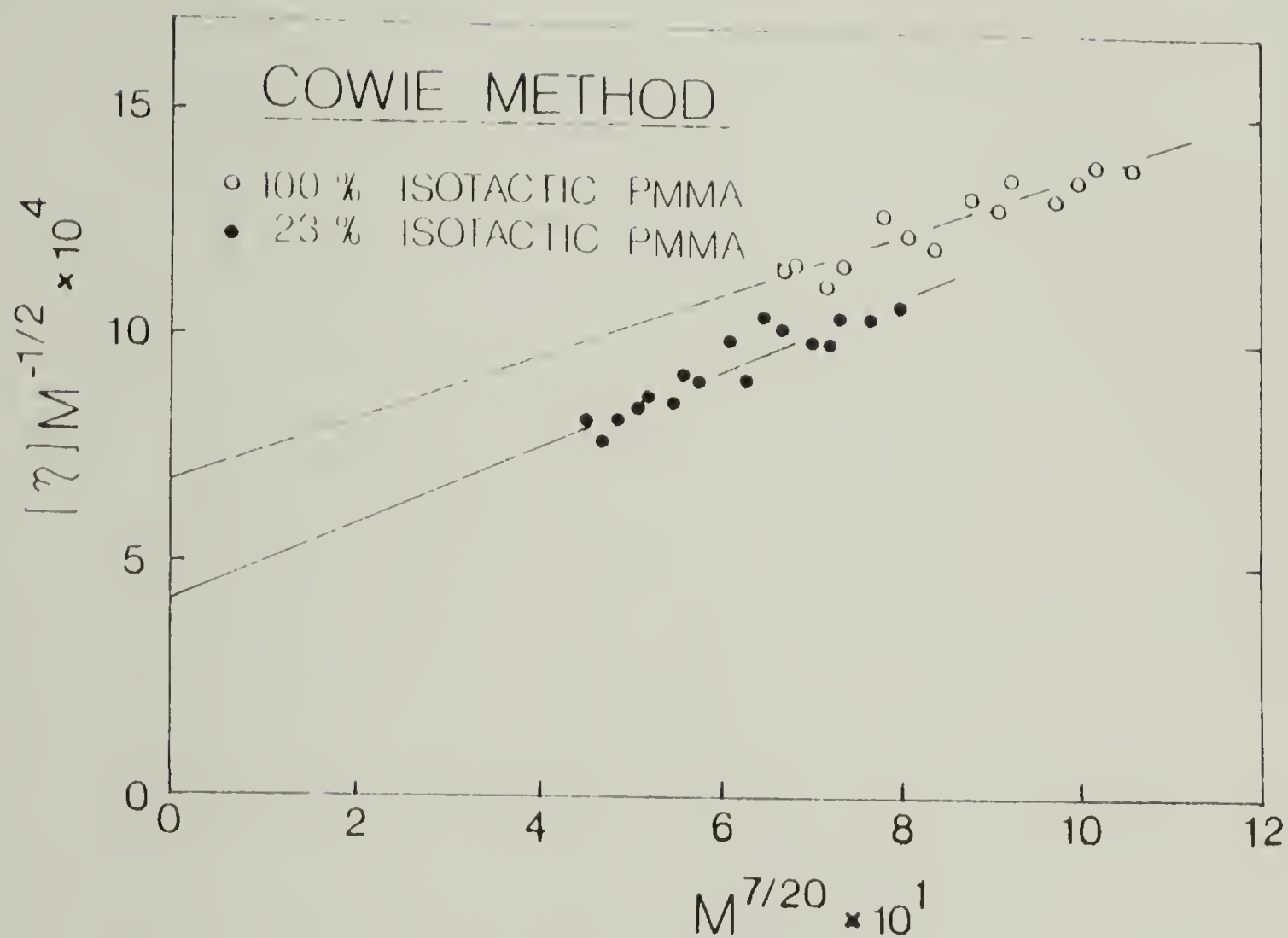


Figure 5.6. Estimation of the unperturbed dimensions for two different stereoregular forms of poly(methyl methacrylate) using the method of Cowie.

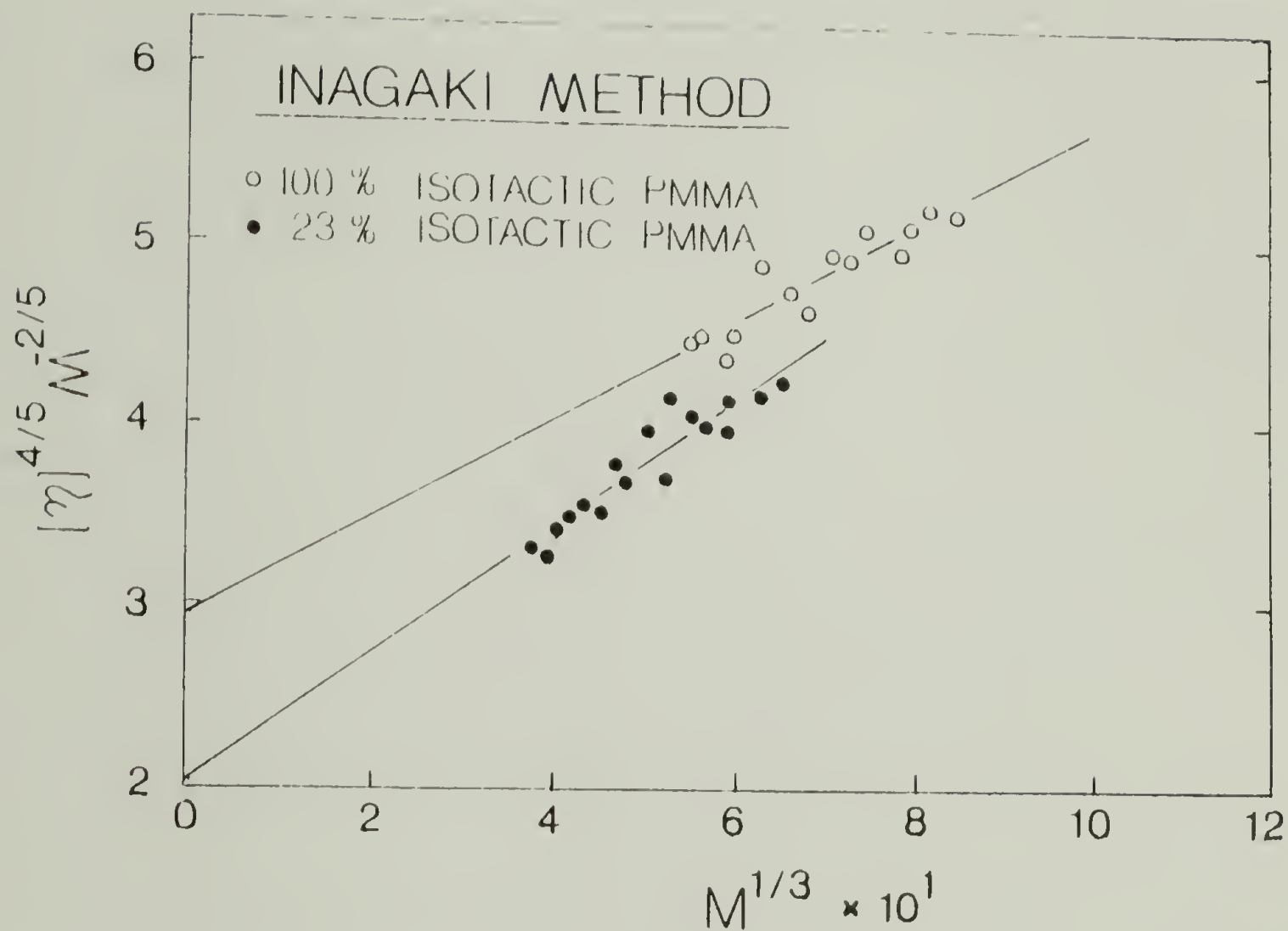


Figure 5.7. Estimation of the unperturbed dimensions for two different stereoregular forms of poly(methyl methacrylate) using the method of Inagaki.

which are listed in Table 5.2 for each of the six samples. In each case the values of K_θ obtained were determined to be accurate to 10%. The error resulting primarily from the extrapolation rather than from scatter in the data.

The agreement between the K_θ values predicted by the six different methods. Equations 5.1-5.6, is quite good. For example, for the 100% isotactic sample, Figures 5.2-5.6, the K_θ values ranged from 7.8 to 9.2×10^{-4} dl/gm with an average value of $8.4 \times 10^{-4} \pm 0.5 \times 10^{-4}$. Whereas for the 23% isotactic sample, also shown in Figures 5.2-5.7, the K_θ values ranged from 4.8 to 6.0×10^{-5} dl/gm with an average value of $5.4 \times 10^{-4} \pm .4 \times 10^{-4}$. It is also apparent from Table 5.2 that there is little measurable difference among the three isotactic samples, 5b, 7 and 8b or among the three syndiotactic samples, 1, 2 and 4a, there is however considerable difference between the sets of isotactic and syndiotactic polymers. Comparison of the values in Table 5.2 with those in the literature from both direct and indirect measurements, see Table 1.1, shows good agreement. Values range from 7.0 to 8.7 for the "isotactic" polymers which compares well with our values of 6.7 to 9.2. For the "syndiotactic" samples literature values range from 4.4 to 6.8, which also compares well with our values of 4.3 to 6.0. The agreement between the six different extrapolation procedures, Equations 5.1 to 5.6, is good, within the precision of the methods, $\pm 10\%$. We thus chose to use the arithmetic average of the K_θ values for calculation of the characteristic ratio in the next section. The average values are reported in Column 8, Table 5.2.

Table 5.2. K_{θ} Values for Stereoregular PMMA.

Sample	$K_{\theta} \times 10^4 \text{ (dl/gm)}$						
	Dondos/ Benoit	Stockmayer/ Fixman	Berry	Inagaki	Fox/Flory	Cowie	Average C_{∞}
(8b) 100% isotactic	8.0	8.6	8.0	8.8	7.8	9.2	8.4 10.2
(7) 92% isotactic	8.2	8.8	8.2	9.0	8.0	9.1	8.5 10.3
(5b) 83% isotactic	7.2	7.5	6.8	7.7	6.7	8.0	7.3 9.3
(4a) 35% isotactic	5.4	5.7	4.8	5.5	4.6	5.9	5.3 7.5
(2) 23% isotactic	5.4	5.8	5.0	5.5	4.8	6.0	5.4 7.5
(1) 15% isotactic	5.2	5.7	4.5	5.4	4.3	5.8	5.1 7.3

K_{θ} Values $\pm 10\%$

Calculation of the characteristic ratio. The characteristic ratio, C_∞ , is a parameter which compares the unperturbed mean square end-to-end distance, $\langle r^2 \rangle_0$, to the dimensions of the chain if each segment were freely rotating. For the case of a freely rotating chain it has been shown⁽⁷⁾ that the dimensions of the chains are simply given by Equation 5.8.

$$\langle r^2 \rangle_0 = nl^2 \quad (5.8)$$

The characteristic ratio is defined by;

$$C_n = \langle r^2 \rangle_0 / nl^2 \quad (5.9)$$

where C_n is the characteristic ratio for a chain of length n . For a freely rotating chain C_n is unity for all values of n , but for all other cases C_n will be larger than unity by an amount which will depend on the extension of the chain.

The characteristic ratio is related to the parameter K_θ and consequently may be obtained from Equation 5.10

$$C_\infty = (K_\theta / \phi)^{2/3} M_b / l^2 \quad (5.10)$$

Where M_b is the mean molecular weight per skeletal bond, l is the bond length, and ϕ is Flory's universal constant. The value for C_∞ will depend on the value chosen for ϕ . As discussed in Chapter I several values ranging from 1.8 to 2.87×10^{21} have been proposed. We have chosen to use the value $\phi = 2.5 \times 10^{21}$, as recommended by Yamakawa⁽⁸⁾. Table 5.2, Column 9 lists the characteristic ratios calculated from the average K_θ values reported in Column 8. For the three isotactic samples, 5b, 7, and 8b, we obtain an average value of 9.9 whereas for the three syndiotactic samples, 1, 2 and 4a, we obtain an average of 7.5. The isotactic polymers are thus shown to exhibit dimensions $\approx 35\%$ larger

than the syndiotactic forms. These values are in very good agreement with those of other researchers as collected in Chapter I, Table 1.1.

Figure 5.8 shows graphically the effect of stereoregularity on the unperturbed dimensions. Here we have plotted the characteristic ratio, C_∞ , versus the fraction of isotactic dyads in the chain, f_i . Whereas the dashed line drawn through the data is presumptuous, the trend is obvious. The more isotactic polymers exhibit approximately 35% larger, unperturbed dimensions. The bars shown in Figure 5.8 represent estimated uncertainties of 10%, that result primarily from the extrapolation used to obtain K_θ from which C_∞ is calculated.

Statistical calculations of unperturbed dimensions. As described in Chapter I, methods have been developed whereby statistical calculations can predict the dimensions of a polymer from the rotational isomeric scheme. Assumptions are required about the geometry of pendent groups. These calculations have been extended⁽¹⁷⁾ to predict the effect of tacticity on the unperturbed dimensions by Monte Carlo methods. The Monte Carlo methods were employed to generate chains generally consisting of 200 units with random sequencing of meso and racemic dyads. The results of these calculations for PMMA⁽⁹⁾ are shown in Chapter I, Figure 1.11, along with published data. The three curves, labeled A, B, and C, Figure 1.11, are attempts by Flory et al⁽⁹⁾ to fit the available data. Flory⁽⁹⁾ concluded that agreement with experimental values of C_∞ is obtained by taking $E_\alpha = 1.1 \text{ kcal mole}^{-1}$ and $E_\beta = -0.6 \text{ kcal mole}^{-1}$, α and β being the statistical weights for the meso, gt and the racemic, tt states, respectively, relative to the meso tt state. Comparison of

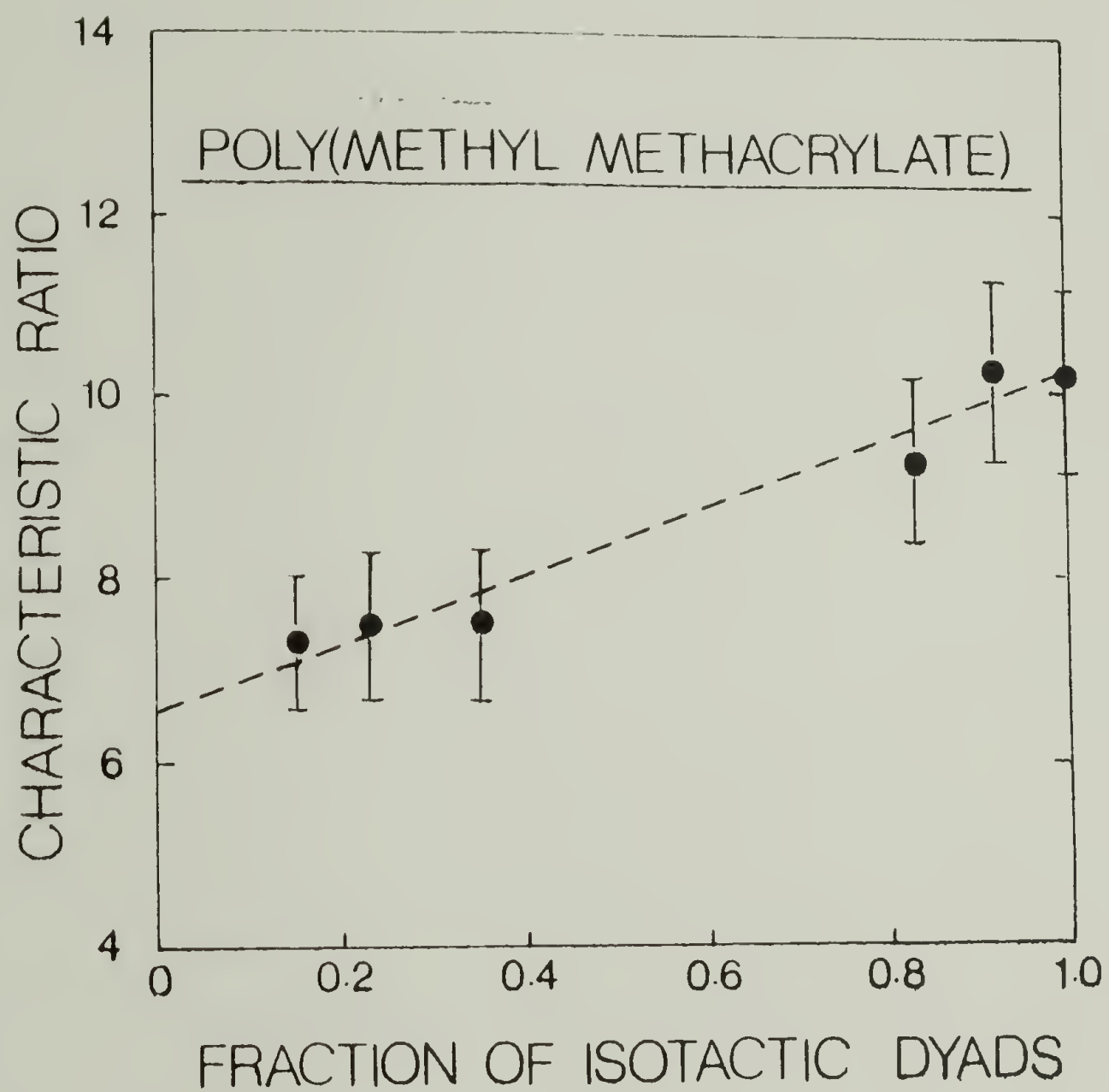


Figure 5.8. The characteristic ratio versus the fraction of isotactic dyads for poly(methyl methacrylate).

our data in Figure 5.8 with the statistical curves shown in Figure 1.11 reveals good agreement. That is, the data obtained by the GPC/LALLS method agrees with curve B for which $E_{\alpha}=1.2 \text{ kcal mole}^{-1}$ and $E_{\beta}=-0.6 \text{ kcal mole}^{-1}$.

Discussion

The reason why isotactic PMMA is 35% more extended than the syndiotactic polymer in its unperturbed state may lie the fact that isotactic PMMA is capable of existing in a helical conformation.⁽¹⁰⁾ X-Ray studies⁽¹⁰⁾ of isotactic PMMA have shown segments of the polymer to exist in a 10_1 - double helix in the crystalline state. It is believed that the helical (trans-to-gauche) segments, because they are in the most energetically stable conformation, might also be capable of existing in the amorphous solid state as well as in dilute solution, although not necessarily in the double helix. The larger dimensions exhibited by isotactic PMMA, as compared to the syndiotactic polymer, in both the perturbed and unperturbed states may then be postulated as resulting from the presence of the helical segments.

Polymer Solvent Interaction Parameter

The slopes of Equations 5.1 to 5.6 reflects the degree of polymer-solvent interaction. Table 5.3 lists the slopes obtained from each of the six different tactic forms of PMMA. In each case the highly isotactic samples, 5b, 7 and 8b, exhibit lower slopes than the syndiotactic samples, 1, 2, and 4a indicating a lesser degree of polymer-solvent interaction.⁽⁸⁾

Table 5.3. Least Squares Slopes Obtained for Equations 5.1 to 5.6

PMMA Sample	Slope of Viscosity Plot					
	Dondos/ Benoit ($\times 10^6$)	Stockmayer/ Fixman ($\times 10^6$)	Berry ($\times 10^8$)	Inagaki ($\times 10^5$)	Fox/Flgry ($\times 10^9$)	Cowie ($\times 10^6$)
(8b) 100% Isotactic	.917	.709	1.65	2.69	7.26	6.84
(7) 92% Isotactic	.919	.693	1.63	2.67	7.22	6.84
(5b) 83% Isotactic	1.11	.954	2.13	3.21	9.09	8.02
(4a) 35% Isotactic	1.21	.998	2.27	3.46	9.53	8.44
(2) 23% Isotactic	1.22	1.01	2.20	3.49	9.19	8.48
(1) 15% Isotactic	1.06	.808	1.97	3.04	8.24	7.35

The parameter we are interested in is B which characterizes the degree of polymer-solvent interaction, and is given by Equation 5.11;

$$B = B/M_S^2 \quad (5.11)$$

where M_S is the molecular weight of the segment and B is the "Binary Cluster Integral". Before we can calculate β from the Fox-Flory method, Equation 5.1, this equation must be rewritten in a form from which β can be obtained.

Yamakawa⁽⁸⁾ has proposed,

$$[\eta]^{2/3}/M^{1/3} = K^{2/3} + 0.858 K^{2/3} \phi_0 BM/[\eta] \quad (5.1a)$$

Table 5.4 lists the values of B as obtained by the six different methods, Equations 5.1 to 5.6, for each of the six stereoregular forms of PMMA. In addition to the six methods used throughout this chapter, Equations 5.1 to 5.6, two additional methods, Equations 5.12 and 5.13 were used to calculate the parameter, B . These

$$[\eta]/M^{1/2} = K_\theta + 0.346\phi_0 BM^{1/2} \quad (5.12)$$

$$[\eta]/M^{1/2} = 1.05K_\theta + 0.287\phi_0 BM^{1/2} \quad (5.13)$$

equations are modifications of the Stockmayer-Fixman equation, Equation 5.2, and were proposed by Yamakawa⁽⁸⁾ in an attempt to compensate for the underestimated values of B obtained from the Stockmayer-Fixman equation.

Table 5.4 shows that the parameter B varies considerably with the method used to obtain B . With the exception of the Cowie method, Equation 5.5, most of the methods are however in qualitative agreement for a particular tactic form of PMMA. For the isotactic

Table 5.4. The Polymer-Solvent Interaction Parameter, B., for Stereoregular PMMA.

Sample	$B \times 10^{28} (\text{cm}^3)$					
	Dondos/ Benoit	Stockmayer/ Fixman	Berry	Inagaki	Fox/Flory	Cowie
(8b) 100% isotactic	7.19	5.56	5.56	7.46	3.99	17.9
(7) 92% isotactic	7.21	5.44	5.42	7.34	3.90	18.1
(5b) 83% isotactic	8.74	7.48	7.78	9.99	5.53	23.9
(4a) 35% isotactic	9.50	7.82	9.86	11.9	7.45	31.9
(2) 23% isotactic	9.59	7.89	9.37	11.9	6.98	31.8
(1) 15% isotactic	8.28	6.33	8.84	9.88	6.74	26.4

samples, 5b, 7 and 8b, values of B are consistently lower than for the syndiotactic samples 1, 2 and 4a. This is indicative of reduced polymer solvent interaction which is consistent with the smaller values obtained for the Mark Houwink exponent, α , for the isotactic samples (see Table 5.1).

Values of B vary from one method to another, Table 5.4, because they depend on the functional form used for α . That is, whether we use closed forms for α of the type α^5 , Equation 1.9 or α^3 , Equation 1.10. According to Yamakawa⁽⁸⁾, a more rigorous experimental test of the theories of α is needed before we can establish a basic equation for viscosity plots to be used for the estimation of B . No published data on B is available for comparison.

Conclusions

From this work it can be concluded that, (a) A measurable difference occurs in the Mark-Houwink relationship between isotactic and syndiotactic PMMA. For a given molecular weight the isotactic polymer exhibits a larger intrinsic viscosity, although at high molecular weights, 10^6 , this difference diminishes. This difference indicates that isotactic PMMA is more highly extended even in a thermodynamically good solvent, THF (b) Isotactic PMMA is $\sim 35\%$ more extended than syndiotactic PMMA in its unperturbed state; (c) Isotactic PMMA exhibits less polymer-solvent interaction than the syndiotactic polymer. An explanation for all three conclusions, a, b, and c lies in the fact that isotactic PMMA exists in a more extended state. It is possible

that the more extended conformation of isotactic PMMA arises from the presence of helical segments. Since the helix is the conformation of lowest potential energy it is postulated that helical segments are possible in both the bulk state and in solution. The presence of these helical segments would be expected to result in the larger perturbed and unperturbed dimensions exhibited by isotactic PMMA in comparison to the syndiotactic polymer. In addition, the combination of bulky side groups, and the presence of helical segments are believed to result in limiting the access of solvent molecules to the polymer and thereby result in a smaller degree of polymer-solvent interaction.

REFERENCES

1. J.M.G. Cowie, *Polymer*, 7, 487 (1966).
2. P.J. Flory, T.G. Fox, *J. Amer. Chem. Soc.*, 73, 1904(1951)
3. W.H. Stockmayer, M.J. Fixman, *J. Polym. Sci.*, C1, 137(1963)
4. G.C. Berry, *J. Chem. Phys.* 46, 1338(1967)
5. A. Dondos, and H. Benoit, *Polymer*, 19, 523 (1978)
6. J.M.G. Cowie, *Polymer London*, 7, 487(1966)
7. P.J. Flory, Statistical Mechanics of Chain Molecules, Interscience, New York(1971)
8. H. Yamakawa, Modern Theory of Polymer Solutions, Harper and Row, New York(1971)
9. P.R. Sundararajan, and P.J. Flory, *J. Amer. Chem. Soc.*, 96, 5025 (1974)
10. H. Kusanagi, H. Tadokoro, and Y. Chatani, *Macromolecules*, 9, 531 (1976)

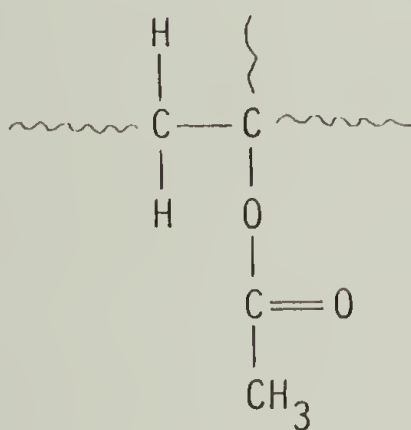
C H A P T E R V I
CHARACTERIZATION OF BRANCHED POLY(VINYL ACETATE) BY GEL
PERMEATION CHROMATOGRAPHY COUPLED WITH ON-LINE LOW
ANGLE LASER LIGHT SCATTERING PHOTOMETRY

Abstract

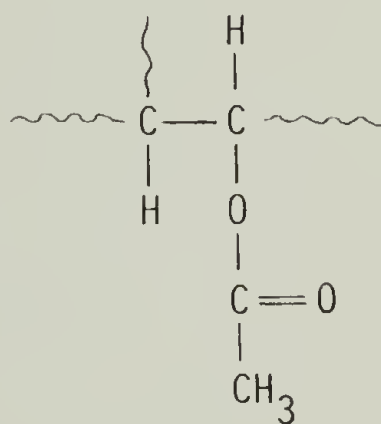
Poly(vinyl acetate) (PVAc) of \bar{M}_w 750,000, \bar{M}_w/\bar{M}_n 3.85 and \bar{B}_n (the number of long branches per molecule) 2.2 was subjected to chain scission by mechanical (high-speed stirring) as well as chemical (saponification and reacetylation) methods to investigate the effect of shear on the branching distribution. The extent of long branching was measured by gel permeation chromatography on-line with low-angle laser light scattering photometry. It was concluded that (i) the branches through the acetate group are long and are ruptured preferentially on shearing, (ii) the branches through the α - and β -carbons are not broken on shearing, (iii) the extent of long branching through the acetate group is about 67% of total branching, (iv) on shearing, 80% of the decrease in molecular weight is due to rupture of the long branches through the acetate group. The remaining 20% of the decrease in molecular weight results from the main chain scission; and (v) the poly(vinyl alcohol) derived from branched PVAc contains a smaller but nevertheless significant amount of branching.

Introduction

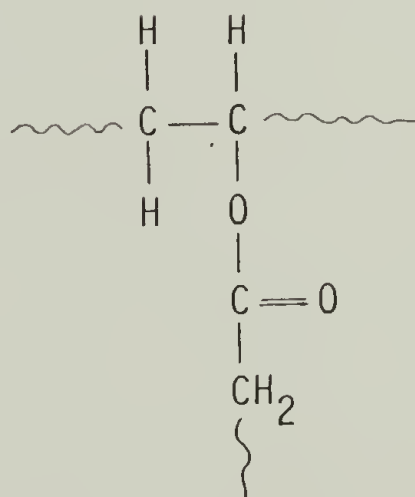
During the polymerization of vinyl acetate extensive branching occurs by chain transfer to polymer and terminal double bond reactions.⁽¹⁻⁸⁾ Branching frequency increases rapidly with conversion and causes a concomitant broadening of the molecular weight distribution.^(4,9-14) The branch points have been previously shown to exist in three chemically distinct structures, through the α -carbon (structure I), the β -carbon (structure II), and through the acetate group (structure III).⁽¹⁵⁾



I



II

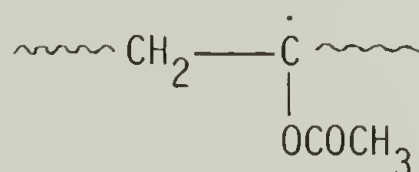


III

Branches may be "short" or "long." Since long branches mainly affect the hydrodynamic properties of the polymer, and are thereby

measurable by intrinsic viscosity measurements, we will be concerned exclusively with the measurement of long branches. The amount of branching through the acetate group was estimated to be about 70% of the total by Graessley and his coworkers.⁽¹⁵⁾ However, this percentage will obviously depend on the conditions of polymerization.

On shearing of branched poly(vinyl acetate) (PVAc) to rupture, it is not certain which main chains or branch units will be ruptured. The strength of a $-C-O-$ bond is higher than that of a $-C-C-$ bond.^(16,17) As a result, $-C-C-$ bonds would be expected to be ruptured preferentially. It has been shown, using electron spin resonance, that



is the principal radical observed on shearing.^(18,19) However, Goto and Fujiwara⁽²⁰⁾ have determined using chemical methods that stirring a solution of PVAc in cyclohexanone did not result in chain scission at the $-C-C-$ linkage, but rather at the pendant ester linkage.

The purpose of our study is to investigate which bonds are ruptured on shearing; that is, whether scission occurs at the main chains or at the branch points shown in structures I, II and III or at a combination of them. To accomplish this, we have carried out chain scission by mechanical as well as by chemical methods. Branching through the acetate group (structure III) can be detected from changes in molecular weights when a sample is saponified to poly(vinyl alcohol) (PVA) and acetylated back to PVAc. The PVAc so obtained has a lower molecular weight than the original PVAc prior to saponification because branches

through the acetate group are broken on saponification and are not re-formed on acetylation.⁽²¹⁾ The branches through the α -carbon (structure I) and the β -carbon (structure II) are not affected by saponification since they are non-hydrolyzable. Hence, PVA obtained by saponification of branched PVAc remains partially branched.⁽¹⁵⁾ To investigate which branches, if any, are ruptured on shear and to what extent, four samples were prepared as described in Table 6.1.

Previously, branching in PVAc has been determined kinetically (1,3,6,7,15), by gel permeation chromatography (GPC) combined with viscometry⁽²²⁻²⁴⁾, GPC combined with ultracentrifugation⁽²⁴⁾ and GPC on-line with low-angle laser light scattering (LALLS) photometry.^(25,26) In this work we use GPC/LALLS and the methods developed in Chapter IV for calculating $[\eta]_i$ and M_{w_i} values from the distribution of the polymer. These values are then used to determine the degree of long chain branching in PVAc.

Experimental

Materials. The PVAc used was obtained from Polysciences, Pa. It had a \bar{M}_w 750,000, \bar{M}_w/\bar{M}_n 3.85 and \bar{B}_n (the number of long branches per molecule) 2.2.

Saponification. A 5% methanolic potassium hydroxide solution was added with stirring to ten times its volume of a 2% methanol solution of PVAc at room temperature. The agitation was continued overnight to insure complete alcoholysis.⁽²¹⁾ The PVA obtained was then filtered and repeatedly washed with methyl acetate.

TABLE 6.1 Description of Poly(Vinyl Acetate) Samples

Sample #	Sample Description
1	Original branched PVAc
2	From sample #1 by saponification and re-acetylation for removal only of branches through acetate group
3	After high-speed stirring of toluene solution of sample #1 (0.03 g/ml)
4	From sample #3 by saponification and re-acetylation

Reacetylation. The drained, but not dry, PVA was then dispersed in an acetylating solution in approximate proportions of 40 ml of solution for each gram of PVA. The acetylating solution consisted of one volume of pyridine, five volumes of acetic acid and fifteen volumes of acetic anhydride. The dispersion was agitated slowly at room temperature for 24 hours longer than the time required for the PVA to dissolve.⁽¹⁾ The reconstituted PVAc was recovered by precipitation with a large excess of water at room temperature. The PVAc was washed extensively with water, purified by reprecipitation into water from an acetone solution and dried overnight under vacuum at 40°C. The purified PVAc was then dissolved in benzene and freeze-dried to remove the last traces of the acetylating solution.^(7,15)

High-speed stirring. High-speed stirring was achieved by use of a Virtis-60 homogenizer. The homogenizer was fitted with a teflon cylinder mounted to a stainless steel shaft. A 250 ml round glass flask with five flutes was used as a degradation vessel. The degradation vessel was set in a cooling cup and temperature was maintained at $10 \pm 0.5^\circ\text{C}$ by packing the cooling cup with crushed ice. The toluene solution of PVAc (0.03 g/ml) was agitated at 50,000 rpm for 5 hrs. to achieve extreme agitation and shear. A turbulent flow was generated during shearing and was believed to be the most probable cause for bond rupture.⁽²⁷⁾

Refractive index increment measurements. Measurement of the specific refractive index increment, dn/dc , for PVAc was described in Chapter II. All measurements were made using a Chromatix KMX-16 differential refractometer using tetrahydrofuran, THF, Fisher certified grade, at 25°C.

The concentration range was varied from 2 to 5 g/l. Since the variation in dn/dc values obtained for the four PVAc samples was less than 2%, (Chapter II), an average value of 0.054 ml/gm was used here.

Gel permeation chromatography on-line with low angle laser light scattering photometry. The apparatus used was the GPC/LALLS system described in Chapter IV. The inlet of the LALLS was fitted with a 0.5μ fluoropore filter (Millipore Corporation, Mass.). This filter provided a good signal relatively free from dust particles, without removal of the high molecular weight fraction of the sample. The flow rate used was 1cc/min. at 25°C. Injection volumes were 0.5cc and concentrations were 1 to 2.5×10^{-4} g/ml.

As discussed in Chapters IV and V data acquisition is limited to a region in the distribution where adequate response is obtained from both the differential refractometer, and the LALLS detectors. For broad MWD samples, i.e., branched PVAc, the offset between the response from the two detectors becomes increasingly large. This offset severely limits the number of useable data points one can obtain from the distribution of the polymer. In our work data was acquired at 1 ml intervals. This procedure generally resulted in approximately 20-30 useable data points for each polymer. Outside this region considerable errors resulted because of limitations in our ability to measure the intensity of the signal. This problem may, of course, be handled electronically as described by Hamielec and Ouano.⁽²⁵⁾

Calculation of the incremental intrinsic viscosity and molecular weight values. The method used to calculate the incremental intrinsic viscosi-

ties, $[\eta]_i$, and molecular weights, M_{w_i} , from the distribution of a polymer, was described in Chapter IV. Basically, the method uses the LALLS to determine M_{w_i} and then relies on the assumption of "Universal Calibration" to obtain $[\eta]_i$. In addition, the method requires that α , the Mark-Houwink exponent be known. The method for obtaining an estimate of α has also been discussed in Chapter IV. However, it is sufficient to note here that, although α may vary with molecular weight for a branched polymer, the method is insensitive to the exact value of α and consequently an average may be used. The average value of α used here was 0.646.⁽²⁷⁾

A series of values of $[\eta]_i$, the intrinsic viscosity of branched polymer, and M_{w_i} were generated across the distribution of the polymer using a computer program. The value of intrinsic viscosity, $[\eta]_{\ell_i}$, for the corresponding linear polymer, at any molecular weight, M_{w_i} , was obtained using the following Mark-Houwink relationship for linear PVAc:⁽²²⁾

$$[\eta]_{\ell_i} = 1.877 \times 10^{-4} M_{w_i}^{0.686} \quad (6.1)$$

The viscosity ratio, G , at any molecular weight M_{w_i} , was then obtained by dividing the intrinsic viscosity of the branched polymer by that for the corresponding linear polymer.

Results and Discussion

It is well accepted that polymers in solution with long branches are more compact than are their corresponding linear analogs. As a result, the intrinsic viscosity of polymers with long chain branching is smaller than that for linear polymers of the same molecular weight.

Figure 6.1 compares intrinsic viscosities as a function of molecular weight for the four PVAc samples under study. At any molecular weight, the intrinsic viscosity of the original polymer (sample #1) is much smaller than that of the linear PVAc with the difference in intrinsic viscosity increasing with molecular weight. This indicates that sample #1 is highly branched, and the extent of branching increases with molecular weight. On shearing the intrinsic viscosity of the polymer for a given molecular weight is increased whereas the average molecular weight is decreased (sample #3). This increase in intrinsic viscosity for a given molecular weight indicates that branches are preferentially ruptured during shear. On saponification and reacetylation of the sheared sample (sample #3), a further increase in the intrinsic viscosity is observed for a given molecular weight. This is consistent with saponification of additional branches joined through the acetate group and produces a more linear polymer (sample #4). Similar results are obtained for Sample #2. That is, the intrinsic viscosity at a given molecular weight is higher than that of the original branched polymer and the average molecular weight is lower. This is because on saponification the branches through the acetate group (structure III) are broken and not reformed on acetylation. However, any branches through the α - and β -carbons (structures I and II) would not be affected by saponification since these branches are non-hydrolyzable. Hence the saponified and reacetylated sample contains a smaller but significant amount of branches. This implies that any PVA derived from a branched PVAc will not be linear. It is interesting to note that the data for sample #2 and #4 coincide (see Figure 6.1). This qualitatively indicates

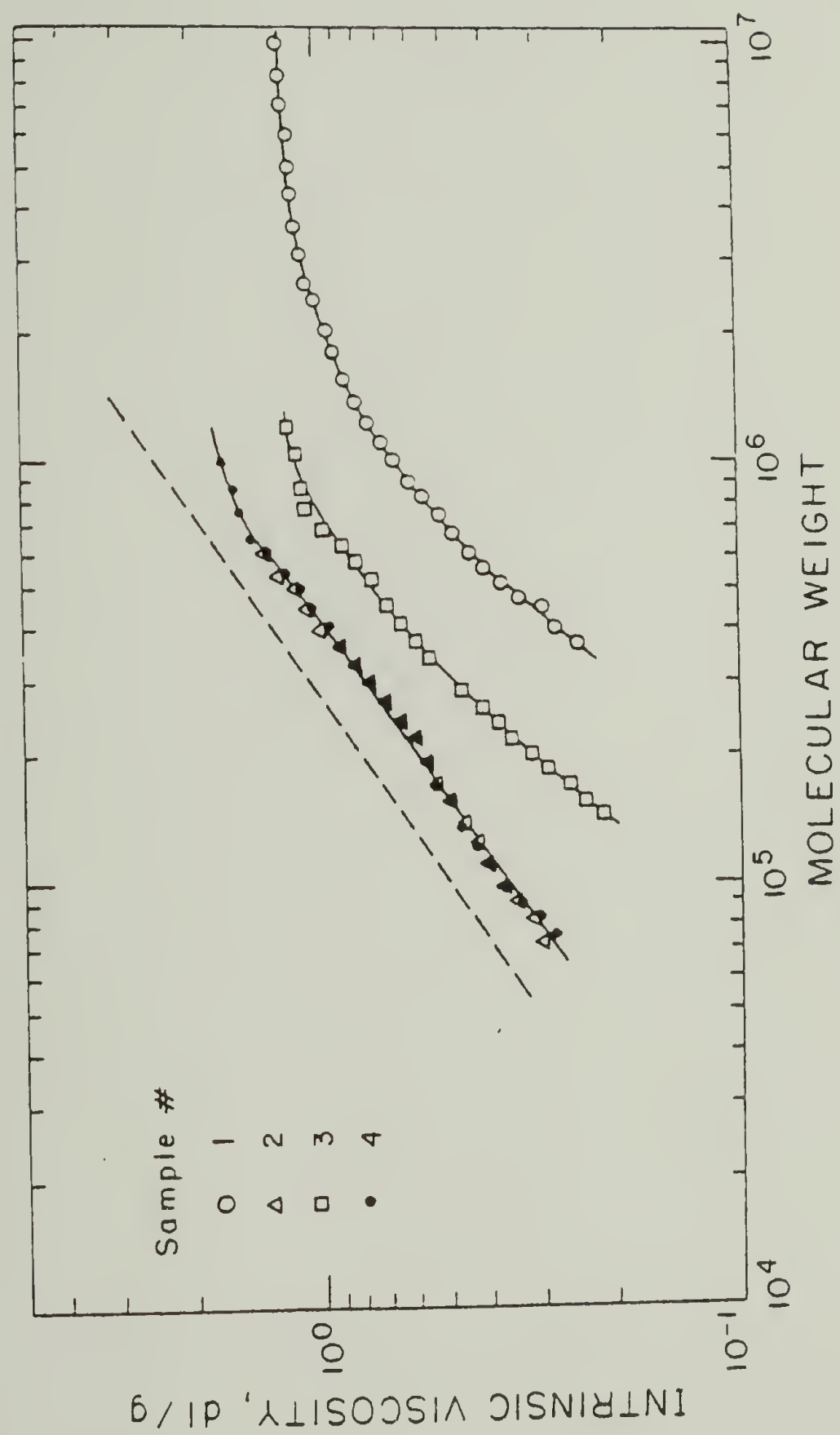


Figure 6.1. Intrinsic viscosity versus molecular weight for branched poly(vinyl acetate).

that, on shearing, non-hydrolyzable branches (structure I and II) are not broken and the branches through the acetate group (structure III) are preferentially ruptured. Those left are then removed on saponification and reacetylation.

The viscosity ratio, G , as a function of molecular weight for the four samples is shown in Figure 6.2. The value of G depends on the type and location of the branches as well as on the number of branch points per molecule.⁽²⁸⁾ The value of G is 1.0 for a linear polymer and decreases with increase in branching. We observe that the value of G for sample #1 is low and decreases with increase in molecular weight, indicating that the extent of branching increases with molecular weight. The value of G increases towards 1.0 on saponification and reacetylation (sample #2). This is because the branches through the acetate group are removed on saponification and reacetylation. The average value of G for sample #2 is 0.74, compared to 0.20 for sample #1. This implies that about 67% of the branching in PVAc occurs through the acetate group. This is in agreement with the results of Graessley et al.,⁽¹⁵⁾ who determined that about 70% of the branches in PVAc were through the acetate group (structure III). The effect of shearing (sample #3) on the value of G is also shown in Figure 6.2. Comparison of the data for sample #1 and #3 indicates that in addition to the decrease in molecular weight, the value of G increases, indicating the removal of some long branches as a result of shearing. In addition, Figure 6.2 shows the results of shearing followed by saponification and reacetylation (sample #4). It is apparent that saponification and reacetylation of the sheared sample #3 results in removal of the remaining branches through the ace-

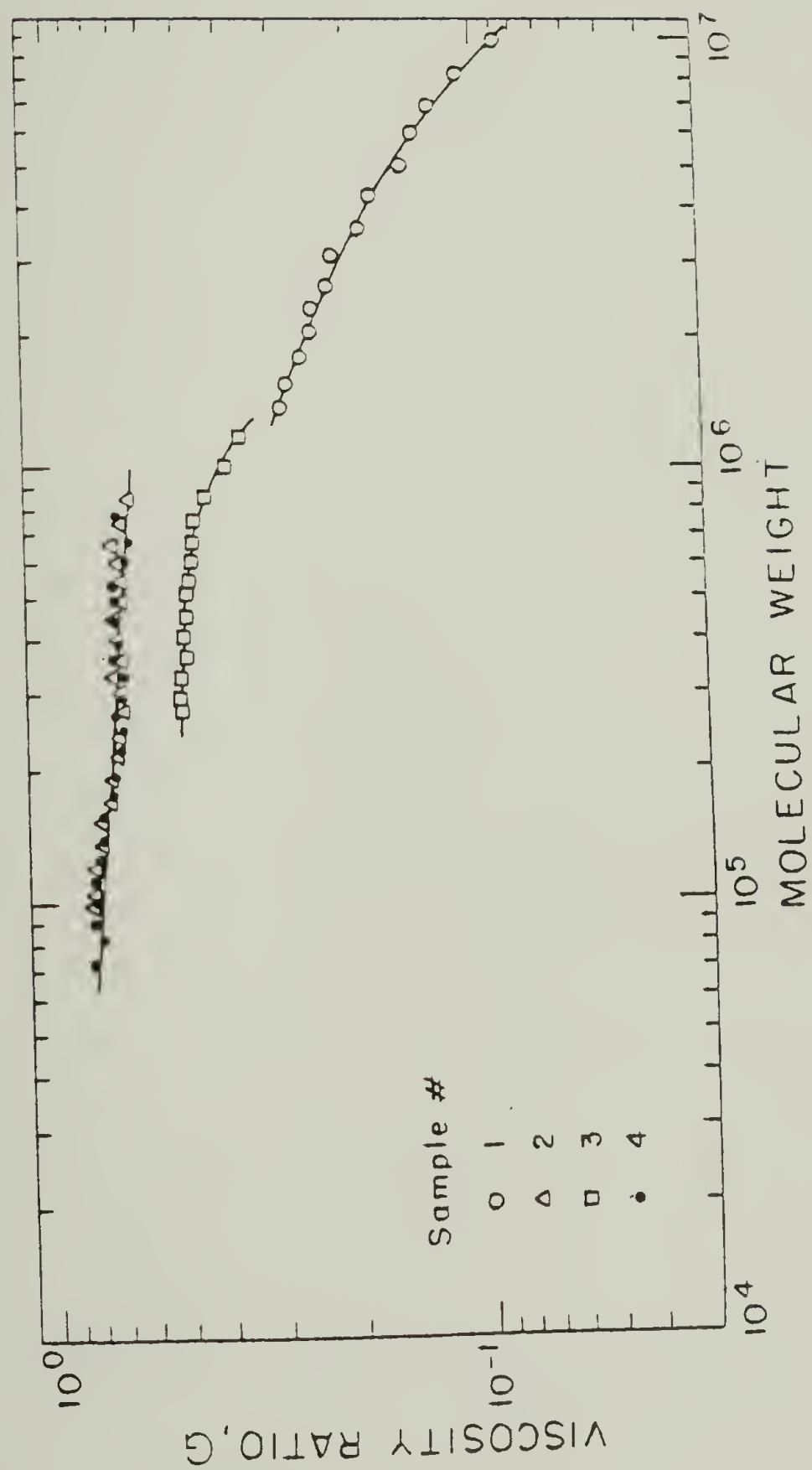


Figure 6.2. The viscosity ratio, G , versus molecular weight for branched poly(vinyl acetate).

tate group, as indicated by the coincidence of the data for sample #2 and #4.

The number average molecular weights, \bar{M}_n , for the four samples are compared in Table 6.2. Each scission, whether by shear or by saponification and reacetylation, increases the number of molecules by one without altering the number of repeating units. Thus, by counting molecules before and after scission, we obtain:⁽¹⁵⁾

$$\text{chain scission/molecule} = \frac{(\bar{M}_n)_b - (\bar{M}_n)_a}{(\bar{M}_n)_a} \quad (6.2)$$

where subscripts b and a signify before and after saponification-reacetylation or shear. The number of chain scissions per molecule thus calculated is shown in Table 6.2.

We may also calculate the amount of scission that occurs on shearing at linkages other than the pendant ester linkages. This is obtained from the difference in the number of scissions per molecule between the sheared and saponified and reacetylated sample (#4) and the sample which was only saponified and reacetylated (#2). This difference is 0.07. This indicates that shear results in only 0.07 scissions per molecule through linkages other than the pendant ester linkages. The remaining 0.28 scissions per molecule (see Table 6.2) on shear must then occur through the acetate group. This implies that 80% of the decrease in molecular weight, on shearing, occurs due to rupture of long branches through the acetate group (structure III). The coincidence of the data for sample #2 and #4 (see Figures 6.1 and 6.2) indicates that branches through the α - and β -carbons (structures I and II) are not ruptured on shearing. Hence the remaining 20% of the decrease in molecular weight

TABLE 6.2 Comparison of Poly(Vinyl Acetate) Samples

Sample #	\bar{M}_n from GPC	chain scission/ molecule
1	194,800	-
2	78,875	1.47
3	144,000	0.35
4	76,625	1.54

must occur due to main chain scission.

Since the strength of the -C—O- bond is higher than that of -C—C- bond, it would be expected that on shearing -C—C- bonds would be ruptured preferentially. However, our results as well as those of Goto and Fujiwara⁽²⁰⁾ indicate that the rupture occurs preferentially through the -C—O- bond of the ester group. This implies that the branches through the acetate group must be long, since long chains would be expected to rupture on shearing,^(17,29) particularly as they can participate in entanglements.

REFERENCES

1. O.L. Wheeler, E. Lavin and R.N. Crozier, J. Polym. Sci., 9, 157 (1952).
2. D.J. Stein, Makromol. Chem., 76, 170 (1964).
3. M.K. Lin-erman, G.E. Ham, Ed., Vinyl Polymerization, Vol. 1, Part 1, Edward Arnold, London, 1967, Chap. 4.
4. W.C. Uy, J. Polym. Sci. A2, 7, 1919 (1969).
5. G. Odian, Principles of Polymerization, McGraw-Hill, New York, 1970, p. 219.
6. K. Nagasubramanian and W.W. Graessley, Chem. Eng. Sci., 25, 1559 (1970).
7. S. Nazakura, Y. Morishima and S. Murahashi, J. Polym. Sci., Polym. Chem. Ed., 10, 2853 (1972).
8. P.A. Small, Adv. Polym. Sci., 18, 1 (1975).
9. W.W. Graessley and H.M. Mittelhauser, J. Polym. Sci. A2, 5, 431 (1967).
10. O. Saito, K. Nagasubramanian and W.W. Graessley, J. Polym. Sci. A2, 7, 1937 (1969).
11. P.J. Flory, Principles of Polymer Chemistry, Cornell University Press, Ithaca, 1975, Chap. 9.
12. K. Nagasubramanian, O. Saito and W.W. Graessley, J. Polym. Sci. A2, 7, 1955 (1969).
13. W.W. Graessley and J.S. Prentice, J. Polym. Sci. A2, 6, 1887 (1968).
14. W.W. Graessley and E.S. Shinbach, J. Polym. Sci., Polym. Phys. Ed., 12, 2047 (1974).
15. W.W. Graessley, R.D. Hartung and W.C. Uy, J. Polym. Sci. A2, 7, 1919 (1969).
16. T.L. Cottrell, The Strength of Chemical Bonds, Butterworth, London, 1958.

17. A. Casale and R.S. Porter, Polymer Stress Reactions, Academic Press, New York, Vol. 1, 1978, Vol. 2, 1979.
18. S.N. Zurkov, E.E. Tomashevskii and V.A. Zakrevskii, Fiz. Tverd. Tela, 3, 2841 (1961); Eng. transl.: Sov. Phys. Solid State, 3, 2074 (1962).
19. P. Yu. Butyagin, Vysokomol. Soedin., A9 (1), 136 (1967); Eng. transl., Polym. Sci. USSR, 9(1), 149 (1967).
20. K. Goto and H. Fujiwara, Kobunshi Kagaku, 21, 716 (1964).
21. O.L. Wheeler, S.L. Ernst and R.N. Crozier, J. Polym. Sci., 8, 409 (1952).
22. Y. Morishima, W. Kim and S. Nozakura, Polym. J., 8, 196 (1976).
23. W.S. Park and W.W. Graessley, J. Polym. Sci., Polym. Phys. Ed., 15, 85 (1977).
24. R. Dietz and M.A. Francis, Polymer, 20, 451 (1979).
25. A.E. Hamielec and A.C. Ouano, J. Liqd. Chrom., 1 (4), 527 (1978).
26. D.E. Axelson and W.C. Knapp, J. Appl. Polym. Sci., 25, 119 (1980).
27. S.H. Agarwal and R.S. Porter, J. Appl. Polym. Sci., 25, 173 (1980).
28. B.H. Zimm and W.H. Stockmayer, J. Chem. Phys., 18, 1301 (1949).
29. N.K. Baramboim, Mechanochemistry of Polymers (translated from Russian by R.J. Moseley), W.F. Watson, Ed., Rubber and Plastic Res. Assoc. of Great Britain, Maclaren, 1964.

CHAPTER VII

SUGGESTIONS FOR FUTURE WORK

Gel Permeation Chromatography Coupled With on-line Low Angle Laser Light Scattering Photometry

Dimensions of polymer. This research project has demonstrated the application of GPC/LALLS to the measurement of the unperturbed dimensions for a series of stereoregular poly (methyl methacrylate), PMMA, samples. The methods used for PMMA should be applicable to any polymer for which "Universal Calibration" is valid. It should therefore be possible to study numerous other stereoregular systems.

A potentially interesting study would involve using the various stereoregular forms of poly (α -chloro alkyl acrylates) for which we have samples of the methyl, ethyl, and isopropyl esters. This study would be interesting from several points of view. First of all, poly (α -chloro methacrylate) might be expected to exhibit similar unperturbed dimensions to PMMA, based on the fact that the α -chloro and α -methyl groups have roughly the same Van der Waals volume. If the dimensions are considerably different we may learn something about the effect of the polar α -chloro group on the conformation of the chains. In addition, one could obtain valuable information concerning the effect of the size of the pendent ester group on the conformation of the chain.

In general the number of systems which can be studied is endless. Future work might involve studying the unperturbed dimensions of stereoregular polystyrene. There are three different stereoregular forms of polystyrene currently available, 100% isotactic, 60% isotactic, and 15% isotactic. In addition, Professor Lenz's group does a lot of work on poly (α -methyl styrene) and these polymers might also be available. Professor Vogl's group is currently synthesizing various head-to-head polymers and these may also be available for study. It would be interesting to compare the unperturbed dimensions of head-to-head versus head-to-tail polymers.

Branching studies. In Chapter VI the application of GPC/LALLS to study the degree of long chain branching in poly (vinyl acetate), PVAc, was demonstrated. It is believed that this is potentially the most useful application of these combined instruments. Our study on PVAc only begins to scratch the surface. I believe that a student willing to do a limited amount of synthesis of PVAc with varying degrees of branching could make a valuable contribution. By controlling the extent of reaction the degree of branching can also be controlled.⁽¹⁾ Samples prepared in this way would be extremely valuable in evaluating the application of GPC/LALLS to the measurement of long chain branching in polymers. Potentially the most useful application of these combined instruments in measuring the degree of long-chain branching, would be for low density polyethylene, the highest volume thermoplastic in the world. This work would however involve using a GPC system capable of working at 135° C. Although we do have the model 200, I don't believe

this unit is worth all the trouble.

Alternative axial dispersion corrections. In this research project we used a modified version of a method originally developed by Benoit et al⁽²⁾ for correcting for axial dispersion. This method is unique in that it involves correcting each incremental value for spreading. Numerous other corrections for spreading have also been proposed, most of which involve correcting the entire chromatogram rather than the incremental values. I believe it would prove very interesting to compare the application of the more conventional methods for correcting for axial dispersion with the results obtained from the incremental correction. In particular, the methods used by Chromatix in their software programs and GPV2 and GPV3 proposed by Yau et al⁽³⁾ have received considerable attention in the literature, and would prove interesting to compare with the method used in this work.

Calculation of the intrinsic viscosity. In this work we were concerned with calculating incremental values of the intrinsic viscosity, $[\eta]_i$. In theory we should then be able to sum these values and obtain the actual viscosity of the whole polymer. This summation was not attempted in this work because of the imprecise values of $[\eta]_i$ obtained at both ends of the distribution. As discussed in Chapter IV we are limited to a region in the polymer distribution where adequate response is obtained from both the LALLS and the differential refractometer. It would be of considerable practical as well as theoretical importance to see if $[\eta]$ could be calculated from a summation of the the incremental $[\eta]_i$ values.

$$[\eta] = \sum c_i [\eta]_i / \sum c_i$$

As a first approximation an attempt could be made to simply extrapolate the useable molecular weight values, M_{w_i} , obtained from the middle of the distribution to the limits of the distribution, V_i and V_F , where V_i is the initial elution volume and V_F is the final. These extrapolated M_{w_i} values along with the appropriate elution volumes could then be used in conjunction with the "Universal Calibration" curve to obtain more accurate values of $[\eta]_i$ at the ends of the distribution. It is hoped that summation of these values would yield a value for the intrinsic viscosity which would agree with the value obtained by conventional viscometry for the bulk polymer.

Rigid rods in GPC. The GPC/LALLS system would seem to be the ideal set-up for investigating the separation mechanism of helical polymers in GPC. Several authors^(4,5,6) have reported that "universal calibration" appears to be valid for rigid rods, based on the fact that \bar{M}_V calculated by GPC, calibrated with polystyrene standards, appears to be in good agreement with \bar{M}_V obtained by viscosity measurements. The on-line light scattering detector would allow us to actually measure the weight average molecular weight of the polymer as it elutes. From this information we could for the first time obtain information concerning the separation mechanism of rigid rods in GPC.

In this laboratory we have attempted some early work on poly(γ -benzyl-L-glutamate), PBLG, and have found considerable tailing for these samples. Since the molecular weight distribution is supposed to be narrow we have assumed that some sort of absorption must occur on the μ -styragel columns. In our studies we used tetrahydrofuran. Possibly

N,N-dimethylacetamide could help prevent this problem since Dawkins et al⁽⁴⁾ have studied PBLG using this solvent with styragel columns.

Differential Refractometry

Conformational and branching effects. The work reported in Chapter II showed that the specific refractive index increment, dn/dc , was affected by the stereoregular composition as well as by the degree of branching. An attempt was made to correlate the change in dn/dc with changes in the hydrodynamic volume of the polymers. It would be interesting to see if this trend is a general one by studying dn/dc of other stereoregular systems or measuring dn/dc as a function of the degree of long chain branching.

Measurement of dn/dc for a 60% isotactic and a 100% isotactic sample of polystyrene was attempted without much success. Whereas conventional (15% isotactic) polystyrene presented no experimental difficulties, the two isotactic samples gave very inconsistent results. It appeared that dn/dc increased almost exponentially as the concentration was decreased. Every effort was made to filter these samples to obtain optically clean samples but the results consistently showed a dramatic increase in dn/dc with decreasing concentration. For all other systems dn/dc was found to be independent of concentration. It would prove interesting to explore this phenomenon further to see if possibly we are observing some sort of transition or just measuring turbidity.

Helix-coil transitions. There is currently considerable interest in studying helix-coil transitions of simple polypeptides since what is learned about these may be applied to more complex systems. In particular PBLG has received considerable attention. Preliminary work in this laboratory has shown that the helix-coil transition in PBLG may be followed using the Chromatix KMX-16 laser differential refractometer. A 4/1 mixture of dichloroacetic acid and 1, 2 dichloroethylene was used as the solvent for PBLG. The temperature was varied from 0° C to 55° C and a transition was observed at 30-35° C. Unfortunately this study was not pursued any further so that the data must be deemed as only preliminary. In addition, no attempt was made to interpret the data. The relation presented in Chapter III relating dn/dc to the specific volume and the difference in refractive index between the polymer and the solvent may be of some use here in interpreting the data. Although this relation is semiempirical one may be able to extract some information concerning the volume change during the helix coil transition.

REFERENCES

1. A.E. Hamielec, A.C. Ouano, L.L. Nebenzahl, J. Liq. Chrom., 1(4), 527 (1978).
2. L. Marais, and H. Benoit, J. Appl. Polym. Sci., 21, 1955 (1977).
3. W.W. Yau, J.J. Kirkland, and D.D. Bly, Modern Size Exclusion Liquid Chromatography, Wiley-Interscience, New York, 1979.
4. J.V. Dawkins, M. Henning, Polymer, 16, 554 (1975).
5. M.R. Ambler, D. McIntyre, J. Polym. Sci., PL. Ed., 13, 589 (1975).
6. Z. Grubisic, L. Reibel, G. Spach, C.R. Acad. Sc. Paris, 264, 1690 (1967).

